



# Biogeographic patterns and diversification dynamics of the genus *Cardiodactylus* Saussure (Orthoptera, Grylloidea, Eneopterinae) in Southeast Asia

Jiajia Dong, Gael Kergoat, Natállia Vicente, Cahyo Rahmadi, Shengquan Xu,  
Tony Robillard

## ► To cite this version:

Jiajia Dong, Gael Kergoat, Natállia Vicente, Cahyo Rahmadi, Shengquan Xu, et al.. Biogeographic patterns and diversification dynamics of the genus *Cardiodactylus* Saussure (Orthoptera, Grylloidea, Eneopterinae) in Southeast Asia. *Molecular Phylogenetics and Evolution*, 2018, 129, pp.1-14. 10.1016/j.ympev.2018.06.001 . hal-02433078

HAL Id: hal-02433078

<https://hal.science/hal-02433078>

Submitted on 8 Jan 2020

**HAL** is a multi-disciplinary open access archive for the deposit and dissemination of scientific research documents, whether they are published or not. The documents may come from teaching and research institutions in France or abroad, or from public or private research centers.

L'archive ouverte pluridisciplinaire **HAL**, est destinée au dépôt et à la diffusion de documents scientifiques de niveau recherche, publiés ou non, émanant des établissements d'enseignement et de recherche français ou étrangers, des laboratoires publics ou privés.

1      **Title**

2

3      **Biogeographic patterns and diversification dynamics of the genus**  
4      ***Cardiodactylus* Saussure (Orthoptera, Grylloidea, Eneopterinae) in**  
5      **Southeast Asia**

6

7      **Authors**

8      Jiajia Dong<sup>a,b,\*</sup>, Gael J. Kerfoot<sup>c</sup>, Natállia Vicente<sup>d</sup>, Cahyo Rahmadi<sup>e</sup>, Shengquan Xu<sup>b</sup>, Tony  
9      Robillard<sup>a</sup>

10

11     **Authors' affiliations**

12     <sup>a</sup> Institut de Systématique, Evolution et Biodiversité (ISYEB), Muséum national d'Histoire  
13     naturelle, CNRS, Sorbonne Université, EPHE, 57 rue Cuvier, CP 50, 75231 Paris Cedex 05,  
14     France

15     <sup>b</sup> College of Life Science, Shaanxi Normal University, 710119, Xi'an, Shaanxi, P.R. China

16     <sup>c</sup> CBGP, INRA, CIRAD, IRD, Montpellier SupAgro, Univ. Montpellier, Montpellier, France

17     <sup>d</sup> Universidade Federal de Viçosa, Programa de pós-graduação em Ecologia. Av. PH Rolfs  
18     s/n. Viçosa, Minas Gerais, CEP 36570-900, Brazil

19     <sup>e</sup> Division of Zoology, RC-Biology, Cibinong Science Center – Indonesian Institute of  
20     Sciences (LIPI), Cibinong Science Center, Jl. Raya Jakarta- Bogor Km. 46, Cibinong, 16911  
21     Indonesia

22     \*Corresponding author: jia\_jia\_dong@hotmail.com

23

24     **Running title:** Biogeography of *Cardiodactylus* crickets

25

26    **Abstract**

27    Southeast Asia harbors an extraordinary species richness and endemism. While only  
28    covering 4% of the Earth's landmass, this region includes four of the planet's 34 biodiversity  
29    hotspots. Its complex geological history generated a megadiverse and highly endemic biota,  
30    attracting a lot of attention, especially in the field of island biogeography. Here we used the  
31    cricket genus *Cardiodactylus* as a model system to study biogeographic patterns in  
32    Southeast Asia. We carried out molecular analyses to: (1) infer phylogenetic relationships  
33    based on five mitochondrial and four nuclear markers, (2) estimate divergence times and  
34    infer biogeographical ancestral areas, (3) depict colonization routes, and summarize  
35    emigration and immigration events, as well as *in situ* diversification, and (4) determine  
36    whether shifts in species diversification occurred during the course of *Cardiodactylus*  
37    evolution. Our results support the monophyly of the genus and of one of its species groups.  
38    Dating and biogeographical analyses suggest that *Cardiodactylus* originated in the  
39    Southwest Pacific during the Middle Eocene. Our reconstructions indicate that Southeast  
40    Asia was independently colonized twice during the Early Miocene (ca. 19-16 Million years  
41    ago), and once during the Middle Miocene (ca. 13 Million years ago), with New Guinea acting  
42    as a corridor allowing westward dispersal through four different passageways: Sulawesi, the  
43    Philippines, Java and the Lesser Sunda Islands. Sulawesi also served as a diversification  
44    hub for *Cardiodactylus* through a combination of high immigration and *in situ* diversification  
45    events, which can be accounted for by the complex geological history of the Wallacea region.

46

47    **Keywords**

48    Biogeography; climate change; crickets; diversification analyses; geological changes;  
49    molecular dating

50

51

52

53

54 **1. Introduction**

55 Southeast Asia (SEA) is considered as one of the most geologically dynamic regions of the  
56 planet (Lohman et al., 2011). It aggregates four major biodiversity hotspots (de Bruyn et al.,  
57 2014; Mittermeier et al., 2004; Zachos and Habel, 2011), which are divided by sharp, yet  
58 porous, biogeographic boundaries (Hearty et al., 2007; Morley et al., 2012; Wallace, 1860).  
59 The complex geological history of SEA generated a megadiverse and highly endemic biota  
60 that has attracted a lot of attention, especially in the field of island biogeography (Condamine  
61 et al., 2013, 2015; Hall, 2009a; Lohman et al., 2011; Metcalfe, 2006; Woodruff, 2010). In  
62 SEA, dynamic geological and climatic histories acted together to generate the world's largest  
63 island complex, in which the spatial distribution of terrestrial habitats has been altered  
64 extensively through time (Bird et al., 2005; Hall, 1996, 2009a, 2011; Hall and Sevastjanova,  
65 2012; Heaney, 1991; Metcalfe, 2006; Voris, 2000; Zahirovic et al., 2014). Volcanic uplifts and  
66 repeated sea-level fluctuations also promoted species diversification by providing countless  
67 opportunities for allopatric speciation (Heaney, 2000; Steppan et al., 2003; Jansa et al., 2006;  
68 Outlaw and Voelker, 2008). The interplay between the movement of tectonic plates,  
69 oscillations in the Earth's orbit, and the variable configuration of landmasses and ocean  
70 currents also affected the climate of SEA (Morley, 2012). As a result, the vegetation and the  
71 distribution of habitats of SEA were profoundly modified through time (Heaney, 1991).  
72 Tropical rainforest in SEA greatly expanded during the Paleogene Period (66.0-23.0 Million  
73 years ago (Ma)) and the beginning of the Neogene Period, due to warmer temperatures and  
74 more humid climates. Tropical rainforests reached a peak during the mid-Miocene Climatic  
75 Optimum (MCO; 17-15 Ma), when their distribution extended further north to southern China  
76 and Japan (Heaney, 1991; Morley, 2012; Zachos et al., 2001). It is not until the Late Miocene  
77 and Early Pliocene that tropical rainforests started to decrease in range as a result of global  
78 cooling (Hall, 2012; Zachos et al., 2001). Lower sea levels, cooler temperatures, and  
79 modified rainfall patterns related with the development of continental glaciers during the  
80 Pleistocene (2.6-0.01 Ma) also had a great impact on SEA vegetation setting (Heaney,  
81 1991). Studies of fossil pollen records from the Last Glacial Maximum (20,000 years ago)

82 indicate that SEA vegetation differed substantially from that of today, being characterized by  
83 an increase in the extent of montane vegetation and savannah, and by the presence of a  
84 continuous belt of evergreen rainforests across Sundaland (Bird et al., 2005). During the Last  
85 Glacial Period (110,000-11,700 years ago), short warmer interglacial periods also resulted in  
86 raises of the global sea level, which led to the fragmentation of some parts of the Sundaland  
87 into islands and peninsulas; for instance, the Thai-Malay Peninsula, Borneo, Sumatra and  
88 Java were separated from each other every time the sea level rose.

89 The complex geological and climate history and the fragmented island habitats have  
90 raised many questions on the origins of the current biota of SEA. In a comprehensive study,  
91 de Bruyn et al. (2014) reviewed previous biogeographical works by conducting meta-  
92 analyses of geological, climatic and biological data. Based on inferences of colonization  
93 routes and ancestral areas derived from meta-analyses of phylogenetic data, they inferred  
94 that Borneo and Indochina acted as major evolutionary hotspots during the Cenozoic. One of  
95 the reasons invoked is the length of their emergent histories (more than 80 million years),  
96 which surpasses by far those of other regions in SEA. De Bruyn et al. (2014) also found out  
97 that within-area diversification (*in situ* diversification) and subsequent emigration played a  
98 major role in Borneo and Indochina, especially during the course of the Neogene and  
99 Quaternary sea-level fluctuations.

100 To investigate biogeographic and species diversification patterns in SEA, we use a  
101 species-rich clade of crickets from the subfamily Eneopterinae, the genus *Cardiodactylus*  
102 Saussure, as a model system. Eneopterinae crickets are mostly distributed in tropical areas  
103 (Vicente et al., 2017) and are characterized by a diversity of traits in relation with acoustic  
104 communication (e.g., Robillard et al., 2007, 2013; ter Hofstede et al., 2015). With 82 known  
105 species, *Cardiodactylus* is currently the most speciose eneopterine genus. It is also the most  
106 widespread one, as its distribution runs from Japan (northern Ryukyu Islands), to the coasts  
107 of Southeast Asia, Northern Australia and the archipelagos of the Western Pacific across the  
108 Caroline Islands, Fiji, Indonesia, New Caledonia, Palau, Papua New Guinea, the Philippines,  
109 the Samoan Islands, the Solomon Islands, the Mariana Islands, Tonga, Vanuatu and Wallis

110 and Futuna (Otte, 2007; Robillard and Ichikawa, 2009; Robillard et al., 2014). The genus is  
111 subdivided in two species groups, *Efordi* (22 known species) and *Novaeguineae* (60 known  
112 species), which show contrasted patterns of geographical distributions. Only one species of  
113 the *Efordi* group is distributed in SEA; the other species are distributed in New Guinea and in  
114 archipelagoes of the Southwest Pacific. In contrast, the *Novaeguineae* species group has a  
115 wider distribution, and is well diversified in SEA (35 species are found in SEA: Dong and  
116 Robillard, 2016; Robillard et al., 2014). Interestingly, the distribution map of the  
117 *Novaeguineae* group indicates that species richness is inconsistent with landmass sizes (see  
118 details in Figure 1). For example, only one species occurs in the northern part of Indochina  
119 (*Cardiodactylus guttulus*, distributed from Japan to Northern Vietnam), while four species are  
120 endemic to Sulawesi. Some species are not endemic to a single island; for example, *C.*  
121 *empagatao* is found in the Philippines and Sulawesi, and *C. borneoe* is widely distributed in  
122 Borneo and in the Thai-Malay Peninsula. Disentangling the origin of such diverse distribution  
123 patterns thus calls for the need of a thorough biogeographical study of the genus.

124 According to the study of Vicente et al. (2017) on Eneopterinae the genus  
125 *Cardiodactylus* did not originate in SEA but in the Southwest Pacific; however, this inference  
126 was potentially biased by the settings of the analysis in terms of time slices, and by the fact  
127 that it relied on a sparse sampling for the genus (only six *Cardiodactylus* species were  
128 sampled). Here, we use a more comprehensive sampling (41 *Cardiodactylus* species) for the  
129 genus and more appropriate time slices to infer the biogeographic patterns and  
130 diversification dynamics of the genus using a time-calibrated species tree. This allows us to  
131 assess with more precision the dynamics of diversification of the genus, and to determine  
132 whether Borneo and Indochina played a major role in its diversification.

133

## 134 **2. Materials and methods**

### 135 *2.1. Taxon sampling*

136 The taxon sampling of *Cardiodactylus* is focused on species distributed in SEA, but also  
137 includes representatives of the whole distribution and taxonomic diversity of the genus. In

138 this study, we sampled 113 individuals representing 41 species of *Cardiodactylus* crickets,  
139 including 28 species from SEA and 13 species from New Guinea and Southwest Pacific  
140 archipelagoes (New Caledonia, Solomon Islands and Vanuatu). For outgroup selection, we  
141 referred to a previous study (Anso et al., 2016), and selected 22 species representing all five  
142 tribes of the Eneopterinae subfamily, as well as two more distant species belonging to the  
143 subfamily Gryllinae. Detailed information on specimens is presented in Appendix S1.

144 Most specimens were collected during recent fieldworks and through collaborative  
145 works in several countries in SEA. In addition, some specimens used in the current study  
146 were obtained from the following institutions: the ‘Muséum d’Histoire Naturelle de Genève’  
147 (MHNG), the ‘Muséum National d’Histoire Naturelle, Paris’ (MNHN), the ‘Museum  
148 Zoologicum Bogoriense, Bogor’ (MZB), the ‘Nationaal Natuurhistorisch Museum, Leiden’  
149 (RMNH), the ‘Natural History Museum, London’ (BMNH), the ‘Naturhistorisches Museum,  
150 Vienna’ (NHMW), the ‘Royal Belgian Institute of Natural sciences, Brussels’ (RBINS), and the  
151 ‘Zoological Institute, Russian Academy of Sciences, Saint Petersburg’ (ZIN).

152

### 153 *2.2. DNA extraction, amplification and sequencing*

154 The molecular work was performed at the ‘Service de Systématique Moléculaire’ of the  
155 MNHN. Whole genomic DNA was extracted from the median/hind femora of dried or alcohol-  
156 preserved specimens using the NucleoSpin® 96 Tissue Kit (Macherey-Nagel, Germany) and  
157 an automatic pipetting robot Eppendorf epMotion® 5075 TMX. Five mitochondrial markers  
158 and four nuclear markers used in previous phylogenetic studies on crickets (Anso et al.,  
159 2016; Chintauan-Marquier et al., 2016; Nattier et al., 2011, 2012; Robillard and Desutter-  
160 Grandcolas, 2006) were amplified and sequenced. Mitochondrial markers were partial  
161 fragments of two non-protein coding(12S ribosomal RNA (12S), 16S ribosomal RNA (16S)),  
162 and three protein-coding, (cytochrome c oxidase subunit I (COI), cytochrome c oxidase  
163 subunit II (COII) and cytochrome b (Cytb)) genes. Nuclear markers included partial  
164 fragments of elongation factor 1 alpha (EF1a), histone H3 (H3), 18S ribosomal subunit (18S)  
165 and 28S ribosomal subunit (28S). The amplified fragment of EF1a consisted of both protein-

166 coding and non-protein coding regions whereas the amplified fragment of H3 only consisted  
167 of protein-coding regions. Whenever possible, we obtained molecular data from the same  
168 previous voucher specimens. We used the primers and settings detailed in Anso et al.  
169 (2016), Nattier et al. (2011) and Chintauan-Marquier et al. (2016). All sequences obtained in  
170 this study were cleaned, checked for sequencing errors and pseudogenes (through BLAST  
171 searches, DNA sequences and amino acid translation alignments and inference of gene  
172 trees), and deposited in GenBank (see details in Appendix S1). The COI sequences for all  
173 sequenced specimens of *Cardiodactylus borneoe* were discarded because of suspicion of  
174 pseudogenes. The complete combined dataset consisted of 4,111 aligned base pairs (bp) for  
175 145 terminals: 528 bp for 16S, 419 bp for 12S, 706 bp for COI, 340 bp for COII, 345 bp for  
176 Cytb, 653 bp for 18S, 375 bp for 28S, 327 bp for H3 and 405 bp for EF1a.

177

### 178 2.3. Phylogenetic analyses

179 To check for possible contaminations and artifacts, preliminary phylogenetic analyses were  
180 carried out for each marker using the IQ-TREE web server (<http://iqtree.cibiv.univie.ac.at/>;  
181 Trifinopoulos et al., 2016) (see the resulting gene trees in Appendix S5). Then the aligned  
182 sequences of all nine markers were concatenated in Geneious R8.1.4 (Biomatters Ltd., New  
183 Zealand, [www.geneious.com](http://www.geneious.com)).

184 The concatenated dataset was then analyzed using Bayesian inference (BI) and  
185 maximum likelihood (ML). For both BI and ML we used PartitionFinder V2.1.1 (Lanfear et al.,  
186 2017) to determine best-fit partitioning schemes and the associated substitution models. One  
187 partition was specified for each of the non-protein coding genes (12S, 16S, 18S and 28S)  
188 and one partition per codon for the protein-coding genes (COI, COII, Cytb and H3), with the  
189 exception of EF1a which included several protein-coding and non-protein coding regions. For  
190 the latter we only used one partition to avoid specifying too many small partitions for the  
191 protein-coding and non-protein coding regions. PartitionFinder analyses were further carried  
192 out using the default ‘greedy’ algorithm option and either the ‘mrbayes’ or ‘raxml’ set of  
193 models (for BI and ML analyses, respectively); we also used the ‘linked branch lengths’

194 option, in order to limit the risk of overparameterization by lowering the number of inferred  
195 partitions. The Bayesian information criterion (BIC) was preferentially used to compare  
196 partitioning schemes and substitution models following Ripplinger and Sullivan (2008).

197 Bayesian inference analyses were performed with MrBayes 3.2.6 (Ronquist et al.,  
198 2012) whereas ML analyses were performed with RAxML 8.2.8 (Stamatakis, 2014) and IQ-  
199 TREE 1.6.2 (Nguyen et al., 2015). All corresponding analyses were performed using the  
200 CIPRES Science Gateway 3.3 (Miller et al., 2015).

201 For ML analyses best-scoring trees were obtained using heuristic searches relying on  
202 100 random-addition replicates. Clade support was assessed using non-parametric bootstrap  
203 (for both RAxML and IQ-TREE analyses); for each analysis 1,000 bootstrap replicates were  
204 conducted. Nodes supported by bootstrap support values (BS)  $\geq$  70% were considered  
205 strongly supported following Hillis and Bull (1993).

206 For BI analyses we conducted two independent runs with eight Markov chain Monte  
207 Carlo (MCMC): one cold and seven incrementally heated that ran for 50 million generations  
208 with trees sampled every 1,000 generations. We used a conservative burn-in of 12.5 million  
209 generations per run after checking for stability on the log-likelihood curves and the split-  
210 frequencies of the runs in Tracer v.1.7 (Rambaut et al., 2014). Support of nodes for MrBayes  
211 analyses was provided by clade posterior probabilities (PP) as directly estimated from the  
212 majority-rule consensus topology. A clade with a PP value higher than 0.95 was considered  
213 as well supported following Erixon et al. (2003). Whenever a *Cardiodactylus* species (for  
214 which multiple specimens were sequenced) or a specific taxonomic group of interest was  
215 recovered paraphyletic, we used Bayes factors ( $B_F$ ) to assess whether there was statistical  
216 support for their non-monophyly. To do so, specific analyses (in which taxa of interest are  
217 constrained to be monophyletic) were carried out using MrBayes.

218

#### 219 *2.4. Divergence time estimation*

220 We generated a species-level dataset (with one specimen per sampled *Cardiodactylus*  
221 species; see details in Appendix S1) to properly conduct dating and all subsequent analyses

222 (i.e. historical biogeography and diversification analyses). Divergence times were estimated  
223 using Bayesian relaxed clocks as implemented in BEAST 1.8.4 (Drummond et al., 2012).  
224 The partitions/clocks and substitution models were selected under PartitionFinder 2.1.1  
225 following the settings presented above but with the ‘beast’ set of models (see details in Table  
226 1). We were not able to fully implement a two steps strategy recommended by several  
227 authors (e.g., see Foster and Ho, 2017). The first step corresponds to a PartitionFinder  
228 analysis with the partition-rich ‘*linked branch lengths*’ option, to be followed by the use of the  
229 ‘ClockstaR’ R package (Duchêne et al., 2014), which requires having no missing gene  
230 fragments in the dataset; the latter step is expected to reduce the number of clocks in  
231 molecular dating procedures (hence limiting the risk of overparameterization). For  
232 comparison purpose, we nonetheless decided to conduct BEAST analyses with both options  
233 (number of partitions/clocks inferred with either the ‘*linked branch lengths*’ or the ‘*unlinked*  
234 *branch lengths*’ option). BEAST analyses were performed on the CIPRES Science Gateway  
235 using BEAGLE to improve and speed up the likelihood calculation (Ayres et al., 2012; Miller  
236 et al., 2015). For each clock model/partitioning scheme an uncorrelated lognormal relaxed  
237 clock was implemented. The *Tree Model* was set to a birth-death speciation process  
238 (Gernhard, 2008) to better account for extinct and missing lineages. The *ucld.mean* prior of  
239 each clock model was set to an uninformative interval (0.0001-1.0) with a uniform prior  
240 distribution.

241 Based on the available worldwide biogeographical framework of Eneopterinae  
242 crickets (Vicente et al., 2017), three secondary calibration points were enforced using normal  
243 distributions centered on previously estimated median ages: (1) the node for the most recent  
244 common ancestor (MRCA) of *Cardiodactylus* was assigned an interval of 33.60-55.19 Ma  
245 (*normalPrior mean*="42.6" *stdev*="6.0"), (2) the node for the MRCA of the *Novaeguineae*  
246 species group was assigned an interval of 23.32-39.73 Ma (*normalPrior mean*="30.0"  
247 *stdev*="6.0"), and (3) the node for the MRCA of *C. guttulus*, *C. oeroe*, *C. tankara* and *C.*  
248 *singapura* was assigned an interval of 17.83-31.17 Ma (*normalPrior mean*="23.4"  
249 *stdev*="6.0").

250 BEAST analyses consisted of 50 million generations of MCMC with the parameters  
251 and trees sampled every 1,000 generations. A burn-in of 25% was applied after checking the  
252 log-likelihood curves. Trees obtained from distinct analyses were combined using  
253 LogCombiner v1.8.4 (<http://beast.bio.ed.ac.uk/>). The maximum credibility tree, median ages  
254 and their 95% highest posterior density (HPD) were generated with TreeAnnotator v1.8.4  
255 (<https://github.com/beast-dev/beast-mcmc/releases/tag/v1.8.4>).

256

257 *2.5. Ancestral area estimation*

258 The package BioGeoBEARS (Matzke, 2014) implemented in R was used to infer the  
259 biogeographical history of *Cardiodactylus* crickets across SEA. The dispersal-extinction-  
260 cladogenesis (DEC; Ree and Smith, 2008), dispersal-vicariance analysis (DIVA; Ronquist,  
261 1997; herein DIVALIKE) and Bayesian Analysis of Biogeography (BayArea, Landis et al.,  
262 2013; herein BAYAREALIKE) models were used to estimate ancestral areas. Because of  
263 concerns with its statistical validity (Ree and Sanmartín, 2018) we did not use the +J model  
264 of Matzke (2014) in our analyses. The analyses were conducted with the maximum clade  
265 credibility (MCC) tree inferred under BEAST. The geographical distribution of each species  
266 was estimated based on fieldwork data, extant literature, and information provided by  
267 museum specimens (see details in Appendix S1). Twelve operational areas were defined  
268 (see details in Appendix S2) based on the distribution ranges of extant *Cardiodactylus*  
269 crickets (Robillard et al., 2014): Indochina (A), Thai-Malay Peninsula (B), Sumatra (C), the  
270 Philippines (minus Palawan) (D), Palawan (E), Borneo (F), Java (G), Sulawesi (H), Lesser  
271 Sunda Islands (I), Moluccas (J), New Guinea (K) and the archipelagoes in the Southwest  
272 Pacific (L).

273 In previous studies (de Bruyn et al., 2014; Hall, 2011; Morley, 2012), it has been  
274 shown that three major Cenozoic collision events had a great influence on the current  
275 archipelago setting: (1) the India-Asia collision at ca. 45 Ma facilitated the isolation of West  
276 Sulawesi from Sundaland, (2) the Australia-Asia collision at ca. 25 Ma generated the Bird's  
277 Head region of New Guinea, and (3) the collision of the Sula Spur promontory with the

278 Southeast Asian margin in Sulawesi ca. 15 Ma formed the region now known as Wallacea  
279 (Hall, 2009a). To account for these major geological events, three distinct time slices were  
280 enforced in our time-stratified biogeographical model; the first time slice runs from 45.0 to  
281 25.0 Ma, the second one from 25.0 to 15.0 Ma and the last one from 15.0 Ma to the present  
282 (Hall, 2013; Hall and Sevastjanova, 2012; see more details in Appendix S2). For each time  
283 slice, we constructed a basal matrix of scaling factors (multipliers) (0, 0.01, 0.1, 0.25, 0.50,  
284 0.75, 1.0) for the dispersal rates between areas according to their geographical position and  
285 changes in sea level. Alternative and more simplified sets of multipliers were also tested (0,  
286 0.01, 0.1, 0.25, 1.0; 0, 0.01, 0.1, 0.50, 1.0; and 0, 0.01, 0.1, 0.75, 1.0). Analyses were  
287 repeated with two, three or four maximum ancestral areas (parameter *max\_range\_size* in  
288 BioGeoBEARS). Therefore, a total of 36 processes (four distinct multipliers sets, three  
289 speciation models (DEC, DIVALIKE and BAYAREALIKE), three distinct maximum range  
290 sizes), were implemented to estimate ancestral areas (the details of these processes are  
291 listed in Appendix S2 and S3).

292 Finally, to ensure that the time framework imposed by the secondary calibration does  
293 not constrain the biogeographical results through strong constraint on allowed areas and  
294 dispersal multipliers, we implemented nine additional processes without time slices  
295 (unstratified analyses) using the basal set of multipliers with three speciation models and  
296 three distinct maximum ancestral areas (see Appendix S3).

297

#### 298 2.6. Colonization events and *in situ* diversification

299 As mentioned above, only one member of the *Efordi* species group is distributed in SEA; in  
300 contrast, the *Novaeguineae* species group is more widely distributed, including in SEA, New  
301 Guinea and the Southwest Pacific. Therefore, we study colonization events and *in situ*  
302 diversification events of *Cardiodactylus* in SEA by focusing on the *Novaeguineae* species  
303 group. Within this clade, major colonization routes were inferred for each time slice.  
304 Emigration and immigration events for each area were analyzed by summarizing colonization

305 events using SPSS Statistics 22 (SPSS Inc.). We also followed de Bruyn et al. (2014) to  
306 estimate *in situ* diversification events using SPSS Statistics v.22 (SPSS Inc.).

307

308 *2.7. Diversification analyses*

309 Bayesian Analysis of Macroevolutionary Mixtures 2.5 (BAMM; Rabosky et al., 2013) was  
310 used: (1) to estimate rates of speciation ( $\lambda$ ), extinction ( $\mu$ ), and net diversification ( $\gamma$ ) either for  
311 all *Cardiodactylus* species or only for the SEA species belonging to the *Novaeguineae*  
312 species group (which constitutes a monophyletic group), (2) to conduct rate-through-time  
313 analysis of these rates, and (3) to identify and visualize shifts in species rates across the  
314 *Cardiodactylus* phylogeny. BAMM accounts for non-random and incomplete taxon sampling  
315 in the phylogenetic trees by allowing all non-sampled species to be associated with a  
316 particular tip or more inclusive clade. Species numbers were obtained from the ‘Orthoptera  
317 species file online’ website (Cigliano et al., 2017) and published sources.

318 Priors for BAMM were generated using the R package BAMMtools v.2.5.0 (Rabosky  
319 et al., 2014a,b) by providing the BEAST maximum clade credibility tree and the total species  
320 numbers across *Cardiodactylus* (see Appendix S4). We used a gradient of prior values  
321 ranging from 0.1 to 1.0 to test the sensitivity to the prior, to account for the recent debate on  
322 the reliability of BAMM estimates (Moore et al., 2016, but see Rabosky et al., 2017). We ran  
323 BAMM by setting four independent MCMC running for 50 million generations and sampled  
324 every 50,000 generations; convergence was assessed by computing ESS of log likelihoods.  
325 After removing 10% of trees as burn-in, the BAMM output were analyzed with employing  
326 BAMMtools package in R and the 95% credible rate shift configurations was estimated using  
327 Bayes factors. The best shift configuration with the highest maximum a posteriori probability  
328 was estimated in this analysis. Rates-through-time plots were generated for speciation ( $\lambda$ ),  
329 extinction ( $\mu$ ) and net diversification ( $\gamma$ ), either for all *Cardiodactylus* species or only for the  
330 SEA species. All visualization was performed using R and C code available through the R  
331 package BAMMtools.

332

333 **3. Results**

334 *3.1. Data collection and phylogenetic analyses*

335 The best-fit partition schemes and substitution models used in BI and ML analyses of the  
336 combined dataset are showed in Table 1. Both BI and ML phylogenetic analyses yielded  
337 robust and largely congruent topologies (Figure 2; see also Appendix S6 for original outputs  
338 of both BI and ML analyses); it is especially the case for the results of RAxML analyses  
339 which are presented in Figure 2 (90% of nodes within *Cardiodactylus* supported by  $BV \geq$   
340 70%). In all analyses the subfamily Eneopterinae and the genus *Cardiodactylus* are  
341 recovered as monophyletic with a high support ( $BS_{RAxML}$  of 100%, PP of 1.0 and  $BS_{IQ-TREE}$  of  
342 100% and 76%, for Eneopterinae and *Cardiodactylus*, respectively). All *Cardiodactylus*  
343 species are also recovered as monophyletic, with the exception of *C. floresiensis*. However,  
344 additional analyses carried out under BI do not support the paraphyly of *C. floresiensis*:  
345 MCMC runs where *C. floresiensis* representatives are constrained to be monophyletic yield a  
346 harmonic mean estimate of -50151.29 versus -50150.18 for the unconstrained MCMC runs;  
347 hence the difference corresponds to a non-statistically significant  $B_F$  of 2.22 ( $B_F < 10$ ; see  
348 Kass and Raftery, 1995).

349 Within *Cardiodactylus*, the monophyly of the *Novaeguineae* species group is strongly  
350 supported in both analyses ( $BS_{RAxML/IQ-TREE}$  of 100%, PP of 1.0). By contrast, the *Efordi*  
351 species group is recovered as paraphyletic in all analyses due to the placement of *C.*  
352 *javarere* and *C. enkraussi*. *Cardiodactylus javarere* is found as sister to the *Novaeguineae*  
353 species group, forming a well-supported clade ( $BS_{RAxML}$  of 97%,  $BS_{IQ-TREE}$  of 78%, PP of 1.0).  
354 Both RAxML and MrBayes analyses recover *Cardiodactylus enkraussi* as sister to the clade  
355 (*C. javarere* + *Novaeguineae* species group), but its position is less robust ( $BS_{RAxML}$  of 85%,  
356 PP of 0.73); with IQ-TREE *C. enkraussi* is grouped with *C. niugini*, this clade being the  
357 sister group of *C. javarere* + *Novaeguineae* species group, with a very weak support ( $BS_{IQ-$   
358  $TREE}$  of 34% and 24% for the two corresponding nodes). Both RAxML and MrBayes analyses  
359 indicate that the remaining species of the *Efordi* species group constitute a well-supported  
360 clade ( $BS_{RAxML}$  of 78% and PP of 0.96) whereas IQ-TREE analyses infer two distinct

361 lineages, due to the placement of *C. enkraussi* (see above). Additional analyses carried out  
362 under BI support the paraphyly of the *Efordi* species group: MCMC runs where members of  
363 the *Efordi* species group are constrained to be monophyletic yield a harmonic mean estimate  
364 of -50162.07 versus -50150.18 for the unconstrained MCMC runs. Hence the difference  
365 corresponds to a statistically significant  $B_F$  of 21.68 ( $B_F > 10$ ; see Kass and Raftery, 1995).

366 Within the *Novaeguineae* species group, *C. haddocki* and *C. novaeguineae* form a  
367 robust clade (BS<sub>RAXML/IQ-TREE</sub> of 100%, PP of 1.0), sister to another well-supported clade  
368 (BS<sub>RAXML</sub> of 99%, BS<sub>IQ-TREE</sub> of 66%, PP of 1.0) comprising all the remaining species of the  
369 group. Within this clade, three species are the first lineages to branch off, sister to the  
370 remaining species of the group; these three species correspond to two species distributed in  
371 New Guinea (*C. lucus* and *C. maaei*) and one in the Western Pacific (*C. tankara*). The  
372 remaining members of the species group form a generally well-supported clade (BS<sub>RAXML</sub> of  
373 76%, PP of 0.97; but BS<sub>IQ-TREE</sub> of only 18%), which splits into two main clades (hereby  
374 referred as clade 1 and clade 2 on Figure 2). Clade 1 is generally well supported (BS of 84%,  
375 PP of 1.0; but BS<sub>IQ-TREE</sub> of only 40%) and consists of lineages that are also well supported  
376 (see Figure 2 for details). Clade 2 is only moderately supported, with low BS (BS<sub>RAXML</sub> of  
377 40%, BS<sub>IQ-TREE</sub> of 19%) and a moderate support under BI (PP of 0.91). Within clade 2, two  
378 main clades (clade 3 and clade 4) can be distinguished. All species belonging to the clade 4  
379 are distributed in SEA, whereas only two species (*C. manus* and *C. quatei*) are not  
380 distributed in SEA in clade 3.

381

382 *3.2. Divergence time estimation*

383 BEAST analyses relying on the 11 partitions/clocks selected through the use of the '*linked*  
384 *branch lengths*' option did not converge, as underlined by low ESS values (below 200) for 53  
385 parameters. On the contrary BEAST analyses relying on the two partitions/clocks selected  
386 through the use of the '*unlinked branch lengths*' option converged quickly, with all  
387 parameters showing ESS values  $\geq 200$ . As a result, we only present and discuss the results  
388 of the latter analyses in our study. The resulting median ages are presented in Figure 3 and

389 the original output results (including those of the analyses with low ESS values) in Appendix  
390 S7. Age estimates for the genus *Cardiodactylus* suggest an origin in the Middle Eocene ca.  
391 43.2 Ma (95% HPD: 33.47-52.93 Ma). The members of the *Efordi* species group form a  
392 monophyletic group, except *C. javarere*, which is recovered as sister to the *Novaeguineae*  
393 species group. Members of the *Efordi* species group apparently started their diversification in  
394 the Late Eocene about 41.0 Ma (95% HPD: 29.22-48.83 Ma). The lineage leading to *C.*  
395 *javarere* then diverged from the *Novaeguineae* species group ca. 39.1 Ma, while members of  
396 the *Novaeguineae* species group started diversifying during the Late Oligocene about 27.0  
397 Ma (95% HPD: 20.39-33.67 Ma). The divergence time for the MRCA of *C. haddocki* and *C.*  
398 *novaeguineae*, which are sister to the remaining members of the *Novaeguineae* species  
399 group, is inferred at ca. 8.4 Ma (95% HPD: 5.18-11.84 Ma), at the end of the Miocene. Most  
400 speciation events within the *Novaeguineae* species group happened during the Miocene (ca.  
401 23.0-5.3 Ma). Only a few lineages appear to have diverged recently (less than 4 Ma).

402

### 403 3.3. Ancestral area estimation

404 DIVALIKE model shows higher statistical support over the DEC and BAYAREA models for all  
405 tested dispersal multiplier matrices (see more details in Appendix S3). Furthermore, the  
406 matrix of scaling factors involving five distinct rates (0, 0.01, 0.25, 0.5, 0.75, 1.0)  
407 implemented with a DIVALIKE model and a maximum range size of two areas was supported  
408 as the best-fit model over more simplified sets of multipliers and more allowed areas; the  
409 corresponding ancestral areas estimation is presented in Figure 3. Analyses without time  
410 slices (unstratified analyses) result in the same biogeographical pattern (see more details in  
411 Appendix S3) in SEA *Novaeguineae* species group, but it inferred an origin in New Guinea  
412 for the genus *Cardiodactylus* and for the *Efordi* species group. However, according to Hall's  
413 work (2009, 2013), New Guinea only began to emerge about 25 Ma; therefore, a New  
414 Guinea origin of *Cardiodactylus* ca. 43 Ma is not compatible with geological evidences. The  
415 latter illustrates the importance of using stratified analyses to account for geological changes  
416 through time; hence for our study we only focus on the results inferred with the stratified

417 analysis relying on the inferred best-fit model (DIVALIKE model with five distinct rates and a  
418 maximum range size of two areas).

419 Ancestral areas estimation suggests an origin of *Cardiodactylus* in the Southwest  
420 Pacific during the Middle Eocene, followed by a complex and dynamic biogeographical  
421 history. Lineages belonging to the *Efordi* species group diverged earlier (ca. 40 Ma) than the  
422 *Novaeguineae* species group (ca. 27 Ma) and colonized New Guinea several times, twice  
423 independently, after 37.1 Myrs (*C. niugini*) and 39.1 Myrs (*C. javarere*), and twice  
424 independently after 22.5 Myrs (*C. busu* and *C. nobilis*).

425 The members of the *Novaeguineae* species group colonized New Guinea four times  
426 from the Southwest Pacific: twice at the end of the Oligocene (once after 24.0 Myrs (*C. lucus*)  
427 and once ca. 22.1 Ma (main clade in SEA), and twice more recently, ca. 8.4 Ma for the clade  
428 made of (*C. haddocki* + *C. novaeguineae*). From New Guinea, *Cardiodactylus* independently  
429 colonized SEA three times: the first one linked New Guinea to SEA through the Philippines  
430 ca. 19.5 Ma; the second one through Sulawesi ca. 16.4 Ma; a third colonization of SEA from  
431 New Guinea occurred more recently, during the Middle Miocene, through Java and the  
432 Lesser Sunda Islands ca. 13 Ma.

433 Through the first passageway, *Cardiodactylus* colonized Palawan after 19 Myrs  
434 through the Philippines, then the Thai-Malay Peninsula and Borneo. *Cardiodactylus*  
435 colonized Indochina twice recently, once from the Thai-Malay Peninsula, ca. 4 Ma (*C.  
436 thailandia*) and once from the Philippines ca. 5 Ma (*C. guttulus*). Meanwhile a lineage from  
437 the Thai-Malay Peninsula dispersed to Borneo after 3.4 Myrs.

438 From the Philippines, *Cardiodactylus* also colonized the Moluccas (*C. halmaheira*)  
439 after 17 Myrs, and recently dispersed to Sulawesi (*C. empagatao*). After colonizing Borneo  
440 ca. 15 Ma, the genus colonized Sumatra ca. 12 Ma and reached Java through Sumatra ca. 8  
441 Ma.

442

443 3.4. Colonization routes, emigration / immigration events and in situ diversification

444 Colonization routes of the *Novaeguineae* species group are presented in Figure 4a. Before  
445 the Miocene, as deduced from our biogeographical analyses, no colonization event  
446 happened. During the Miocene, 10 distinct colonization routes are inferred; interestingly New  
447 Guinea is recovered as a major biogeographical crossroad (four different routes are inferred,  
448 to Java, Sulawesi, the Lesser Sunda Island and the Philippines), followed by the Philippines  
449 (three routes), the Southwest Pacific (two routes), and Borneo and Sumatra (one route each).  
450 Along these routes, colonization events from the Southwest Pacific to New Guinea happened  
451 twice. During the Plio-Pleistocene eight colonization routes are identified: three depart from  
452 the Philippines; two depart from New Guinea, and two from the Thai-Malay; and one goes  
453 from the Southwest Pacific to New Guinea.

454 Estimated emigration and immigration events through time are presented in Figure 4b.  
455 When summing the total numbers of events for each area, six areas only had immigration  
456 events inferred (Indochina, Java, the Lesser Sunda Islands, Palawan, Sulawesi and the  
457 Moluccas). The total number of inferred emigration events is higher than that of immigration  
458 events for New Guinea, the Philippines, the Southwest Pacific and the Thai-Malay Peninsula,  
459 while the opposite (more immigration than emigration events) is inferred only for Borneo.  
460 Moreover, the total number of emigration and immigration events is at equilibrium only for  
461 Sumatra.

462 *In situ* diversification events through time are presented in Figure 4c. When summing  
463 the total numbers of events for each area, three areas (New Guinea, Sulawesi and the  
464 Philippines) are associated with the highest number of *in situ* diversification events (four  
465 events), followed by the Lesser Sunda Islands and the Thai-Malay Peninsula (three events),  
466 Sumatra and the Southwest Pacific (two events) and Borneo (one event).

467

### 468 3.5. Diversification analyses

469 A *poissonRatePrior* of 0.5 was recovered as the best-fit prior by BAMMtools (see more  
470 details in Appendix S10). Convergence of the MCMC chains in the BAMM analyses was  
471 observed after discarding the burn-in period (ESS > 900 for both the number of shifts and log

472 likelihoods). The 95% credible set of rate shift configurations sampled with BAMM provides  
473 more support (probability of 0.36) for a scenario without shifts in diversification rates within  
474 *Cardiodactylus* (Figure 5); less supported scenarios (probabilities of 0.16, 0.17 and 0.17)  
475 inferred a single shift in diversification rates near the base of the *Novaeguinae* species group  
476 (the placement of the shift differs, as illustrated in Figure 5). BAMM analyses strongly support  
477 a diversity-dependent speciation process across *Cardiodactylus* with the following rates: (1)  
478 net diversification rate of 0.06 species/Myr (95% quantile=0.023-0.071), (2) speciation rate of  
479 0.12 species/Myr (95% quantile=0.075-0.202), and (3) extinction rate of 0.06 species/Myr  
480 (95% quantile=0.003-0.170). Rate-through-time plots for the three corresponding rates are  
481 presented in Figure 6, for the whole genus and within the *Novaeguineae* species group. The  
482 resulting plots indicate that *Cardiodactylus* speciation and net diversification rates have  
483 decreased through time, with the exception of an increase in speciation and net  
484 diversification rates occurring from 20.0 to 15.0 Ma. By contrast, the inferred extinction rates  
485 are quite constant and relatively low. A similar trend was recovered in the *Novaeguineae*  
486 species group. For the whole genus, speciation and net diversification rates rised slowly with  
487 several fluctuations between the Late Oligocene (ca. 26 Ma) and the Middle Miocene (ca. 15  
488 Ma) (Figure 6a). These tendencies are similar for the *Novaeguineae* species group, with a  
489 sharper peak during the Early Miocene (ca. 18-23 Ma) (Figure 6b).

490

#### 491 **4. Discussion**

##### 492 *4.1. Phylogenetic relationships*

493 Both BI and ML analyses recovered a similar placement of the genus *Cardiodactylus* within  
494 the subfamily Eneopterinae in the tribe Lebinthini (Figure 2), as in previous studies (Anso et  
495 al., 2016; Nattier et al., 2011; Robillard and Desutter-Grandcolas, 2004, 2006; Vicente et al.,  
496 2017). Within *Cardiodactylus*, we were able to assess the status of the two species groups  
497 defined by Otte (2007) on morphological grounds.

498 Our results clearly support the monophyly of the species group *Novaeguineae* and  
499 the paraphyly of the *Efordi* species group (-50150.18 versus -50162.0,  $B_F$  of 21.78;  $B_F > 10$ ).  
500 The paraphyly of the latter can be accounted for by the placement of two species: *C. javarere*  
501 and *C. enkraussi*. When using  $B_F$  we found out that the placement of *C. enkraussi* outside of  
502 the *Efordi* species group is not statistically supported (harmonic mean estimate of -50150.18  
503 versus -50151.98,  $B_F$  of 3.6;  $B_F < 10$ ); it is also the case for *C. javarere* (harmonic mean  
504 estimate of -50150.18 versus -50149.44;  $B_F$  of 1.48,  $B_F < 10$ ). Further molecular analyses with  
505 a denser sampling will be necessary to reach a stable conclusion on the status of the *Efordi*  
506 species group. Within the *Novaeguineae* species group, our results strongly support a clade  
507 grouping *C. novaeguineae* and *C. haddocki* as the sister group of all remaining species of  
508 the group. When comparing results of BI and ML analyses, similar relationships are inferred  
509 within the species group, except for the positions of *C. manus* and *C. quatei*, perhaps as a  
510 consequence of missing taxa from New Guinea and the Southwest Pacific. Nevertheless, the  
511 species distributed in SEA are clearly nested within a clade including species from New  
512 Guinea and the Southwest Pacific.

513

#### 514 4.2. Origin of *Cardiodactylus* in the Southwest Pacific

515 Our study estimated the divergence time and ancestral areas of *Cardiodactylus* by  
516 implementing secondary calibrations based on the study of Vicente et al. (2017), which  
517 inferred that *Cardiodactylus* diverged from its sister clade within the tribe Lebinthini in SEA.  
518 As a result, similar age estimates for the MRCA of *Cardiodactylus* were recovered: 43.2 Ma  
519 in our study vs. 42.57 Ma in the study of Vicente et al. (2017). Secondary calibrations may be  
520 a source of bias in dating procedures (Graur and Martin, 2004; Schenk, 2016); however, it is  
521 worth highlighting that another study (relying on a larger phylogenetic context) using a  
522 different set of secondary calibrations gave a similar age range for *Cardiodactylus* (Anso et  
523 al., 2016).

524 All DIVALIKE stratified analyses infer an origin for *Cardiodactylus* in the Southwest  
525 Pacific; it is also the case for all DEC stratified analyses and some of the BAYAREA stratified  
526 analyses. This result seems to conflict with the widely accepted assertion that less diverse  
527 island communities are easier to invade (Bellemain and Ricklefs, 2008). However, the global  
528 biogeographical history of the tribe Lebinthini, as inferred by Vicente et al. (2017), suggests  
529 that *Cardiodactylus* diverged from its sister clade in SEA before colonizing the islands of the  
530 Southwest Pacific during the Middle Eocene. During that time, the species richness in SEA  
531 was likely much higher than that of the Southwest Pacific. The genus probably first occurred  
532 in islands now under water, since many islands in this region had not emerged yet (e.g., the  
533 Solomon and Fiji Islands) or were just coral reef formations (i.e. New Caledonia; Neall and  
534 Trewick, 2008). In fact, the origin of *Cardiodactylus* in the Southwest Pacific and its recent  
535 recolonization of SEA support the “reverse colonization” hypothesis (from small Pacific  
536 islands back to continent) as presented in Bellemain and Ricklefs (2008). This hypothesis  
537 was recently supported by several studies of other insect clades, such as in *Polyura*  
538 butterflies (Toussaint and Balke, 2016) and *Camponotus* ants (Clouse et al., 2015), while it  
539 was not recovered for other clades (Economou et al., 2015). Our results consequently bring  
540 some new insights into the discussion of Pacific island biogeography and of the role of  
541 Pacific clades in contribution to the diversity of surrounding archipelagoes (e.g., Claridge et  
542 al., 2017). In the case of *Cardiodactylus*, additional studies with a denser sampling of the  
543 species distributed in the archipelagoes of the Southwest Pacific will be necessary to precise  
544 their origin in the Southwest Pacific. As a reminder, our conclusions are based on ca. 50% of  
545 the species of *Cardiodactylus* only. Consequently, some conclusions are likely to change as  
546 our knowledge on this genus will continue improving and be further implemented in future  
547 biogeographical studies.

548

#### 549 4.3. New Guinea as a corridor between the Southwest Pacific and SEA

550 During the period ranging from its origin in the Middle Eocene to the collision between  
551 Australia and Asia (ca. 25 Ma), there is no evidence that *Cardiodactylus* colonized any area

552 other than New Guinea (Figure 3). Our results inferred colonization events from the  
553 Southwest Pacific to New Guinea after the emergence of the Bird's Head region of New  
554 Guinea (ca. 25 Ma). New Guinea thus appeared to have been a significant corridor between  
555 the Southwest Pacific and SEA, even if this aspect of the biogeography of *Cardiodactylus* is  
556 likely not yet addressed with a sufficient taxonomic sampling.

557 Two independent colonization events of SEA from New Guinea are inferred before  
558 the emergence of the Wallacea (ca. 15 Ma), and a third colonization event occurred  
559 afterward immediately (ca. 13 Ma). This result is consistent with the dispersal route  
560 documented in flightless beetles, which crossed Lydekker's line from New Guinea and  
561 reached the Moluccas ca. 5 Ma (Tanzler et al., 2016). *Cardiodactylus* initially departed from  
562 New Guinea and colonized SEA by crossing the Wallace line, which is a good example of  
563 faunal boundaries permeation between Wallace's line and Lydekker's line (Lohman et al.,  
564 2011). It was also found in other insect groups: Müller et al. (2013) inferred that colonization  
565 events happened several times between Wallacea and New Guinea in Pieridae butterflies;  
566 similarly, Kalkman et al. (2018) found that the Odonate family Argiolestidae colonized  
567 Sulawesi from the north of Australia.

568

569 *4.4. Colonization routes from east to west in SEA and priority of adjacent area in colonization*  
570 *routes*

571 *Cardiodactylus* colonized SEA three times independently from east to west across New  
572 Guinea, through four different passageways: the Philippines, Sulawesi, the Lesser Sunda  
573 Islands and Java.

574 The colonization of SEA through the Philippines occurred during the early Miocene (ca.  
575 19 Ma), when the Philippines (minus Palawan), a true oceanic island archipelago, began to  
576 emerge, initially scattered along the margin of the Philippine Sea Plate (Yumul et al., 2004).  
577 From the Philippines, the genus rapidly dispersed to the rest of the region. It also colonized  
578 Sulawesi twice, first ca. 16.4 Ma, then recently as a range expansion of *C. empagatao*.

579       The colonization of SEA through Sulawesi ca. 16.4 Ma was followed by subsequent *in*  
580       *situ* diversification within this island. This is consistent with the “predominantly tectonic  
581       dispersal origin” of 20 taxa in Sulawesi, as shown by the review of Stelbrink et al. (2012)  
582       based on 27 animal datasets: in this study, the authors inferred that speciation on Sulawesi  
583       did not occur before the Miocene, which is consistent with geological evidence indicating an  
584       increase of landmasses along with more heterogeneous landscapes (Hall, 2009b).

585       During the Late Miocene, colonization events occurred less frequently and were only  
586       confined to adjacent areas: the Thai-Malay Peninsula / Indochina, Java / Sumatra, the  
587       Philippines / Indochina (Figure 3 and Figure 4a). However, the frequent transgressing events  
588       along the Wallace’s line (or the modified Huxley’s line) documented in the beetle genus  
589       *Rhantus* and the avian family Campephagidae (Lohman et al., 2011), were not found in  
590       *Cardiodactylus*. These results are consistent with the conclusions on flightless weevils  
591       (Tänzler et al., 2016), which showed that the Sunda Arc (region including Borneo, Java and  
592       Sumatra) could be a potential dispersal corridor between mainland SEA and Melanesia  
593       through its continuous chain of islands.

594       The study of de Bruyn et al. (2014) inferred that colonization events happened more  
595       frequently between adjacent areas than between distant ones. This conclusion is verified in  
596       our study, but it could however be tempered by the fact that the probabilities of transition  
597       amongst our areas were set proportionally to the distance between them.

598

599       4.5. *Weak influence of recent sea level changes on Cardiodactylus diversification dynamics*  
600       The drastic changes of sea level during the Plio-Pleistocene have been considered of greater  
601       influence on species diversification in SEA, through the fragmentation of areas when the sea  
602       level rose and the increasing landmass area when the sea level decreased (Guo et al., 2015;  
603       Lohman et al., 2011). Interestingly, according to the results of BAMM analyses, net  
604       diversification rates of *Cardiodactylus* rose rapidly during the Miocene, and then decreased  
605       before the Plio-Pleistocene (Figure 6). Moreover, inferred colonization events during the Plio-

606 Pleistocene in SEA are far less common than expected. These recent events only happened  
607 from the Philippines to the Moluccas, Palawan and Sulawesi, and from the Thai-Malay  
608 Peninsula to Borneo and Indochina, but they did not generate any detectable diversification  
609 (Figures 3 and 4a). It may indicate that the recent changes of sea level and their  
610 consequences in terms of fragmentation of habitats were not sufficient to establish stable  
611 barriers between the populations, or that the flight abilities of the species prevent speciation  
612 to occur.

613 These results are consistent with the Thai-Malay Peninsula position as a  
614 biogeographic crossroad between Indochina and the Sundaic faunal regions (Borneo, Java  
615 and Sumatra; Lohman et al., 2011). One interesting point in our results is the absence of  
616 inferred immigration of *Cardiodactylus* in Java and Sumatra (Figure 4b in Plio-Pleistocene),  
617 which differs from the conclusion of de Bruyn et al. (2014), where these two areas are  
618 characterized by higher levels of immigration than emigration. This is related with the low  
619 diversity of the genus in these islands, which can in turn be linked with missing knowledge of  
620 the species distributed in large areas of Sumatra and Java, which could not be sampled.

621

#### 622 4.6. Dynamics of diversification through the history of *Cardiodactylus*

623 Our diversification analysis indicates that there was no distinct rate shift within  
624 *Cardiodactylus* and that the speciation rate of the genus changed slowly through time  
625 (Figures 5 and 6). However, when we focus on the diversity in each area of SEA, each  
626 lineage of *Cardiodactylus* shows a contrasted history.

627 According to the meta-analysis implemented by de Bruyn et al. (2014), the diversity of  
628 SEA biota may have arisen through the accumulation of immigrants, by *in situ* diversification,  
629 or by a combination of the two. In our results (Figures 4b and 4c), the highest level of  
630 immigration occurred in Borneo, Indochina, Java, Moluccas and Sulawesi, and to a lesser  
631 extend in the remaining areas.

632       The areas are however characterized by significantly different levels of *in situ*  
633 diversification. There was no event of *in situ* diversification in Indochina, Palawan, Java and  
634 the Moluccas, and only one in Borneo. Sulawesi and the Philippines show the highest level  
635 of *in situ* diversification, followed by the Thai-Malay Peninsula and the Lesser Sunda Islands.  
636 The early colonization of Sulawesi, the Philippine and the Thai-Malay Peninsula from New  
637 Guinea and the fragmentation of these areas from the Miocene to the present day may  
638 explain that the levels of *in situ* diversification are higher compared with other areas. This  
639 result is consistent with the conclusions of de Bruyn et al. (2014), who showed that the level  
640 of *in situ* diversification in ancient areas (originating area) was higher than in others. However,  
641 the higher level of *in situ* diversification found in the Lesser Sunda Islands contrasts with this  
642 conclusion: this group of islands is relatively small and recent, since they emerged during the  
643 Middle Miocene. They partly come from microcontinental fragments sliced from Java or/and  
644 Australia, while some parts of these islands truly emerged from the ocean. During their  
645 history, connections and disconnections between the Lesser Sunda Islands were very  
646 common (Hall, 2009a) and this may have resulted in higher speciation rate. Linking the  
647 complex geological history in the Lesser Sunda Islands easily explains the species diversity  
648 found in this area, despite its recent age and small size. These results suggest that higher  
649 levels of species diversification can be driven by frequent connection and disconnection  
650 between two areas, at least in some parts of the genus distribution. However, we cannot  
651 exclude that this level of *in situ* diversification could partly be linked to a positive sampling  
652 bias, since extensive field work has been done recently in this archipelago, while other  
653 regions of SEA remain less sampled (Robillard et al., 2014). Similarly, the low level of *in situ*  
654 diversification estimated in large islands colonized almost as early as Sulawesi, such as Java  
655 and Borneo, could be explained by biases in taxonomic sampling in these areas.

656       To summarize, the species diversity of *Cardiodactylus* in SEA seemingly results from:  
657 (1) the accumulation of colonizers in Indochina, Palawan, Java and Moluccas, and (2) both  
658 the accumulation of colonizers and *in situ* diversification in the Thai-Malay Peninsula,  
659 Sumatra, the Philippines, Borneo, Sulawesi and the Lesser Sunda Islands.

660

661 **5. Conclusion**

662 In summary, the historical biogeography of *Cardiodactylus* appears to be linked to the early  
663 geological history of SEA. After originating from the Southwest Pacific (diverging from its  
664 sister group among the Lebinthini tribe), *Cardiodactylus* lineages crossed the Lydekker's line  
665 multiple times, but more rarely transgressed the Wallace's line. SEA was colonized three  
666 times independently by members of the *Novaeguineae* species group and once by the *Efordi*  
667 species group. In addition, the New Guinea acted as a major colonization source of  
668 *Cardiodactylus* in SEA from east to west, while the Thai-Malay Peninsula served as an  
669 important corridor between Indochina and Borneo. In addition, Sulawesi served as a  
670 diversification hub for *Cardiodactylus* through a combination of high immigration and *in situ*  
671 diversification events.

672

673 **6. Acknowledgements**

674 We thank Alfried Vogler and two anonymous reviewers for numerous valuable comments  
675 and suggestions on a previous version of the manuscript. This work was conducted in the  
676 context of the PhD thesis of JD, which was funded by China Scholarship Council (CSC), the  
677 Innovation Funds of Graduate Programs of Shaanxi Normal University [2012CXB019], the  
678 National Science Foundation of China [Grant No. 31402006] and a supporting grant from "La  
679 Société des Amis du Muséum" and the Institut de Systematique, Evolution, Biodiversité  
680 (ISYEB). NV was supported by the post-doc funding "CNPq - Conselho Nacional de  
681 Desenvolvimento Científico e Tecnológico [Processo: 164922/2017-2]" in Brazil. Laboratory  
682 access and assistance was provided by the "Service de Systematique Moléculaire" of the  
683 Muséum national d'Histoire naturelle, Paris (CNRS UMS 2700). The molecular work was  
684 partly supported by agreement no. 2005/67 between the Genoscope (Evry, France) and the  
685 MNHN project 'Macrophylogeny of life'; sequencing was also undertaken in the project  
686 @SpeedID proposed by F-BoL, the French Barcode of Life initiative and the network

687 ‘Bibliothèque du vivant’ funded by the CNRS, INRA and MNHN; and through several MNHN  
688 grants (ATM “Génomique et collections” (Sarah Samadi and Régis Debruyne; ATM blanche  
689 2016). Fieldwork was supported by the following projects and institutions: the Muséum  
690 national d’Histoire naturelle, Paris (grants from ATM “Biodiversité actuelle et fossile”,  
691 Stéphane Peigné and Philippe Janvier; ATM “Formes possibles, formes réalisées”, Vincent  
692 Bels & Pierre-Henry Gouyon); the Project Lengguru 2014 ([www.lengguru.org](http://www.lengguru.org)), conducted by  
693 the French Institut de Recherche pour le Développement (IRD), the Indonesian Institute of  
694 Sciences (LIPI), the University of Papua (UNIPA), the University of Cendrawasih (UNCEN),  
695 the University of Musamus (UNMUS) and the Sorong Fisheries Academy (APSOR) with  
696 corporate sponsorship from COLAS Group, Veolia Water and the Total Foundation; the  
697 project “Our Planet Reviewed Papua-New-Guinea 2012-2013” set up by Pro-Natura  
698 International, MNHN (France), IRD (France) in partnership with the Royal Belgian Institute of  
699 Natural Sciences, the New Guinea Binatang Research Center, the University of Papua New  
700 Guinea, and the Divine Word University of Madang and with core funding of Prince Albert II  
701 of Monaco Foundation, the Stavros Niarchos Foundation, the Total Foundation, the  
702 Fondation d’entreprise EDF, the Fonds Pacifique, Spiecapag, Entrepose Contracting, the  
703 New-Caledonia Government, the Reef Foundation and the Belgian National Lottery. We  
704 thank Jérôme Constant and Carole Paleco (RBINS) for their help during the study of the  
705 collections of the Royal Belgian Institute of Natural sciences, Brussels, funded by the  
706 SYNTHESYS European program (BE-TAF-6640), Judith Marshall and George Beccaloni  
707 (BMNH) for their help during the study in the Natural History Museum, London, funded by the  
708 SYNTHESYS European program (GB-TAF-531); Andrej Gorochov (ZIN) for providing  
709 *Cardiodactylus* samples from the collections of Saint Petersburg; Rob de Vries and Caroline  
710 Pepermans (RMNH) for their help during the study in Leiden collections, funded by a grant  
711 from the PPF "État et structure phylogénétique de la biodiversité actuelle et fossile", MNHN  
712 (Philippe Janvier); Peter Schwendinger and John Hollier (MHNG) for their help during the  
713 study of Genève collections; and Oscar Effendi and Erni Ernawati (MZB, Indonesia) for their

714 help during the study of eneopterine crickets in Cibinong, Indonesia (MZB), and Shepherd  
715 Myers and Franck Howarth (BPBM) for loaning crickets from the collections of Honolulu.  
716

717 **7. References**

718 Anso, J., Barrabe, L., Desutter-Grandcolas, L., Jourdan, H., Grandcolas, P., Dong, J.,  
719 Robillard, T., 2016. Old Lineage on an old Island: *Pixibinthus*, a new cricket genus  
720 endemic to New Caledonia shed light on gryllid diversification in a hotspot of  
721 biodiversity. PLoS One 11, e0150920.

722 Ayres, D.L., Darling, A., Zwickl, D.J., Beerli, P., Holder, M.T., Lewis, P.O., Huelsenbeck, J.P.,  
723 Ronquist, F., Swofford, D.L., Cummings, M.P., Rambaut, A., Suchart, M.A. 2012.  
724 BEAGLE: an application programming interface and high-performance computing  
725 library for statistical phylogenetics. Syst. Biol. 61, 170–173.

726 Bellemain, E., Ricklefs, R.E., 2008. Are islands the end of the colonization road? Trends  
727 Ecol. Evol. 23, 461–468.

728 Bird, M.I., Taylor, D., Hunt, C., 2005. Palaeoenvironments of insular Southeast Asia during  
729 the Last Glacial Period: a savanna corridor in Sundaland? Quat. Sci. Rev. 24, 2228–  
730 2242.

731 Chintauan-Marquier, I.C., Legendre, F., Hugel, S., Robillard, T., Grandcolas, P., Nel, A.,  
732 Zuccon, D., Desutter-Grandcolas, L., 2016. Laying the foundations of evolutionary and  
733 systematic studies in crickets (Insecta, Orthoptera): a multilocus phylogenetic analysis.  
734 Cladistics 32, 54–81.

735 Cigliano, M.M., Braun, H., Eades, D.C., Otte, D., 2017. Orthoptera Species File. Version  
736 5.0/5.0. [01/09/2017]. <<http://Orthoptera.SpeciesFile.org>>

737 Claridge, E.M., Gillespie, R.G., Brewer, M.S., Roderick, G.K., 2017. Stepping-stones across  
738 space and time: repeated radiation of Pacific flightless broad-nosed weevils  
739 (Coleoptera: Curculionidae: Entiminae: *Rhyncogonus*). J. Biogeogr. 44, 784–796.

740 Clouse, R.M., Janda, M., Blanchard, B., Sharma, P., Hoffmann, D.H., Andersen, A.N.,  
741 Czekanski-Moir, J.E., Krushelnicky, P., Rabeling, C., Wilson, E.O., Economo, E.P.,

- 742 Sarnat, E.M., General, D.M., Alpert, G.D., Wheeler, W.C., 2014. Molecular phylogeny  
743 of Indo-Pacific carpenter ants (Hymenoptera: Formicidae, *Camponotus*) reveals waves  
744 of dispersal and colonization from diverse source areas. *Cladistics* 31, 1–14.
- 745 Condamine, F.L., Toussaint, E.F.A., Clamens, A.-L., Genson, G., Sperling, F.A.H., Kergoat,  
746 G.J., 2015. Deciphering the evolution of birdwing butterflies 150 years after Alfred  
747 Russell Wallace. *Sci. Rep.* 5, 11860.
- 748 Condamine, F.L., Toussaint, E.F.A., Cotton, A.M., Sperling, F.A.H., Genson, G., Kergoat,  
749 G.J., 2013. Fine-scale biogeographical and temporal diversification processes of  
750 peacock swallowtails (*Papilio* subgenus *Achillides*) in the Indo-Australian  
751 Archipelago. *Cladistics* 29, 88–111.
- 752 De Bruyn, M., Stelbrink, B., Morley, R.J., Hall, R., Carvalho, G.R., Cannon, C.H., Van den  
753 Bergh, G., Meijaard, E., Metcalfe, I., Boitani, L., Maiorano, L., Shoup, R., Von Rintelen,  
754 T., 2014. Borneo and Indochina are major evolutionary hotspots for Southeast Asian  
755 biodiversity. *Syst. Biol.* 63, 879–901.
- 756 Drummond, A.J., Suchard, M.A., Xie, D., Rambaut, A., 2012. Bayesian phylogenetics with  
757 BEAUti and the BEAST 1.7. *Mol. Biol. Evol.* 29, 1969–1973.
- 758 Duchêne, S., Molak, M., Ho, S.Y.W., 2014. ClockstaR: choosing the number of relaxed-clock  
759 models in molecular phylogenetic analysis. *Bioinformatics* 30, 1017–1019.
- 760 Economo, E.P., Sarnat, E.M., Janda, M., Clouse, R., Klimov, P.B., Fischer, G., Blanchard,  
761 B.D., Ramirez, L.N., Andersen, A.N., Berman, M., Guénard, B., Lucky, A., Rabeling, C.,  
762 Wilson, E.O., Knowles, L.L., 2015. Breaking out of biogeographical modules: range  
763 expansion and taxon cycles in the hyperdiverse ant genus *Pheidole*. *J. Biogeogr.* 42,  
764 2289–2301.
- 765 Erixon, P., Svensson, B., Britton, T., Oxelman, B., 2003. Reliability of Bayesian posterior  
766 probabilities and bootstrap frequencies in phylogenetics. *Syst. Biol.* 52, 665–673.
- 767 Foster, C.S.P., Ho, S.Y.W., 2017. Strategies for partitioning clock models in phylogenomic  
768 dating: application to the angiosperm evolutionary timescale. *Genome Biol. Evol.* 9,  
769 2752–2763.

- 770 Gernhard, T., 2008. The conditioned reconstructed process. *J. Theor. Biol.* 253, 769–778.
- 771 Graur, D., Martin, W., 2004. Reading the entrails of chickens: molecular timescales of  
772 evolution and the illusion of precision. *Trends Genet.* 20, 81–86.
- 773 Guo, Y.Y., Luo, Y.B., Liu, Z.J., Wang, X.Q., 2015. Reticulate evolution and sea-level  
774 fluctuations together drove species diversification of slipper orchids (*Paphiopedilum*) in  
775 South-East Asia. *Mol. Ecol.* 24, 2838–2855.
- 776 Hall, R., 1996. Reconstructing Cenozoic SE Asia, in: Hall, R. and Blundell, D (Eds), *Tectonic  
777 Evolution of Southeast Asia*, Geological Society, London, pp. 153–184.
- 778 Hall, R., 2009. Southeast Asia's changing palaeogeography. *Blumea*. 54, 148–161.
- 779 Hall, R., 2009b. Continental growth at the Indonesian margins of southeast Asia. *Arizona  
780 Geol.Soc. Digest.* 22, 245–258.
- 781 Hall, R., 2011. Australia-SE Asia collision: plate tectonics and crustal flow, in: Hall, R.,  
782 Cottam, M. A., Wilson, M. E. J. (Eds), *The SE Asian Gateway: History and Tectonics of  
783 the Australia-Asia Collision*. Geological Society, London, Special Publications, 355, 75–  
784 109.
- 785 Hall, R., 2012. Sundaland and Wallacea: geology, plate tectonics and palaeogeography, in:  
786 Gower, D.J., Richardson, J.E., Rosen, B.R., Rüber, L., Williams, S.T. (Eds.), *Biotic  
787 evolution and environmental change in Southeast Asia*, Cambridge University Press,  
788 Cambridge, pp. 32–78.
- 789 Hall, R., 2013. The palaeogeography of Sundaland and Wallacea since the Late Jurassic. *J.  
790 Limnol.* 72, 1–17.
- 791 Hall, R., Sevastjanova, I., 2012. Australian crust in Indonesia. *Aus. J. Earth Sci.* 59, 827–844.
- 792 Hearty, P.J., Hollin, J.T., Neumann, C.A., O'Leary, M.J., McCulloch, M., 2007. Global sea-  
793 level fluctuations during the last Interglaciation (MIS 5e). *Quat. Sci. Rev.* 26, 2090–  
794 2112.
- 795 Heaney, L.R., 1991. A synopsis of climatic and vegetational change in Southeast Asia. *Clim.  
796 Change.* 19, 53–61.

- 797 Heaney, L.R., 2000. Dynamic disequilibrium: a long-term, large-scale perspective on the  
798 equilibrium model of island biogeography. *Glob. Ecol. Biogeogr.* 9, 59–74.
- 799 Hillis, D.M., Bull, J.J., 1993. An empirical test of bootstrapping as a method for assessing  
800 confidence in phylogenetic analysis. *Syst. Biol.* 42, 182–192.
- 801 Jansa, S.A., Barker, F.K., Heaney, L.R., 2006. The Pattern and Timing of Diversification of  
802 Philippine Endemic Rodents Evidence from Mitochondrial and Nuclear Gene  
803 Sequences. *Syst. Biol.* 55, 73–88.
- 804 Kalkman, V.J., Dijkstra, D.B., Dow, R.A., Stokvis, F.R., van Tol, J., 2018. Out of Australia: the  
805 Argiolestidae reveal the Melanesian Arc System and East Papua Composite Terrane  
806 as possible ancient dispersal routes to the Indo-Australian Archipelago (Odonata:  
807 Argiolestidae). *Int. J. Odonat.* 21, 1–14.
- 808 Kass, R.E., Raftery, A.E., 1995. Bayes factors. *J. Am. Stat. Assoc.* 90, 773–795.
- 809 Landis, M., Matzke, N.J., Moore, B.R., Hulsenbeck, J.P., 2013. Bayesian analysis of  
810 biogeography when the number of areas is large. *Syst. Biol.* 62, 789–804.
- 811 Lanfear, R., Frandsen, P.B., Wright, A.M., Senfeld, T., Calcott, B., 2017. PartitionFinder 2:  
812 new methods for selecting partitioned models of evolution for molecular and  
813 morphological phylogenetic analyses. *Mol. Biol. Evol.* 34, 772–773.
- 814 Lohman, D.J., de Bruyn, M., Page, T., von Rintelen, K., Hal, R., Ng, P.K.L., Shih, H.-T.,  
815 Carvalho, G.R., von Rintelen, T., 2011. Biogeography of the Indo-Australian  
816 Archipelago. *Annu. Rev. Ecol. Evol. Syst.* 42, 205–226.
- 817 Matzke, N.J., 2014. Model selection in historical biogeography reveals that founder-event  
818 speciation is a crucial process in island clades. *Syst. Biol.* 63, 951–970.
- 819 Metcalfe, I., 2006. Paleozoic and Mesozoic tectonic evolution and palaeogeography of East  
820 Asian crustal fragments: The Korean Peninsula in context. *Gondwana Res.* 9, 24–46.
- 821 Miller, M.A., Schwartz, T., Pickett, B.E., He, S., Klem, E.B., Scheuermann, R.H., Passarotti,  
822 M., Kaufman, S., O'Leary, M.A., 2015. A RESTful API for access to phylogenetic tools  
823 via the CIPRES Science Gateway. *Evol. Bioinform.* 11, 43–48.

- 824 Mittermeier, R.A., Gil, P.R., Hoffmann, M., Pilgrim, J., Brooks, T., Mittermeier, C.G.,  
825 Lamoreux, J., Da Fonseca, G.A.B., 2004. Hotspots Revisited - Earth's biologically  
826 richest and most endangered terrestrial ecoregions. The University of Chicago Press,  
827 Chicago.
- 828 Moore, B.R., Höhna, S., May, M.R., Rannala, B., Huelsenbeck, J.P. 2016. Critically  
829 evaluating the theory and performance of Bayesian analysis of macroevolutionary  
830 mixtures. Proc. Natl. Acad. Sci. USA 113, 9569–9574.
- 831 Morley, R.J., 2012. A review of the Cenozoic palaeoclimate history of Southeast Asia, in:  
832 Gower, D., Johnson, K., Richardson, J., Rosen, B., Rüber, L., Williams, S. (Eds), Biotic  
833 evolution and environmental change in Southeast Asia, Cambridge University Press,  
834 Cambridge, pp. 79–114.
- 835 Müller, C.J., Matos-Maravi, P.E., Beheregaray, L.B., 2013. Delving into *Delias* Hübner  
836 (Lepidoptera: Pieridae): fine-scale biogeography, phylogenetics and systematics of the  
837 world's largest butterfly genus. J. Biogeogr. 40, 881–893.
- 838 Nattier, R., Grandcolas, P., Elias, M., Desutter-Grandcolas, L., Jourdan, H., Couloux, A.,  
839 Robillard, T., 2012. Secondary sympatry caused by range expansion informs on the  
840 dynamics of microendemism in a biodiversity hotspot. PLoS One 7, e48047.
- 841 Nattier, R., Robillard, T., Desutter-Grandcolas, L., Couloux, A., Grandcolas, P., 2011. Older  
842 than New Caledonia emergence? A molecular phylogenetic study of the eneopterine  
843 crickets (Orthoptera: Grylloidea). J. Biogeogr. 38, 2195–2209.
- 844 Neall, V.E., Trewick, S.A., 2008. The age and origin of the Pacific islands: a geological  
845 overview. Phil. Trans. R. Soc. B. 363, 3293–3308.
- 846 Nguyen, L.T., Schmidt, H.A., von Haeseler, A., Minh, B.Q., 2015. IQTREE: A fast and  
847 effective stochastic algorithm for estimating maximum likelihood phylogenies. Mol. Biol.  
848 Evol. 32, 268–274.
- 849 Otte, D., 2007. New species of *Cardiodactylus* from the western Pacific region (Gryllidae:  
850 Eneopterinae). Proc. Acad. Nat. Sci. Phila. 156, 341–400.

- 851 Outlaw D.C., Voelker, G., 2008. Pliocene climatic change in insular Southeast Asia as an  
852 engine of diversification in *Ficedula* flycatchers. *J. Biogeogr.* 35, 739–752.
- 853 Rabosky, D.L., Donnellan, S.C., Grundler, M., Lovette, J.J., 2014a. Analysis and visualization  
854 of complex macroevolutionary dynamics: an example from Australian scincid lizards.  
855 *Syst. Biol.* 63, 610–627.
- 856 Rabosky, D.L., Grundler, M., Anderson, C., Title, P., Shi, J.J., Brown, J.W., Huang, H.,  
857 Larson, J.G., Kembel, S., 2014b. BAMMtools: an R package for the analysis of  
858 evolutionary dynamics on phylogenetic trees. *Methods Ecol. Evol.* 5, 701–707.
- 859 Rabosky, D.L., Mitchell, J.S., Chang, J., 2017. Is BAMM flawed? Theoretical and practical  
860 concerns in the analysis of multi-rate diversification models. *Syst. Biol.* 66, 477–498.
- 861 Rabosky, D.L., Santini, F., Eastman, J., Smith, S.A., Sidlauskas, B., Chang, J., Alfaro, M.E.,  
862 2013. Rates of speciation and morphological evolution are correlated across the  
863 largest vertebrate radiation. *Nat. Comm.* 4, 1958.
- 864 Rambaut, A., Suchard, M.A., Xie, D., Drummond, A.J., 2014. Tracer v1.6, Available from  
865 <http://beast.bio.ed.ac.uk/Tracer>.
- 866 Ree, R.H., Sanmartín, I., 2018. Conceptual and statistical problems with the DEC+J model of  
867 founder-event speciation and its comparison with DEC via model selection. *J.*  
868 *Biogeogr.* 45, 741–749.
- 869 Ree, R.H., Smith, S.A., 2008. Maximum likelihood inference of geographic range evolution  
870 by dispersal, local extinction, and cladogenesis. *Syst. Biol.* 57, 4–14.
- 871 Ripplinger, J., Sullivan, J., 2008. Does Choice in Model Selection Affect Maximum Likelihood  
872 Analysis? *Syst. Biol.* 57, 76–85.
- 873 Robillard, T., Desutter-Grandcolas, L., 2004. Phylogeny and the modalities of acoustic  
874 diversification in extant Eneopterinae (Insecta, Orthoptera, Grylloidea, Eneopteridae).  
875 *Cladistics* 20, 271–293.
- 876 Robillard, T., Desutter-Grandcolas, L., 2006. Phylogeny of the cricket subfamily  
877 Eneopterinae (Orthoptera, Grylloidea, Eneopteridae) based on four molecular loci and  
878 morphology. *Mol. Phylogen. Evol.* 40, 643–661.

- 879 Robillard, T., Grandcolas, P., Desutter-Grandcolas, P., 2007. A shift toward harmonics for  
880 high-frequency calling shown with phylogenetic study of frequency spectra in  
881 Eneopterinae crickets (Orthoptera, Grylloidea, Eneopteridae). Can. J. Zool. 85, 1264–  
882 1274.
- 883 Robillard, T., Ichikawa, A., 2009. Redescription of two *Cardiodactylus* species (Orthoptera,  
884 Grylloidea, Eneopterinae): the supposedly well-known *C. novaeguineae* (Haan, 1842),  
885 and the semi-forgotten *C. guttulus* (Matsumura, 1913) from Japan. Zool. Sci. 26, 878–  
886 891.
- 887 Robillard, T., Montealegre-Z, F., Desutter-Grandcolas, L., Grandcolas, P., Robert, D., 2013.  
888 Mechanisms of high-frequency song generation in brachypterous crickets and the role  
889 of ghost frequencies. J. Exp. Biol. 216, 2001–2011.
- 890 Robillard, T., Dong, J.J., 2016. The *Cardiodactylus* crickets from Eastern New Guinea, with  
891 description of five new species (Orthoptera: Gryllidae: Eneopterinae), in: Robillard, T.,  
892 Legendre, F., Villemant, C., Leponce, M. (Eds.), Insects of Mount Wilhelm, Papua New  
893 Guinea, Mémoires du Muséum National d'Histoire Naturelle 209, Muséum national  
894 d'Histoire Naturelle, Paris, pp. 203–258.
- 895 Robillard, T., Gorochov, A.V., Poulain, S., Suhardjono, Y.R., 2014. Revision of the cricket  
896 genus *Cardiodactylus* (Orthoptera, Eneopterinae, Lebinthini): the species from both  
897 sides of the Wallace line, with description of 25 new species. Zootaxa 3854, 1–104.
- 898 Ronquist, F., 1997. Dispersal-Vicariance Analysis: A new approach to the quantification of  
899 historical biogeography. Syst. Biol. 46, 195–203.
- 900 Ronquist, F., Teslenko, M., van der Mark, P., Ayres, D.L., Darling, A., Höhna, S., Larget, B.,  
901 Liu, L., Suchard, M. A, Huelsenbeck, J.P., 2012. MrBayes 3.2: efficient Bayesian  
902 phylogenetic inference and model choice across a large model space. Syst. Biol. 61,  
903 539–542.
- 904 Schenk, J.J., 2016. Consequences of secondary calibrations on divergence time estimates.  
905 PLoS One 11, e0148288.

- 906 Stelbrink, B., Albrecht, C., Hall, R., von Rintelen, T., 2012. The biogeography of Sulawesi  
907 revisited: is there evidence for a vicariant origin of taxa on Wallace's "anomalous  
908 island"? *Evolution* 66, 2252–2271.
- 909 Steppan, S.J., Zawadzki, C., Heaney, L.R., 2003. Molecular phylogeny of the endemic  
910 Philippine rodent *Apomys* (Muridae) and the dynamics of diversification in an oceanic  
911 archipelago. *Biol. J. Linn. Soc.* 80, 699–715.
- 912 Tanzler, R., Van Dam, M.H., Toussaint, E.F.A., Suhardjono, Y.R., Balke, M., Riedel, A.,  
913 2016. Macroevolution of hyperdiverse flightless beetles reflects the complex geological  
914 history of the Sunda Arc. *Sci. Rep.* 6, 18793.
- 915 Ter Hofstede, H.M., Schöneich, S., Robillard, T., Hedwig, B., 2015. Evolution of a  
916 communication system by sensory exploitation of startle behavior. *Curr. Biol.*, 25,  
917 3245–3252.
- 918 Toussaint, E.F.A., Balke, M., 2016. Historical biogeography of *Polyura* butterflies in the  
919 oriental Palaeotropics: trans-archipelagic routes and South Pacific island hopping. *J.*  
920 *Biogeogr.* 43, 1560–1572.
- 921 Trifinopoulos, J., Nguyen, L.T., von Haeseler, A., Minh, B.Q., 2016. W-IQ-TREE: a fast online  
922 phylogenetic tool for maximum likelihood analysis. *Nucleic Acids Res.* 44, W232–  
923 W235.
- 924 Vicente, N., Kergoat, G.J., Dong, J., Yotoko, K., Legendre, F., Nattier, R., Robillard, T., 2017.  
925 In and out of the Neotropics: historical biogeography of Eneopterinae crickets. *J.*  
926 *Biogeogr.* 44, 2199–2210.
- 927 Voris, H.K., 2000. Maps of Pleistocene sea levels in Southeast Asia: shorelines, river systems  
928 and time durations. *J. Biogeogr.* 27, 1153–1167.
- 929 Wallace, A.R., 1860. On the zoological geography of the Malay archipelago. *Zool. J. Linn.*  
930 *Soc.* 4, 172–184.
- 931 Woodruff, D.S., 2010. Biogeography and conservation in Southeast Asia: how 2.7 million  
932 years of repeated environmental fluctuations affect today's patterns and the future of  
933 the remaining refugial-phase biodiversity. *Biodivers. Conserv.* 19, 919–941.

- 934 Yumul, G.P., Dimalanta, C.B., Tamayo, R.A., Maury, R.C., Bellon, H., Polv , M.,  
935 Maglambayan, V.B., Querubin, C.L., Cotten, J., 2004. Geology of the Zamboanga  
936 Peninsula, Mindanao, Philippines: an enigmatic South China continental fragment?  
937 Geol. Soc. London Spec. Publ. 266, 289–312.
- 938 Zachos, F.E., Habel, J.C., 2011. Biodiversity hotspots: Distribution and protection of  
939 conservation priority areas. Springer-Verlag, Berlin.
- 940 Zachos, J., Pagani, M., Sloan, L., Thomas, E., Billups, K., 2001. Trends, rhythms and  
941 aberrations in global climate 65 Ma to present. Science 292, 686–693.
- 942 Zahirovic, S., Seton, M., M ller, R.D., 2014. The Cretaceous and Cenozoic tectonic evolution  
943 of Southeast Asia. Solid Earth 5, 227–273.
- 944

945 **Figure titles**

946

947 **Figure 1.** Distribution map of *Cardiodactylus* in Southeast Asia. In this study, we sampled 28  
948 out of 35 *Cardiodactylus* species distributed in Southeast Asia. The sampled species  
949 are written in black (collecting localities in black circles), and species missing in the  
950 sampling are shown in grey.. Map modified after Robillard et al. (2014).

951

952 **Figure 2.** Phylogeny of the genus *Cardiodactylus* inferred from Maximum likelihood (ML) and  
953 Bayesian inference (BI). Values on nodes indicate branch support; the first two values  
954 correspond to non-parametric bootstrap values (BV from RAxML analyses first, then  
955 BV from IQ-TREE analyses) whereas the third value corresponds to BI posterior  
956 probabilities (PP). Asterisks are used to indicate maximum support (100% for BV and  
957 1.0 for PP). Signs ‘-‘ indicate topological incongruences between analyses, the  
958 topology inferred with RAxML being represented. The bold red circles with letters  
959 indicate the secondary calibration points used in the dating analyses; the circled  
960 numbers highlight clades discussed in the text.

961

962 **Figure 3.** Reconstruction of historical biogeography for *Cardiodactylus* using a stratified  
963 dispersal-vicariance analysis (DIVALIKE) model. The left panel and map represent the  
964 12 areas implemented in the biogeographical model. Present-day distributions of each  
965 species are given at the tips by colored circles corresponding to colored areas on map;  
966 a colored square represents the inferred area(s) with the highest relative probability in  
967 the DIVALIKE analysis; corner positions represent geographic ranges immediately after  
968 a cladogenesis event. The red numbers near each node correspond to the median age  
969 inferred in Beast analysis and the gray lines indicate its 95% height posterior  
970 distribution (HPD). Bayesian posterior probabilities below 0.50 are not shown.

971

972     **Figure 4.** Colonization routes, numbers of emigration and immigration events and *in situ*  
973       diversification events inferred from ancestral area estimation for lineages of the  
974       *Novaeguineae* species group during the pre-Miocene, Miocene and Plio-Pleistocene.  
975       a) Colonization routes; line colors correspond to inferred area of origin (same color  
976       code as in simplified map): multiple lines of the same color correspond to multiple  
977       colonization events. b) Number of emigration (positive bars) and immigration (negative  
978       bars) events inferred from colonization events (Figure 4a) for each area in the pre-  
979       Miocene, Miocene and Plio-Pleistocene; column colors correspond to inferred areas as  
980       above. c) *In situ* diversification events inferred from ancestral area estimation for each  
981       area in the pre-Miocene, Miocene and Plio-Pleistocene.

982

983     **Figure 5.** Rate shift configurations with the four highest posterior probabilities from the 95%  
984       credible set within *Cardiodactylus*. The tree topology referred to Figure 3. The colored  
985       histogram indicates the speciation ( $\lambda$ ), the color gradient corresponds the speciation  
986       rate.

987

988     **Figure 6.** Rates-through-time analysis of speciation ( $\lambda$ ), extinction ( $\mu$ ) and net diversification  
989       ( $\gamma$ ) in *Cardiodactylus* (a) and within *Novaeguineae* species group (b).

990

991

992 **Table**

993 **Table** . Best-fit models of sequence evolution and partitioning schemes selected with  
 994 PartitionFinder ('*unlinked branch lengths*' option) for phylogenetic reconstructions using  
 995 Bayesian Inference (MrBayes/BEAST) and Maximum Likelihood (RAxML/IQ-TREE).  
 996 Codon position is denoted by pos1, pos2 and pos3. Subsets are denoted by p1 and p2.

Analyses	Partitions	Models
Bayesian inference (BI) analyses	p1: 16S, COI_pos2, Cytb_pos2, 18S, 28S, H3_pos1, H3_pos2, H3_pos3, EF1a; p2: 12S, COI_pos1, COI_pos3, COII_pos1, COII_pos2, COII_pos3, Cytb_pos1, Cytb_pos3;	GTR+I+G
Maximum likelihood (ML) analyses	p1: 16S, COI_pos2, Cytb_pos2, 18S, 28S, H3_pos1, H3_pos2, H3_pos3, EF1a; p2: 12S, COI_pos1, COI_pos3, COII_pos1, COII_pos2, COII_pos3, Cytb_pos1, Cytb_pos3;	GTR+I+G
Bayesian evolutionary analyses by sampling trees (BEAST)	p1: 16S, COI_pos2, Cytb_pos2, 18S, 28S, H3_pos1, H3_pos2, H3_pos3, EF1a; p2: 12S, COI_pos1, COI_pos3, COII_pos1, COII_pos2, COII_pos3, Cytb_pos1, Cytb_pos3;	GTR+I+G

997

998

999    **Supporting Information**  
1000

1001    Appendix S1. Taxon sampling.

1002    Appendix S2. Time-stratified biogeographical standard implemented in BioGeoBEARS  
1003        analyses.

1004    Appendix S3. Summary of ancestral area estimation with different models and dispersal rate  
1005        multipliers with time slices (Table S3a) and without time slices (Table S3b). The gray  
1006        line highlights the model with the highest statistical support.

1007    Appendix S4. Sampling of species groups in BAMM analysis.

1008    Appendix S5. Gene trees inferred for each marker: 16S (a), 12S (b), COI (c), COII (d), Cytb  
1009        (e), 18S (f), 28S (g), EF1a (h), H3 (i).

1010    Appendix S6. Original output results of Bayesian inference (BI) and maximum likelihood (ML)  
1011        analyses for the concatenated dataset.

1012    Appendix S7. Original outputs for dating analyses.

1013    Appendix S8. Results of ancestral area estimation in BioGeoBEARS based on the most  
1014        complex set of dispersal rate multipliers with three time slices, two maximum  
1015        ancestral areas and DIVALIKE speciation model.

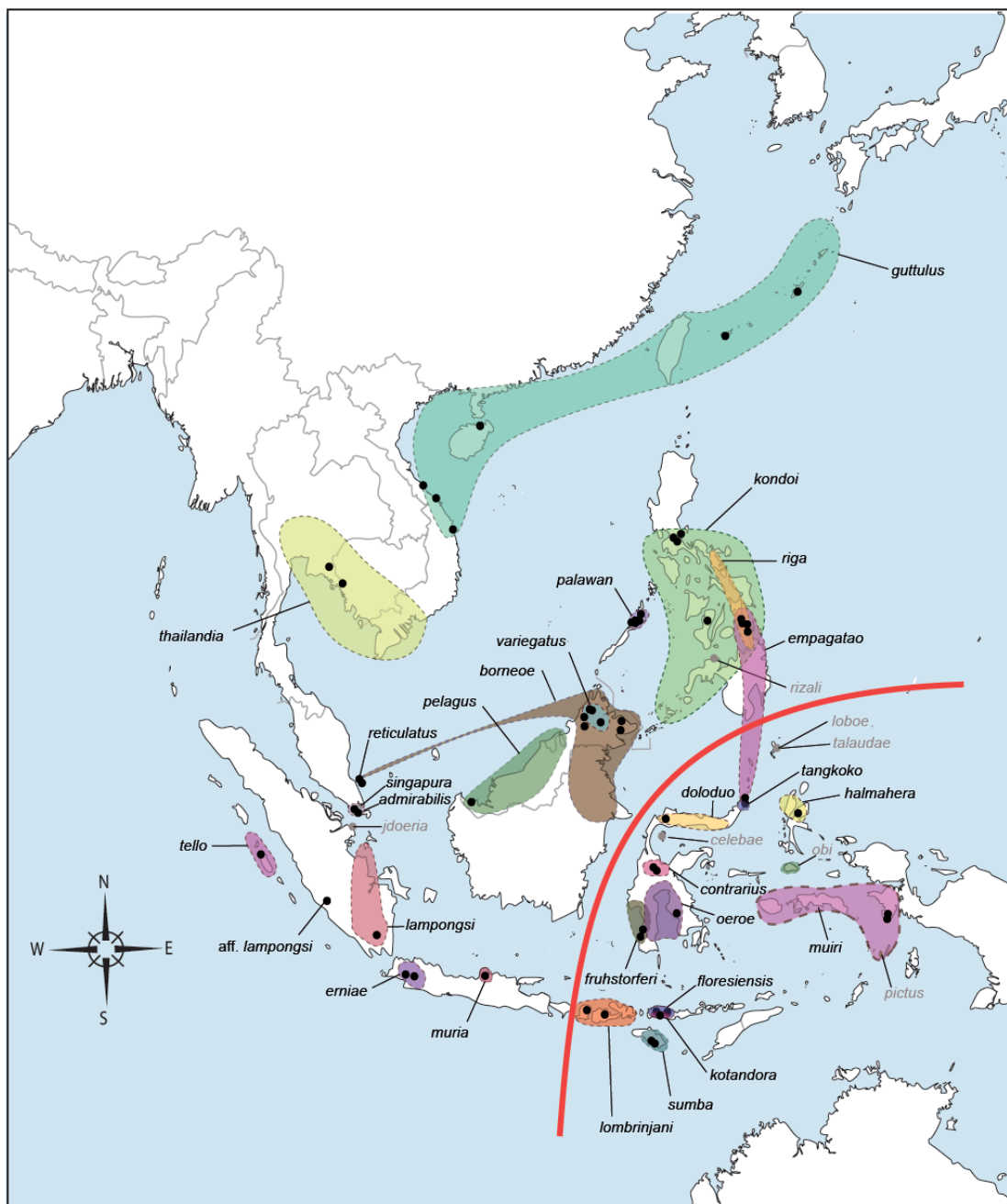
1016    Appendix S9. Results of ancestral area estimation in BioGeoBEARS based on the most  
1017        complex set of dispersal rate multipliers without time slices, two maximum ancestral  
1018        areas and DIVALIKE speciation model.

1019    Appendix S10. Summary of diversification rate under BAMM analysis with gradient of prior  
1020        values ranging from 0.1 to 1.0. The gray line highlights the model with the highest  
1021        statistical support.

1022

1023

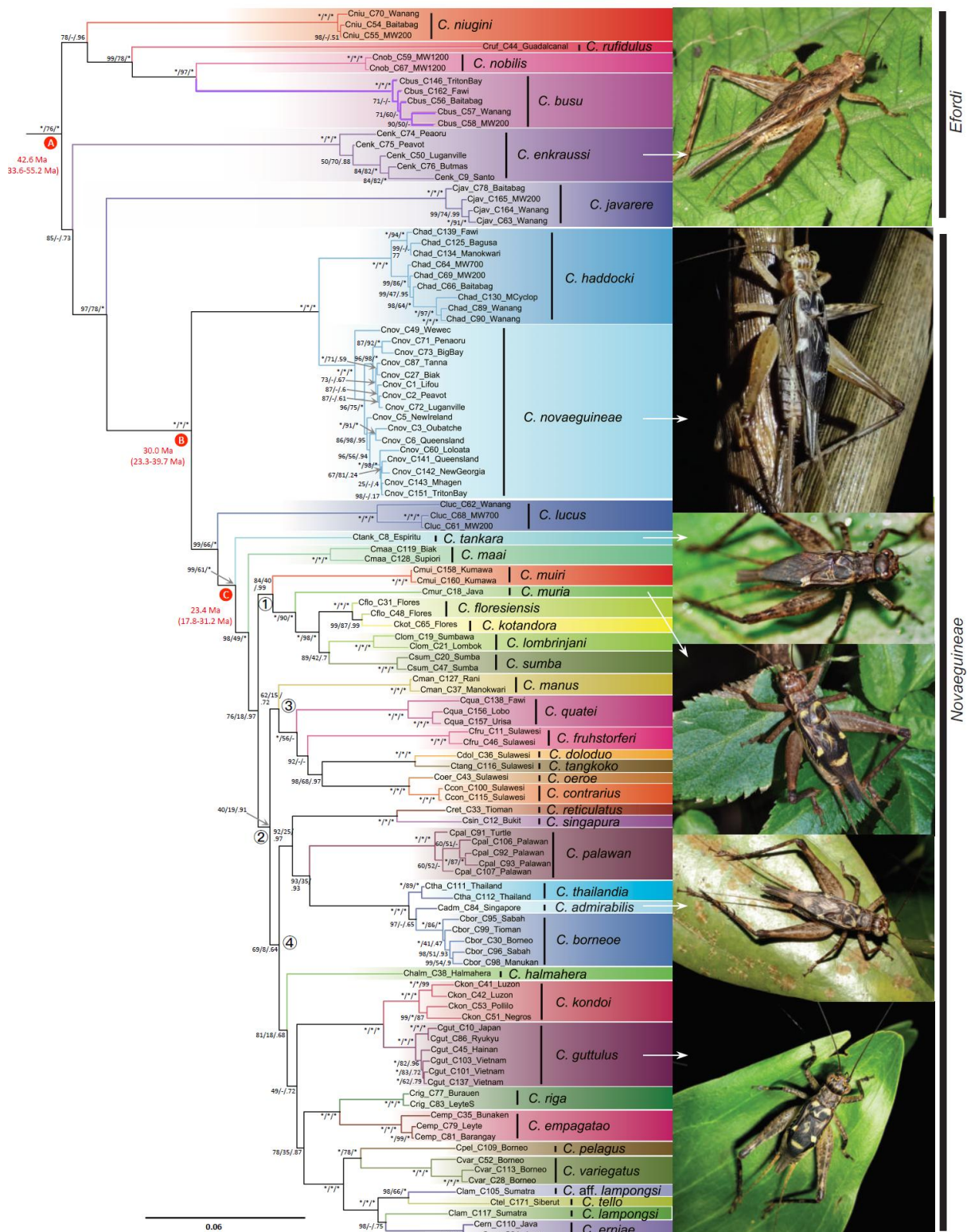
1024 Fig.1



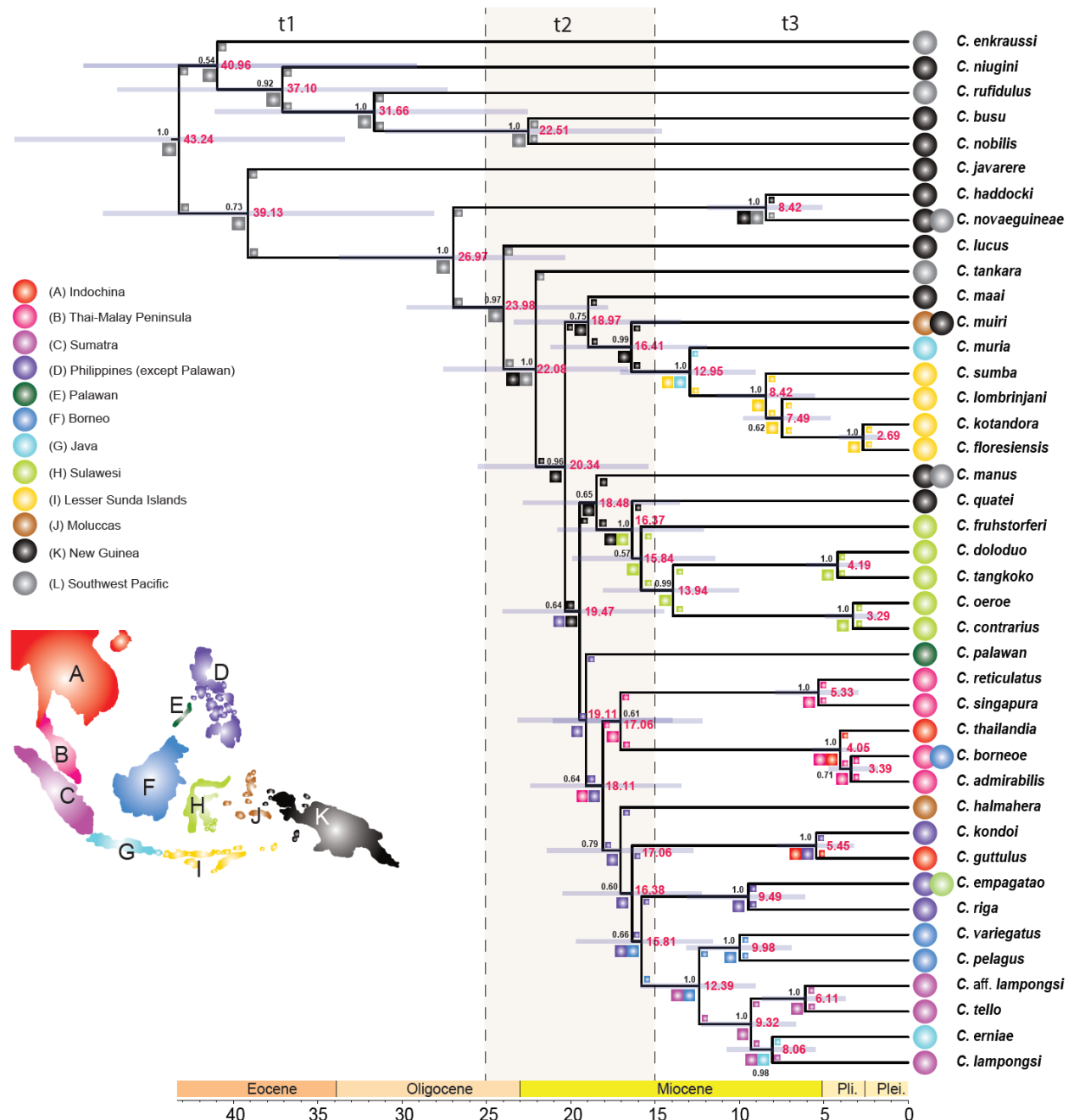
1025

1026

1027 Fig.2



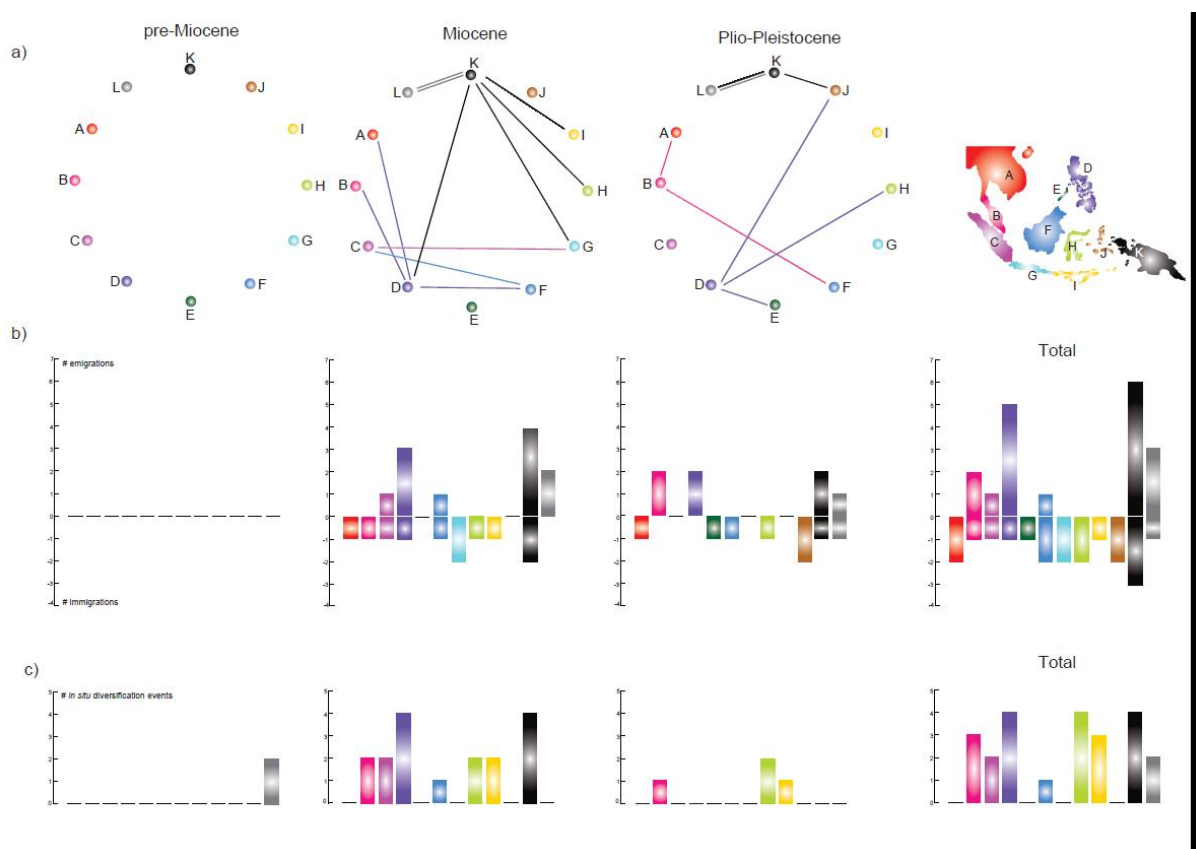
1030 Fig.3



1031

1032

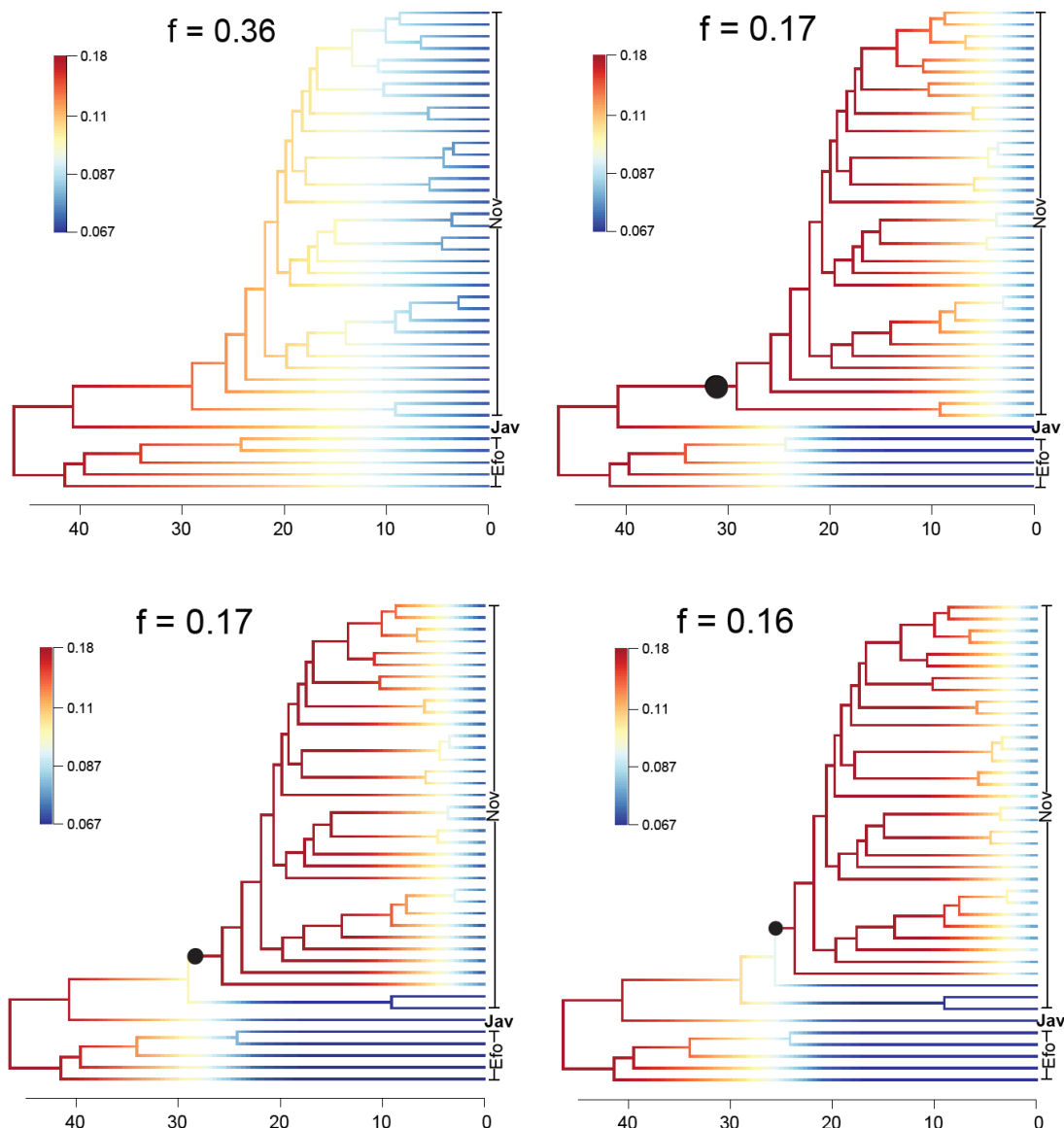
1033 Fig.4



1034

1035

1036 Fig.5.

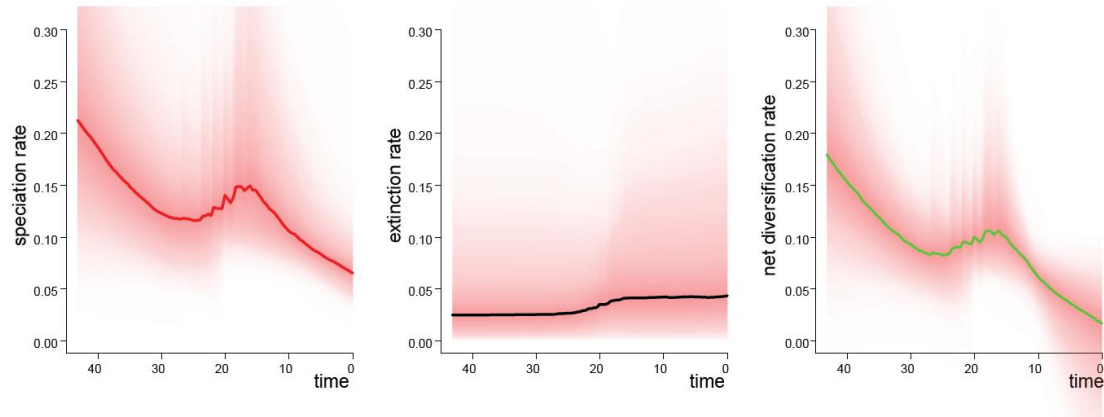


1037

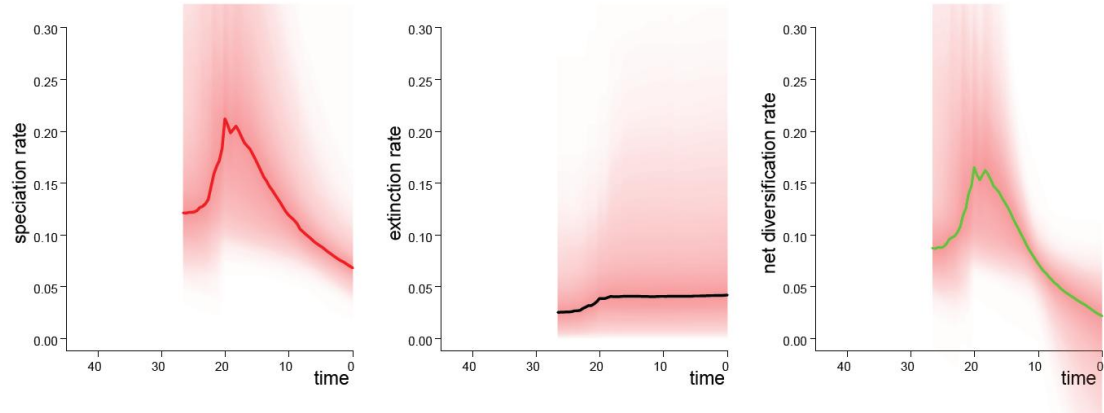
1038

1039 Fig.6.

a) Rates-through-time analysis of speciation ( $\lambda$ ), extinction ( $\mu$ ) and net diversification ( $\gamma$ ) within genus *Cardiodactylus*



b) Rates-through-time analysis of speciation ( $\lambda$ ), extinction ( $\mu$ ) and net diversification ( $\gamma$ ) in *Novaeguineae* species group



1040

1041

1042 **Supporting information**

1043

1044 **Appendix S1. Taxon sampling.**

1045 List of all *Cardiodactylus* and outgroups used in this study with current geographical  
 1046 distribution and GenBank accession numbers of each marker. The abbreviations of  
 1047 taxonomic status indicate as following: subfamily Gryllinae (GRYL), subfamily  
 1048 Eneopterinae (ENEO), subfamily Gryllinae (Gry), tribe Lebinthini (Leb), tribe  
 1049 Eneopterini (Ene), tribe Eurepini (Eur), tribe Nisitrini (Nis), tribe Xenogryllini (Xen).  
 1050 NA means missing data. The samples used in the dating analyses to represent each  
 1051 species are show with an asterisk (\*).

1052

1053

Species	Taxonomy	Voucher	Molecular code	Geographic area/code	16S	12S	COI	COII	Cytb	18S	28S	EF1a	H3
<i>Acheta domesticus</i> (Linnaeus, 1758)	GRYL/Gry	MNHN-EO-ENSIF3523	Adom	France (Laboratory strain)	AF248698	ADZ97611	JX897403	JX897439	AF248682	AD18SITS1	JX897465	GQ886692	KR903150
<i>Agnotecous albifrons</i> Desutter-Grandcolas, 1997	ENEO/Leb	MNHN-EO-ENSIF-2767	AalCT	New Caledonia	JX897353	JX897394	JX897418	JX897446	JX897314	JX897583	JX897490	JX897527	JX897572
<i>Agnotecous albifrons</i> Desutter-Grandcolas, 1997	ENEO/Leb	MNHN-EO-ENSIF-1771	AalGe	New Caledonia	JX897354	JX897396	JX897416	JX897445	JX897316	JX897585	NA	JX897529	JX897574
<i>Agnotecous azurensis</i> Desutter-Grandcolas, 2006	ENEO/Leb	MNHN-EO-ENSIF-2777	AazGK	New Caledonia	JX897360	JX897389	JX897426	NA	JX897331	JX897593	JX897472	JX897505	JX897565
<i>Agnotecous azurensis</i> Desutter-Grandcolas, 2006	ENEO/Leb	MNHN-EO-ENSIF-2780	AazRB	New Caledonia	JX897358	JX897376	JX897423	JX897453	JX897329	JX897595	JX897475	JX897502	JX897566
<i>Agnotecous meridionalis</i> Desutter-Grandcolas, 2006	ENEO/Leb	MNHN-EO-ENSIF-2772	AmelDP	New Caledonia	JX897349	JX897401	JX897420	NA	JX897311	JX897579	JX897488	JX897519	JX897553
<i>Agnotecous meridionalis</i> Desutter-Grandcolas, 2006	ENEO/Leb	MNHN-EO-ENSIF-2771	AmePB	New Caledonia	JX897350	JX897402	JX897410	JX897442	JX897313	JX897597	JX897489	JX897520	JX897550
<i>Agnotecous obscurus</i> (Chopard, 1970)	ENEO/Leb	MNHN-EO-ENSIF-2786	AobAo2	New Caledonia	JX897356	JX897398	JX897415	JX897449	JX897319	JX897591	NA	JX897510	NA
<i>Agnotecous obscurus</i> (Chopard, 1970)	ENEO/Leb	MNHN-EO-ENSIF-2785	AobMa	New Caledonia	JX897357	JX897393	JX897412	JX897450	JX897320	JX897587	JX897487	JX897525	JX897576
<i>Agnotecous robustus</i> (Chopard, 1915)	ENEO/Leb	MNHN-EO-ENSIF-2752	AroAo2	New Caledonia	JX897359	JX897375	JX897406	JX897443	JX897333	JX897588	NA	JX897498	JX897555
<i>Agnotecous sarramea</i> Desutter-Grandcolas, 1997	ENEO/Leb	MNHN-EO-ENSIF-2764	AsaMA	New Caledonia	JX897372	JX897380	JX897430	JX897456	JX897342	JX897598	JX897471	JX897511	JX897561
<i>Agnotecous occidentalis</i> Desutter-Grandcolas, 2006	ENEO/Leb	MNHN-EO-ENSIF-2765	AspCR2	New Caledonia	JX897362	JX897386	JX897434	JX897461	JX897322	JX897589	NA	JX897512	JX897570
<i>Agnotecous clarus</i> Desutter-Grandcolas, 2006	ENEO/Leb	MNHN-EO-ENSIF-2788	AspTRPP	New Caledonia	JX897347	JX897400	JX897407	JX897451	JX897324	JX897590	JX897492	JX897523	JX897554
<i>Agnotecous yahoue</i> Otte, 1987	ENEO/Leb	MNHN-EO-ENSIF-2766	AyaKo2	New Caledonia	JX897366	JX897387	JX897438	JX897463	JX897334	JX897602	JX897478	JX897500	JX897549
<i>Agnotecous yahoue</i> Otte, 1987	ENEO/Leb	MNHN-EO-ENSIF-2773	AyaMo5	New Caledonia	JX897367	JX897388	JX897437	JX897462	JX897337	NA	JX897479	JX897501	NA
* <i>Cardiodactylus admirabilis</i> Tan & Robillard, 2014	ENEO/Leb	MNHN-EO-ENSIF3441	Cadm_C84_Singapore/B	*this study	*this study	*this study	*this study	*this study	*this study	*this study	*this study	*this study	*this study
<i>Cardiodactylus borneo</i> Robillard & Gorochov, 2014	ENEO/Leb	RMNH	Cbor_C30_Borneo	Borneo/F	this study	this study	NA	this study					
<i>Cardiodactylus borneo</i> Robillard & Gorochov, 2014	ENEO/Leb	ZIN	Cbor_C95_Sabah	Borneo/F	this study	this study	NA	NA	this study	NA	NA	NA	this study
<i>Cardiodactylus borneo</i> Robillard & Gorochov, 2014	ENEO/Leb	ZIN	Cbor_C96_Sabah	Borneo/F	this study	this study	NA	this study					
<i>Cardiodactylus borneo</i> Robillard & Gorochov, 2014	ENEO/Leb	ZIN	Cbor_C98_Manukan	Borneo/F	this study	this study	NA	this study	NA				
* <i>Cardiodactylus borneo</i> Robillard & Gorochov, 2014	ENEO/Leb	ZIN	Cbor_C99_Tioman	Malaysia/B	*this study	*this study	NA	*this study					
<i>Cardiodactylus busu</i> Otte, 2007	ENEO/Leb	Leng-TR119	Cbus_C146_TritonBaya	New Guinea/K	this study	NA	this study						

1054

*Continued*

Species	Taxonomy	Voucher	Molecular code	Geographic area/code	16S	12S	COI	COII	Cytb	18S	28S	EF1a	H3
<i>Cardiodactylus busu</i> Otte, 2007	ENEO/L eb	ZIN	Cbus_C16_2_Fawi	New Guinea/K	this study	NA	NA	this study	this study				
<i>Cardiodactylus busu</i> Otte, 2007	ENEO/L eb	MNHN-ENSIF1 84	Cbus_C56_Baitabag	New Guinea/K	NA	this study	this study	this study	NA	this study	this study	NA	this study
* <i>Cardiodactylus busu</i> Otte, 2007	ENEO/L eb	MNHN-EO-ENSIF1 01	Cbus_C57_Wanang	New Guinea/K	*this study								
<i>Cardiodactylus busu</i> Otte, 2007	ENEO/L eb	MNHN-ENSIF1 09	Cbus_C58_MW200	New Guinea/K	this study								
<i>Cardiodactylus contrarius</i> Gorochov, 2014	ENEO/L eb	ZIN	Ccon_C10_0_Sulawesi	Sulawesi/H	this study								
* <i>Cardiodactylus contrarius</i> Gorochov, 2014	ENEO/L eb	MNHN-EO-ENSIF3 653	Ccon_C11_5_Sulawesi	Sulawesi/H	*this study								
* <i>Cardiodactylus doloduo</i> Gorochov, 2014	ENEO/L eb	ZIN	Cdol_C36_Sulawesi	Sulawesi/H	*this study								
<i>Cardiodactylus empagatao</i> Otte, 2007	ENEO/L eb	ZIN	Cemp_C35_Bunaken	Sulawesi/H	this study								
* <i>Cardiodactylus empagatao</i> Otte, 2007	ENEO/L eb	MNHN-EO-ENSIF3 353	Cemp_C79_Leyte	Philippines /D	*this study								
<i>Cardiodactylus empagatao</i> Otte, 2007	ENEO/L eb	UPLB MNH	Cemp_C81_Barangay	Philippines /D	this study	NA	this study	this study					
<i>Cardiodactylus enkraussi</i> Otte, 2007	ENEO/L eb	MNHN-EO-ENSIF2 313	Cenk_C50_Luganville	Vanuatu/L	this study	this study	this study	this study	NA	this study	NA	NA	this study
<i>Cardiodactylus enkraussi</i> Otte, 2007	ENEO/L eb	MNHN-EO-ENSIF2 398	Cenk_C74_Peaoru	Vanuatu/L	NA	this study	this study	this study	NA	this study	NA	NA	this study
<i>Cardiodactylus enkraussi</i> Otte, 2007	ENEO/L eb	MNHN-EO-ENSIF2 335	Cenk_C75_Peavot	Vanuatu/L	NA	this study	NA	NA	NA				
* <i>Cardiodactylus enkraussi</i> Otte, 2007	ENEO/L eb	MNHN-EO-ENSIF2 354	Cenk_C76_Butmas	Vanuatu/L	*this study	*this study	*this study	NA	*this study				
<i>Cardiodactylus enkraussi</i> Otte, 2007	ENEO/L eb	MNHN-EO-ENSIF2 366	Cenk_C9_Santo	Vanuatu/L	JF97 2518	JF97 2502	KU7 0556 1	KU7 0555 0	NA	JF97 2533	NA	NA	KU7 0559 5
<i>Cardiodactylus erniae</i> Robillard & Gorochov, 2014	ENEO/L eb	MNHN-EO-ENSIF3 492	Cern_C11_0_Java	Java/G	this study								
* <i>Cardiodactylus erniae</i> Robillard & Gorochov, 2014	ENEO/L eb	MNHN-EO-ENSIF3 489	Cern_C24_Java	Java/G	*this study								
* <i>Cardiodactylus floresiensis</i> Robillard, 2014	ENEO/L eb	MZB	Cflo_C31_Flores	Flores island/l	*this study								
<i>Cardiodactylus floresiensis</i> Robillard, 2014	ENEO/L eb	MZB	Cflo_C48_Flores	Flores island/l	this study								
<i>Cardiodactylus fruhstorferi</i> Gorochov & Robillard, 2014	ENEO/L eb	MNHN-EO-ENSIF1 596	Cfru_C11_Sulawesi	Sulawesi/H	this study	this study	NA	this study					
* <i>Cardiodactylus fruhstorferi</i> Gorochov & Robillard, 2015	ENEO/L eb	MNHN-ENSIF1 123	Cfru_C46_Sulawesi	Sulawesi/H	*this study	*this study	NA	*this study					
<i>Cardiodactylus guttulus</i> (Matsumura, 1913)	ENEO/L eb	ZIN	Cgut_C101_Vietnam	Vietnam/A	this study								
<i>Cardiodactylus guttulus</i> (Matsumura, 1913)	ENEO/L eb	ZIN	Cgut_C103_Vietnam	Vietnam/A	this study								
<i>Cardiodactylus guttulus</i> (Matsumura, 1913)	ENEO/L eb	MNHN-ENSIF1 193	Cgut_C10_Japan	Japan/A	JF97 2519	JF97 2503	KU7 0556 2	NA	JF97 2487	JF97 2534	KU7 0558 0	KU7 0561 2	KU7 0559 6
<i>Cardiodactylus guttulus</i> (Matsumura, 1913)	ENEO/L eb	ZIN	Cgut_C137_Vietnam	Vietnam/A	this study	this study	NA	this study					
* <i>Cardiodactylus guttulus</i> (Matsumura, 1913)	ENEO/L eb	LibinMa	Cgut_C45_Hainan	Hainan/A	*this study								
<i>Cardiodactylus guttulus</i> (Matsumura, 1913)	ENEO/L eb	MNHG	Cgut_C86_Ryukyu	Ryukyu island/A	this study								

Species	Taxonomy	Voucher	Molecular code	Geographic area/code	16S	12S	COI	COII	Cytb	18S	28S	EF1a	H3	
<i>Cardiodactylus haddocki</i> Dong & Robillard, 2016	ENEO/Leb	ZIN	Chad_C125_Bagusa	Bagusa/K	this stud y									
<i>Cardiodactylus haddocki</i> Dong & Robillard, 2016	ENEO/Leb	ZIN	Chad_C130_MCyclop	New Guinea/K	this stud y									
<i>Cardiodactylus haddocki</i> Dong & Robillard, 2016	ENEO/Leb	ZIN	Chad_C134_Manokwari	New Guinea/K	this stud y									
<i>Cardiodactylus haddocki</i> Dong & Robillard, 2016	ENEO/Leb	ZIN	Chad_C139_Fawi	New Guinea/K	this stud y									
* <i>Cardiodactylus haddocki</i> Dong & Robillard, 2016	ENEO/Leb	MNHN-EO-ENSIF354 1	Chad_C64_MW700	New Guinea/K	*this stud y									
<i>Cardiodactylus haddocki</i> Dong & Robillard, 2016	ENEO/Leb	MNHN-EO-ENSIF354 8	Chad_C66_Baitabag	New Guinea/K	this stud y									
<i>Cardiodactylus haddocki</i> Dong & Robillard, 2016	ENEO/Leb	MNHN-EO-ENSIF354 9	Chad_C69_MW200	New Guinea/K	this stud y									
<i>Cardiodactylus haddocki</i> Dong & Robillard, 2016	ENEO/Leb	MNHN-EO-ENSIF354 6	Chad_C89_Wanang	New Guinea/K	this stud y	NA	this stud y	this stud y						
<i>Cardiodactylus haddocki</i> Dong & Robillard, 2016	ENEO/Leb	MNHN-EO-ENSIF354 7	Chad_C90_Wanang	New Guinea/K	this stud y	NA	this stud y	this stud y						
* <i>Cardiodactylus halmahera</i> Gorochov & Robillard, 2014	ENEO/Leb	ZIN	Chalm_C38_Halmahera	Moluccas/J	*this stud y									
<i>Cardiodactylus javarare</i> Otte, 2007	ENEO/Leb	MNHN-EO-ENSIF91	Cjav_C164_Wanang	New Guinea/K	NA	this stud y	NA	this stud y	NA					
<i>Cardiodactylus javarare</i> Otte, 2007	ENEO/Leb	MNHN-EO-ENSIF60	Cjav_C165_MW200	New Guinea/K	NA	this stud y	this stud y	NA	this stud y	this stud y	this stud y	NA	this stud y	this stud y
<i>Cardiodactylus javarare</i> Otte, 2007	ENEO/Leb	MNHN-EO-ENSIF103	Cjav_C63_Wanang	New Guinea/K	this stud y	this stud y	NA	this stud y	this stud y					
* <i>Cardiodactylus javarare</i> Otte, 2007	ENEO/Leb	MNHN-EO-ENSIF353 8	Cjav_C78_Baitabag	New Guinea/K	*this stud y									
<i>Cardiodactylus kondoi</i> Otte, 2007	ENEO/Leb	MNHN-EO-ENSIF155 5	Ckon_C41_Luzon	the Philippines /D	this stud y									
* <i>Cardiodactylus kondoi</i> Otte, 2007	ENEO/Leb	MNHN-EO-ENSIF315 4	Ckon_C42_Luzon	the Philippines /D	*this stud y									
<i>Cardiodactylus kondoi</i> Otte, 2007	ENEO/Leb	UPLB-MNH	Ckon_C51_Negros	the Philippines /D	NA	this stud y	NA	this stud y						
<i>Cardiodactylus kondoi</i> Otte, 2007	ENEO/Leb	MNHN-EO-ENSIF316 0	Ckon_C53_Pollilo	the Philippines /D	this stud y	this stud y	NA	this stud y						
* <i>Cardiodactylus kotandora</i> Robillard, 2014	ENEO/Leb	MNHN-EO-ENSIF351 9	Ckot_C65_Flores	Flores Island/I	*this stud y	NA	*this stud y	*this stud y	*this stud y					
* <i>Cardiodactylus aff. lampongsi</i> Robillard & Gorochov, 2014	ENEO/Leb	ZIN	Clam_C105_Sumatra	Sumatra/C	*this stud y	*this stud y	NA	*this stud y	*this stud y	NA	*this stud y	*this stud y	*this stud y	
* <i>Cardiodactylus lampongsi</i> Robillard & Gorochov, 2014	ENEO/Leb	MNHN-EO-ENSIF349 5	Clam_C117_Sumatra	Sumatra/C	*this stud y	*this stud y	NA	*this stud y						
* <i>Cardiodactylus lombrijani</i> Robillard, 2014	ENEO/Leb	MNHN-EO-ENSIF367 5	Clom_C19_Sumbawa	Sumbawa/I	*this stud y									
<i>Cardiodactylus lombrijani</i> Robillard, 2014	ENEO/Leb	MNHN-EO-ENSIF367 3	Clom_C21_Lombok	Sumbawa/I	this stud y									
<i>Cardiodactylus lucus</i> Dong & Robillard, 2016	ENEO/Leb	MNHN-EO-ENSIF68	Cluc_C61_W200	New Guinea/K	this stud y	NA	this stud y							
<i>Cardiodactylus lucus</i> Dong & Robillard, 2016	ENEO/Leb	MNHN-EO-ENSIF67	Cluc_C62_Wanang	New Guinea/K	this stud y	NA	this stud y							
* <i>Cardiodactylus lucus</i> Dong & Robillard, 2016	ENEO/Leb	MNHN-ENSIF94	Cluc_C68_W700	New Guinea/K	*this stud y	*this stud y	NA	*this stud y						

Species	Taxonomy	Voucher	Molecular code	Geographic area/code	16S	12S	COI	COII	Cytb	18S	28S	EF1a	H3
* <i>Cardiodactylus maaei</i> Otte, 2007	ENEO/Leb	ZIN	Cmaa_C119_Biak	New Guinea/K	*this study								
<i>Cardiodactylus maaei</i> Otte, 2007	ENEO/Leb	ZIN	Cmaa_C128_Supiori	New Guinea/K	this study								
<i>Cardiodactylus manus</i> Otte, 2007	ENEO/Leb	ZIN	Cman_C127_Rani	New Guinea/K	this study								
* <i>Cardiodactylus manus</i> Otte, 2007	ENEO/Leb	ZIN	Cman_C37_Manokwari	New Guinea/K	*this study								
<i>Cardiodactylus muiri</i> Otte, 2007	ENEO/Leb	MNHN-E0-ENSIF4179	Cmui_C158_Kumawa	New Guinea/K	this study	NA							
* <i>Cardiodactylus muiri</i> Otte, 2007	ENEO/Leb	LEN2014-TR617(MZB)	Cmui_C160_Kumawa	New Guinea/K	*this study								
* <i>Cardiodactylus muria</i> Robillard, 2014	ENEO/Leb	MNHN-E0-ENSIF3481	Cmur_C18_Java	Java/G	*this study								
* <i>Cardiodactylus niugini</i> Dong & Robillard, 2016	ENEO/Leb	MNHN-E0-ENSIF113	Cniu_C54_Baitabag	New Guinea/K	*this study								
<i>Cardiodactylus niugini</i> Dong & Robillard, 2016	ENEO/Leb	MNHN-E0-ENSIF1583	Cniu_C55_MW200	New Guinea/K	this study								
<i>Cardiodactylus niugini</i> Dong & Robillard, 2016	ENEO/Leb	MNHN-E0-ENSIF73	Cniu_C70_Wanang	New Guinea/K	this study	NA	this study	this study					
<i>Cardiodactylus nobilis</i> Dong & Robillard, 2016	ENEO/Leb	MNHN-E0-ENSIF102	Cnob_C59_MW1200	New Guinea/K	this study	this study	this study	NA	this study				
* <i>Cardiodactylus nobilis</i> Dong & Robillard, 2016	ENEO/Leb	MNHN-E0-ENSIF131	Cnob_C67_MW1200	New Guinea/K	*this study	*this study	NA	*this study					
<i>Cardiodactylus novaeguineae</i> (Haan, 1842)	ENEO/Leb	ZIN	Cnov_C141_Queensland	Australia/L	this study								
<i>Cardiodactylus novaeguineae</i> (Haan, 1842)	ENEO/Leb	ZIN > MNHN-E0-ENSIF38	Cnov_C142_NewGeorgia	Solomon Island/L	this study	NA	this study	this study	this study				
<i>Cardiodactylus novaeguineae</i> (Haan, 1842)	ENEO/Leb	ZIN	Cnov_C143_Mhagen	New Guinea/K	this study								
<i>Cardiodactylus novaeguineae</i> (Haan, 1842)	ENEO/Leb	MNHN-E0-ENSIF4384	Cnov_C151_TritonBay	New Guinea/K	this study	NA	this study	NA					
<i>Cardiodactylus novaeguineae</i> (Haan, 1842)	ENEO/Leb	MNHN-E0-ENSIF1921	Cnov_C1_Lifou	New Caledonia/L	this study	this study	KU7 05564	KU7 05552	this study	KU7 05588	KU7 05588	KU7 05614	KU7 05597
<i>Cardiodactylus novaeguineae</i> (Haan, 1842)	ENEO/Leb	MZB	Cnov_C27_Biak	New Guinea/K	this study	NA	NA	NA	NA				
<i>Cardiodactylus novaeguineae</i> (Haan, 1842)	ENEO/Leb	MNHN-E0-ENSIF2030	Cnov_C2_Peavot	Vanuatu/L	JF97 2521	JF97 2506	KU7 05563	KU7 05551	JF97 2490	JF97 2537	KR9 03500	KU7 05613	KR9 03151
<i>Cardiodactylus novaeguineae</i> (Haan, 1842)	ENEO/Leb	MNHN-E0-ENSIF2038	Cnov_C3_Oubatche	New Caledonia/L	JF97 2520	JF97 2504	this study	this study	JF97 2488	JF97 2535	this study	this study	this study
* <i>Cardiodactylus novaeguineae</i> (Haan, 1842)	ENEO/Leb	MNHN-E0-ENSIF1466	Cnov_C49_Wewec	New Caledonia/L	*this study								
<i>Cardiodactylus novaeguineae</i> (Haan, 1842)	ENEO/Leb	MNHN-E0-ENSIF1512	Cnov_C5_NewIreland	New Guinea/K	this study	NA	this study						
<i>Cardiodactylus novaeguineae</i> (Haan, 1842)	ENEO/Leb	MNHN-E0-ENSIF3550	Cnov_C60_Loloata	New Guinea/K	this study								
<i>Cardiodactylus novaeguineae</i> (Haan, 1842)	ENEO/Leb	CSIRO	Cnov_C6_Queensland	Australia/L	this study	this study	NA	this study	this study	this study	this study	NA	this study
<i>Cardiodactylus novaeguineae</i> (Haan, 1842)	ENEO/Leb	MNHN-E0-ENSIF2032	Cnov_C71_Penaoru	Vanuatu/L	this study								
<i>Cardiodactylus novaeguineae</i> (Haan, 1842)	ENEO/Leb	MNHN-E0-ENSIF1925	Cnov_C72_Luganville	Vanuatu/L	this study								

Species	Taxonomy	Voucher	Molecular code	Geographic area/code	16S	12S	COI	COII	Cytb	18S	28S	EF1 a	H3
<i>Cardiodactylus novaeguineae</i> (Haan, 1842)	ENEO/Leb	MNHN-EO-ENSIF2020	Cnov_C73_BigBay	Vanuatu/L	this stud y	this stud y	this stud y	NA	this stud y	this stud y	NA	NA	NA
<i>Cardiodactylus novaeguineae</i> (Haan, 1842)	ENEO/Leb	MNHN-EO-ENSIF1474	Cnov_C87_Tanna	Vanuatu/L	this stud y	this stud y	this stud y	this stud y	this stud y	this stud y	this stud y	this stud y	this stud y
* <i>Cardiodactylus oerœ Robillard, 2014</i>	ENEO/Leb	RMNH	Coer_C43_Sulawesi	Sulawesi/H	*this stud y	*this stud y	*this stud y	*this stud y	*this stud y	*this stud y	*this stud y	*this stud y	*this stud y
<i>Cardiodactylus palawan Gorochov, 2014</i>	ENEO/Leb	ZIN	Cpal_C106_Palawan	Palawan/E	this stud y	this stud y	this stud y	this stud y	this stud y	this stud y	this stud y	this stud y	this stud y
<i>Cardiodactylus palawan Gorochov, 2014</i>	ENEO/Leb	ZIN	Cpal_C107_Palawan	Palawan/E	this stud y	this stud y	this stud y	this stud y	this stud y	this stud y	this stud y	this stud y	this stud y
* <i>Cardiodactylus palawan Gorochov, 2014</i>	ENEO/Leb	MNHN-EO-ENSIF1506	Cpal_C91_Turtle	Palawan/E	*this stud y	*this stud y	*this stud y	*this stud y	*this stud y	*this stud y	*this stud y	*this stud y	*this stud y
<i>Cardiodactylus palawan Gorochov, 2014</i>	ENEO/Leb	MNHN-EO-ENSIF1468	Cpal_C92_Palawan	Palawan/E	this stud y	this stud y	this stud y	this stud y	this stud y	this stud y	this stud y	this stud y	this stud y
<i>Cardiodactylus palawan Gorochov, 2014</i>	ENEO/Leb	MNHN-EO-ENSIF1497	Cpal_C93_Palawan	Palawan/E	this stud y	this stud y	this stud y	this stud y	this stud y	this stud y	this stud y	this stud y	this stud y
* <i>Cardiodactylus pelagus</i> Otte, 2007	ENEO/Leb	ZIN	Cpel_C109_Borneo	Borneo/F	*this stud y	*this stud y	*this stud y	*this stud y	*this stud y	*this stud y	*this stud y	*this stud y	*this stud y
<i>Cardiodactylus quatei</i> Otte, 2007	ENEO/Leb	ZIN	Cqua_C13_8_Fawi	New Guinea/K	this stud y	this stud y	this stud y	this stud y	this stud y	NA	this stud y	this stud y	this stud y
* <i>Cardiodactylus quatei</i> Otte, 2007	ENEO/Leb	2014-TR367	Cqua_C15_6_Lobo	New Guinea/K	*this stud y	*this stud y	*this stud y	*this stud y	*this stud y	*this stud y	*this stud y	*this stud y	*this stud y
<i>Cardiodactylus quatei</i> Otte, 2007	ENEO/Leb	2014-TR437	Cqua_C15_7_Urisa	New Guinea/K	this stud y	this stud y	this stud y	this stud y	this stud y	this stud y	this stud y	this stud y	this stud y
* <i>Cardiodactylus reticulatus</i> Gorochov, 2014	ENEO/Leb	ZIN	Cret_C33_Tioman	Malaysia/B	*this stud y	*this stud y	*this stud y	*this stud y	*this stud y	*this stud y	*this stud y	*this stud y	*this stud y
* <i>Cardiodactylus riga</i> Otte, 2007	ENEO/Leb	UPLB-MNH	Crig_C77_Burauen	the Philippines/D	*this stud y	*this stud y	*this stud y	*this stud y	*this stud y	*this stud y	*this stud y	*this stud y	*this stud y
<i>Cardiodactylus riga</i> Otte, 2007	ENEO/Leb	MNHN-EO-ENSIF3352	Crig_C83_LeyteS	the Philippines/D	this stud y	this stud y	this stud y	this stud y	this stud y	this stud y	this stud y	this stud y	this stud y
* <i>Cardiodactylus rufidulus</i> Saussure, 1878	ENEO/Leb	NHM-UK-BM1984-865	Cruk_C44_Guadalcanal	Solomon/L	*this stud y	*this stud y	NA	*this stud y	*this stud y	NA	*this stud y	NA	*this stud y
* <i>Cardiodactylus singapura</i> Robillard, 2011	ENEO/Leb	MNHN-EO-ENSIF2759	Csin_C12_Bukit	Singapour/B	*this stud y	*this stud y	*this stud y	*this stud y	*this stud y	*this stud y	*this stud y	*this stud y	*this stud y
* <i>Cardiodactylus sumba</i> Robillard, 2014	ENEO/Leb	MNHN-EO-ENSIF3661	Csum_C20_Sumba	Sumba/I	*this stud y	*this stud y	*this stud y	*this stud y	*this stud y	*this stud y	*this stud y	*this stud y	*this stud y
<i>Cardiodactylus sumba</i> Robillard, 2014	ENEO/Leb	MNHN-EO-ENSIF3658	Csum_C47_Sumba	Sumba/I	this stud y	this stud y	NA	this stud y	this stud y	this stud y	this stud y	this stud y	this stud y
* <i>Cardiodactylus tangkoko</i> Gorochov, 2014	ENEO/Leb	ZIN	Ctang_C116_Sulawesi	Sulawesi/H	*this stud y	*this stud y	*this stud y	*this stud y	*this stud y	*this stud y	*this stud y	*this stud y	*this stud y
* <i>Cardiodactylus tankara</i> Robillard, 2009	ENEO/Leb	MNHN-ENSIF2416	Ctank_C8_Espiritu	Vanuatu/L	*this stud y	*this stud y	*this stud y	*this stud y	*this stud y	*this stud y	*this stud y	*this stud y	*this stud y
* <i>Cardiodactylus tello</i> Robillard, 2014	ENEO/Leb	MNHN-EO-ENSIF160	Ctel_C171_Siberut	Sumatra/C	*this stud y	*this stud y	NA	NA	NA	NA	NA	NA	NA
<i>Cardiodactylus thailandia</i> Robillard, 2011	ENEO/Leb	ZIN	Ctha_C111_Thailand	Thailand/A	this stud y	this stud y	this stud y	this stud y	this stud y	this stud y	this stud y	NA	this stud y
* <i>Cardiodactylus thailandia</i> Robillard, 2011	ENEO/Leb	ZIN	Ctha_C112_Thailand	Thailand/A	*this stud y	*this stud y	*this stud y	*this stud y	*this stud y	*this stud y	*this stud y	*this stud y	*this stud y
<i>Cardiodactylus variegatus</i> Gorochov & Robillard, 2014	ENEO/Leb	ZIN	Cvar_C113_Borneo	Borneo/F	this stud y	this stud y	NA	NA	NA	NA	NA	NA	NA
* <i>Cardiodactylus variegatus</i> Gorochov & Robillard, 2014	ENEO/Leb	MNHN-EO-ENSIF3510	Cvar_C28_Borneo	Borneo/F	this stud y	this stud y	NA	this stud y	this stud y	this stud y	this stud y	NA	this stud y
* <i>Cardiodactylus variegatus</i> Gorochov & Robillard, 2014	ENEO/Leb	RMNH	Cvar_C52_Borneo	Borneo/F	*this stud y	*this stud y	*this stud y	*this stud y	*this stud y	*this stud y	*this stud y	NA	*this stud y
<i>Eneoptera guyanensis</i> Chopard, 1931	ENEO/Ene	MNHN-EO-ENSIF2741	Egu	French Guiana	AY9 0530 1	AY9 052 72 34	JX8 055 04 65	KU7 053 53 55	KU7 053 31 59	AY9 055 033 09	AY9 053 81 59	KU7 055 974 09	JX8 975 95 02
<i>Eurepinis</i> sp.	ENEO/Eur	MNHN-EO-ENSIF3155	Eursp	Australia	0367 4	038 34	055 65	055 54	039 31	040 28	035 03	NA	031 53
<i>Gryllus bimaculatus</i> De Geer, 1773	GRYL/Gry	MNHN-EO-ENSIF3524/3404	Gbi	France (Laboratory strain)	AF2 4868 5	AY9 052 92	KU7 055 55	AF2 486 145 59	AF2 145 09	KR9 030 02	KR9 030 NA	KR9 031 54	KR9

Species	Taxonomy	Voucher	Molecular code	Geographic area/code	16S	12S	COI	COII	Cytb	18S	28S	EF1a	H3
<i>Pixibinthus sonicus</i> Anso & Robillard, 2016	ENEO/Leb	MNHN-EO-ENSIF99	L59LeN CRBa	New Caledonia	KU70 5530	KU70 8012	KU70 5577	NA	KU70 5538	KU70 5546	KU70 5592	NA	KU70 5608
<i>Pixibinthus sonicus</i> Anso & Robillard, 2016	ENEO/Leb	MNHN-EO-ENSIF83	L66LeN CFN2	New Caledonia	KU70 5532	KU70 8015	KU70 5574	NA	KU70 5540	KU70 5547	KU70 5590	NA	KU70 5605
<i>Lebinthus luae</i> Robillard & Tan, 2013	ENEO/Leb	MNHN-EO-ENSIF2740	LbiS1	Singapore	JF97 2524	KR90 4017	KU70 5567	KU70 5557	JF97 2493	KR90 4199	KR90 3665	KU70 5615	KR90 3321
<i>Lebinthus lifouensis</i> Desutter-Grandcolas, 1997	ENEO/Leb	MNHN-EO-ENSIF1346	Lli	New Caledonia	AY90 5309	AY90 5279	KU70 5566	KU70 5556	AY90 5364	AY90 5336	KU70 5583	NA	KU70 5599
<i>Lebinthus nattawa</i> Robillard, 2009	ENEO/Leb	MNHN-EO-ENSIF2564	LnaN	Vanuatu	JF97 2525	JF97 2510	KU70 5568	KU70 5558	JF97 2494	JF97 2541	KU70 5584	NA	KU70 5600
<i>Lebinthus sp.</i> Stål, 1877	ENEO/Leb	MNHN-EO-ENSIF117	Lpng1	Papua New Guineae	JF97 2528	JF97 2513	KU71 5289	KU71 5288	KU70 5536	JF97 2544	KU71 5290	KU71 5292	KU71 5291
<i>Lebinthus santoensis</i> Robillard, 2009	ENEO/Leb	MNHN-EO-ENSIF2484	LsaPe	Vanuatu	KU70 5528	KU70 8011	KU70 5569	NA	KU70 5535	KU70 5543	KU70 5585	NA	KU70 5601
<i>Lebinthus santoensis</i> Robillard, 2009	ENEO/Leb	MNHN-EO-ENSIF2437	LsaV	Vanuatu	JF97 2527	JF97 2511	JX89 7405	JX89 7441	JF97 2495	JF97 2542	JX89 7467	NA	JX89 7548
<i>Lebinthus villemantae</i> Robillard, 2010	ENEO/Leb	MNHN-EO-ENSIF2739	Lvl	Sulawesi	JF97 2526	JF97 2512	KU70 5570	KU70 5559	JF97 2496	JF97 2543	KU70 5586	NA	KU70 5602
<i>Nisitrus vittatus</i> (Haan, 1842)	ENEO/Nis	MNHN-EO-ENSIF2742	NviS	Singapore	this study	this study	KU70 5572	NA	this study	AY90 5340	KR90 3667	JN88 7883	JX89 7546
<i>Nisitrus vittatus</i> (Haan, 1842)	ENEO/Nis	MNHN-EO-ENSIF3134	Nvith	Malaysia	AY90 5314	AY90 5284	KU70 5571	NA	AY90 5369	AY90 5340	KU70 5587	NA	KU70 5603
<i>Paranisitra longipes</i> Chopard, 1925	ENEO/Nis	MNHN-EO-ENSIF3157	Plo2	the Philippines	KR90 3827	KR90 4020	KU71 5287	NA	NA	KR90 4202	KR90 3668	NA	KR90 3325
<i>Swetzwilderia</i> sp.	ENEO/Leb	MNHN-EO-ENSIF2737	Ssp	Fiji	JF97 2529	JF97 2514	KU70 5579	NA	JF97 2498	JF97 2545	NA	NA	KR90 3327
<i>Xenogryllus marmoratus</i> Bolívar, 1890	ENEO/Xen	MNHN-EO-ENSIF3161	Xma2	Japan	KR90 3830	KR90 4024	NA	KU70 5560	KR90 3491	KR90 4206	NA	KU70 5610	KR90 3329

1065

1066

1067

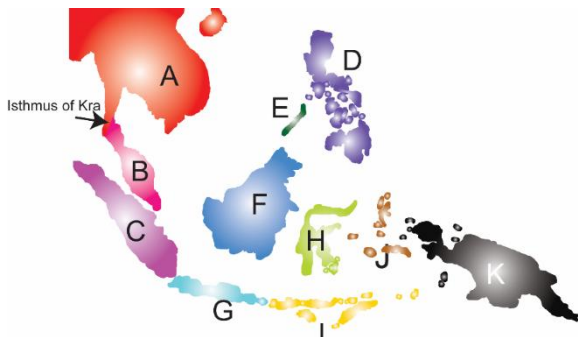
1068  
1069 **Appendix S2. Time-stratified biogeographical standards implemented in**  
1070 **BioGeoBEARS analyses.**

1071  
1072 **1. Definition of geographical areas**

1073 The map of SEA and surrounding regions was subdivided into 12 areas for the  
1074 purpose of the biogeographic analyses: A: Indochina, B: Thai-Malay Peninsula, C:  
1075 Sumatra, D: Philippines (except Palawan island), E: Palawan, F: Borneo, G: Java, H:  
1076 Sulawesi, I: Lesser Sunda Islands, J: Moluccas, K: New Guinea, L: Southwest  
1077 pacific.

1078 Here Indochina corresponds to the Southeast Asia mainland, including the  
1079 northern Ryukyu Islands (not showed on the simplified map), southeastern China  
1080 (including Taiwan), Vietnam and

1081 northern Thailand. The boundary  
1082 between Indochina and the Thai-Malay  
1083 Peninsula corresponds to the Isthmus  
1084 of Kra which intersects the north and



1085 southwest pacific is not shown on the map, but it includes the  
1086 archipelagoes located east from New Guinea.

1087

1088 **2. Dispersal rates:**

1089 Matrix of scaling factors (between 0 and 1.0) for dispersal rates between areas were  
1090 constructed according to the geographical position of the areas during a given time  
1091 slice, interpreting greater distances and/or the extent of geographical barriers (inland  
1092 river, shallow sea, deep sea) as being inversely proportional to expected rates  
1093 (Condamine et al., 2013; Toussaint and Balke, 2016). Dispersal rates were set as  
1094 follows: no barrier between two connected areas: 1.0; minor barrier between two

1095 areas, e.g., inland river, shallow sea water: 0.75; large barrier between two areas,  
1096 e.g., deep sea, strait, high mountain: 0.25; long-distance dispersal between two  
1097 areas: 0.01; absence of one area at a given time: 0. In addition, whenever two areas  
1098 were separated by one area, dispersal rates were modified as follows: 0.5 when not  
1099 involving a minor barrier; 0.25 when the area in between includes a minor barrier;  
1100 and 0.1 when the area in between encompass a major barrier.

1101

1102 **3. Time slices and dispersal multiplier matrices:**

1103 Collision events and the resumption of subduction that happened during the  
1104 Cenozoic had a great impact on SEA terrestrial biogeographic patterns and on the  
1105 current archipelago setting (Hall, 2013). Time-stratified biogeographical models were  
1106 defined according to three distinct time slices following three major paleogeological  
1107 events in SEA:

1108

1109 **3.1. Time slice 1 (45-25 Ma): Eocene to Mid Oligocene**

1110 The India-Asia collision was related to the 45 Ma plate reorganization during the  
1111 Eocene, resulting in Australia's northward moving. The Makassar Straits became a  
1112 wide marine barrier and separated west Sulawesi from core SEA. The Reed Bank-  
1113 Palawan-Mindoro Block separated from the South China margin by the opening of  
1114 the South China Sea during the Oligocene (Hall, 2002). However, at that period  
1115 Palawan was still a part of Southeast China Mainland. In the Eocene, the southern  
1116 part of the Philippines, along with the Halmahera Arc, formed part of an arc system  
1117 which extended into the Southwest Pacific at an equatorial/southern hemisphere  
1118 position. The northern Philippines, principally Luzon, was connected via the Sulu-  
1119 Cagayan Arc to northern Borneo and Sabah before the Miocene (Hall, 2002). Despite

1120 marked geological activities (collision and subduction events), oceanic islands in the  
1121 Wallacean region and New Guinea did not emerge from the sea (Hall, 2013). During  
1122 this period, some islands or parts of current island in the Southwest pacific began to  
1123 emerge, which is for example the case of New Caledonia that emerged ca. 37 Ma  
1124 (Grandcolas et al., 2008) or the Fiji islands, which were formed by subduction with  
1125 the oldest rocks being from a volcanic island-arc of late Eocene (37-34 Ma; Neall and  
1126 Trewick, 2008).

1127 Dispersal rates between well-connected areas (no barrier) were set to 1.0; this  
1128 corresponds to dispersal events between Indochina [A] and the Thai-Malay  
1129 Peninsula [B], Indochina [A] and Palawan [E], Sumatra [C] and Java [G], and Borneo  
1130 [F] and Java [G]. Dispersal areas between slightly less connected areas (minor  
1131 barrier) were assigned a rate of 0.75 (for example between the Thai-Malay Peninsula  
1132 [B] and Palawan [E]; see below for the remaining pairings). Dispersal rates between  
1133 Palawan [E] and Borneo [F] and the Philippines (minus Palawan) [D] and Borneo [F]  
1134 were set to 0.5 considering the presence of small continuous fragments of islands  
1135 between these areas. As explained above whenever two areas were separated by  
1136 one barrier, lower dispersal rates were used (0.25 and 0.1; see below for all  
1137 corresponding pairings). Finally, dispersals from the Southwest Pacific to Southeast  
1138 Asia were considered as long-distance dispersal events (rate of 0.01; see below for  
1139 all corresponding pairings).

1140  
1141

Matrix of scaling factors for dispersal rates in time slice 1 (45-25 Ma)

	A	B	C	D	E	F	G	H	I	J	K	L
A	1	1	0.5	0.25	1	0.5	0.25	0.1	0	0	0	0.01
B		1	1	0.25	0.75	0.75	0.75	0.1	0	0	0	0.01
C			1	0.25	0.75	1	1	0.1	0	0	0	0.01
D				1	0.1	0.5	0.25	0.1	0	0	0	0.01
E					1	0.75	0.5	0.1	0	0	0	0.01
F						1	1	0.25	0	0	0	0.01
G							1	0.25	0	0	0	0.01

H								1	0	0	0	0.01
I								0	0	0	0	0
J									0	0	0	0
K										0	0	0
L												1

1142

1143

1144

1145 **3.2. Time slice 2 (25-15 Ma): Mid Oligocene to Mid Miocene**

1146 Between the Eocene and Early Miocene, the southern and southeast margin of  
 1147 Sundaland were constituted of volcanic arcs (Hall, 2002). The volcanic arcs located  
 1148 on the southern and southeast margin of Sundaland were active and these events  
 1149 created a minor inner barrier within Sundaland. The Palawan Continental Terrane  
 1150 was isolated from the mainland because of the opening of Southeast China Sea and  
 1151 it drifted towards Borneo (Walia et al., 2012). New Guinea began to emerge,  
 1152 probably as small islands along the northern edge, but most of the areas, which is  
 1153 nowadays a mountain range, were covered by shallow sea (Hall, 2009, 2013).  
 1154 Oceanic islands emerged from the sea and rift deformation formed some parts of the  
 1155 Philippines and Sulawesi. In addition, deformation and uplift began in Borneo, Java  
 1156 and Sulawesi.

1157 Therefore, there are several minor barriers within Sundaland (dispersal rate of  
 1158 0.75). Long-distance dispersal was assigned to dispersal events between SEA and  
 1159 New Guinea, as well as between SEA and Southwest pacific. However, the  
 1160 emergence of continuous small fragments / islands between Sulawesi and New  
 1161 Guinea probably increased the chances for dispersal events (dispersal rate of 0.75).

1162

1163

Matrix of scaling factors for dispersal rates in time slice 2 (25-15 Ma).

	A	B	C	D	E	F	G	H	I	J	K	L
A	1	1	0.5	0.1	0.25	0.75	0.25	0.1	0	0	0.01	0.01

B		1	0.75	0.25	0.5	0.75	0.25	0.1	0	0	0.01	0.01
C			1	0.25	0.5	0.75	0.75	0.1	0	0	0.01	0.01
D				1	0.25	0.5	0.25	0.5	0	0	0.1	0.01
E					1	0.75	0.25	0.1	0	0	0.01	0.01
F						1	0.75	0.25	0	0	0.01	0.01
G							1	0.1	0	0	0.01	0.01
H								1	0	0	0.75	0.01
I									0	0	0	0.01
J										0	0	0.01
K											1	0.1
L												1

1164

1165 **3.3. Time slice 3 (15-0 Ma): Mid Miocene to present-day**

1166 The Australian margin drifted from the continent, forming the Bird's Head region of  
 1167 New Guinea, (Sula Spur promontory). By the Mid Miocene, about 15 Ma, the Sula  
 1168 Spur promontory collided with the margin of SEA in Sulawesi, forming the region now  
 1169 known as Wallacea, including the Philippines, the Moluccas, a completed Sulawesi  
 1170 and the Lesser Sunda Islands (Hall, 2009; Spakman and Hall 2010). The geological  
 1171 pattern in SEA did not change so much since these geological events. Thus,  
 1172 dispersal rates within Sundaland were assigned the same values as before (time  
 1173 slice 25-15 Ma). Considering the persistence of strings of small islands involved in  
 1174 the origin of the Wallacean region, dispersal rates between the Philippines and  
 1175 Palawan, the Philippines and Borneo, the Philippines and the Moluccas, and the  
 1176 Moluccas and New Guinea were set to 0.75.

1177

1178 Matrix of scaling factors for dispersal rates in time slice 3 (15 Ma to present day).

	A	B	C	D	E	F	G	H	I	J	K	L
A	1	1	0.5	0.1	0.25	0.75	0.1	0.1	0.01	0.01	0.01	0.01
B		1	0.75	0.1	0.25	0.75	0.25	0.1	0.1	0.01	0.01	0.01
C			1	0.25	0.25	0.75	0.75	0.1	0.25	0.01	0.01	0.01
D				1	0.75	0.75	0.25	0.5	0.25	0.75	0.25	0.01
E					1	0.75	0.25	0.1	0.25	0.1	0.01	0.01
F						1	0.75	0.25	0.5	0.1	0.01	0.01
G							1	0.1	0.75	0.1	0.01	0.01
H								1	0.5	0.75	0.25	0.01
I									1	0.5	0.25	0.01
J										1	0.75	0.25
K											1	0.5

L												1
---	--	--	--	--	--	--	--	--	--	--	--	---

1179

#### 1180 **4. Alternative dispersal multipliers**

1181 We implemented alternative sets of dispersal multiplier to test the robustness of our  
 1182 biogeographical analyses and limit the impact of the arbitrariness of the probability  
 1183 attributed to each event. Three more simplified sets of multipliers were tested using  
 1184 the following changes: except the probabilities of 0, 0.01, 0.1 and 1 that remained  
 1185 unchanged, the events with probabilities of 0.25, 0.50 and 0.75 were given  
 1186 homogenous values (either 0.15, 0.50 or 0.75) in the alternative sets of multipliers.

1187 The three resulting simplified sets of multipliers are presented below.

1188

1189

1190

1191

1192

1193

1194

1195

1196 Simplified set of dispersal multipliers 1 (0, 0.01, 0.1, 0.25, 1.0) – probabilities of 0.25, 0.5 and 0.75 in  
 1197 the base matrix are given a probability of 0.25.  
 1198

time slice 1: 45-25 Ma													
	A	B	C	D	E	F	G	H	I	J	K	L	
A	1	1	0.25	0.25	1	0.25	0.25	0.1	0	0	0	0.01	
B		1	1	0.25	0.25	0.25	0.25	0.1	0	0	0	0.01	
C			1	0.25	0.25	1	1	0.1	0	0	0	0.01	
D				1	0.1	0.25	0.25	0.1	0	0	0	0.01	
E					1	0.25	0.25	0.1	0	0	0	0.01	
F						1	1	0.25	0	0	0	0.01	
G							1	0.25	0	0	0	0.01	
H								1	0	0	0	0.01	
I									0	0	0	0	
J										0	0	0	
K											0	0	

L													1
time slice 2: 25-15 Ma													
	A	B	C	D	E	F	G	H	I	J	K	L	
A	1	1	0.25	0.1	0.25	0.75	0.25	0.1	0	0	0.01	0.01	
B		1	0.25	0.25	0.25	0.75	0.25	0.1	0	0	0.01	0.01	
C			1	0.25	0.25	0.75	0.75	0.1	0	0	0.01	0.01	
D				1	0.25	0.25	0.25	0.25	0	0	0.1	0.01	
E					1	0.25	0.25	0.1	0	0	0.01	0.01	
F						1	0.25	0.25	0	0	0.01	0.01	
G							1	0.1	0	0	0.01	0.01	
H								1	0	0	0.25	0.01	
I									0	0	0	0.01	
J										0	0	0.01	
K											1	0.1	
L												1	
time slice 3: 15 Ma to present													
	A	B	C	D	E	F	G	H	I	J	K	L	
A	1	1	0.25	0.1	0.25	0.25	0.1	0.1	0.01	0.01	0.01	0.01	
B		1	0.25	0.1	0.25	0.25	0.25	0.1	0.1	0.01	0.01	0.01	
C			1	0.25	0.25	0.25	0.75	0.1	0.25	0.01	0.01	0.01	
D				1	0.25	0.25	0.25	0.25	0.25	0.75	0.25	0.01	
E					1	0.25	0.25	0.1	0.25	0.1	0.01	0.01	
F						1	0.25	0.25	0.25	0.1	0.01	0.01	
G							1	0.1	0.25	0.1	0.01	0.01	
H								1	0.25	0.25	0.25	0.01	
I									1	0.25	0.25	0.01	
J										1	0.25	0.25	
K											1	0.25	
L												1	

1199

1200

1201

Simplified set of dispersal multipliers 2 (0, 0.01, 0.1, 0.5, 1.0) – probabilities of 0.25, 0.5 and 0.75 in the base matrix are given a probability of 0.5.

time slice 1: 45-25 Ma													
	A	B	C	D	E	F	G	H	I	J	K	L	
A	1	1	0.5	0.5	1	0.5	0.5	0.1	0	0	0	0.01	
B		1	1	0.5	0.5	0.5	0.5	0.1	0	0	0	0.01	
C			1	0.5	0.5	1	1	0.1	0	0	0	0.01	
D				1	0.1	0.5	0.5	0.1	0	0	0	0.01	
E					1	0.5	0.5	0.1	0	0	0	0.01	
F						1	1	0.5	0	0	0	0.01	
G							1	0.5	0	0	0	0.01	
H								1	0	0	0	0.01	
I									0	0	0	0	
J										0	0	0	
K											0	0	
L												1	
time slice 2: 25-15 Ma													

	A	B	C	D	E	F	G	H	I	J	K	L
A	1	1	0.5	0.1	0.5	0.5	0.5	0.1	0	0	0.01	0.01
B		1	0.5	0.5	0.5	0.5	0.5	0.1	0	0	0.01	0.01
C			1	0.5	0.5	0.5	0.5	0.1	0	0	0.01	0.01
D				1	0.5	0.5	0.5	0.5	0	0	0.1	0.01
E					1	0.5	0.5	0.1	0	0	0.01	0.01
F						1	0.5	0.5	0	0	0.01	0.01
G							1	0.1	0	0	0.01	0.01
H								1	0	0	0.5	0.01
I									0	0	0	0.01
J										0	0	0.01
K											1	0.1
L												1

time slice 3: 15 Ma to present

	A	B	C	D	E	F	G	H	I	J	K	L
A	1	1	0.5	0.1	0.5	0.5	0.1	0.1	0.01	0.01	0.01	0.01
B		1	0.5	0.1	0.5	0.5	0.5	0.1	0.1	0.01	0.01	0.01
C			1	0.5	0.5	0.5	0.5	0.1	0.5	0.01	0.01	0.01
D				1	0.5	0.5	0.5	0.5	0.5	0.5	0.5	0.01
E					1	0.5	0.5	0.1	0.5	0.1	0.01	0.01
F						1	0.5	0.5	0.5	0.1	0.01	0.01
G							1	0.1	0.5	0.1	0.01	0.01
H								1	0.5	0.5	0.5	0.01
I									1	0.5	0.5	0.01
J										1	0.5	0.5
K											1	0.5
L												1

1203

1204

1205

Simplified set of dispersal multipliers 3 (0, 0.01, 0.1, 0.75, 1.0) – probabilities of 0.25, 0.5 and 0.75 in the base matrix are given a probability of 0.75.

1206

	time slice 1: 45-25 Ma											
	A	B	C	D	E	F	G	H	I	J	K	L
A	1	1	0.75	0.75	1	0.75	0.75	0.1	0	0	0	0.01
B		1	1	0.75	0.75	0.75	0.75	0.1	0	0	0	0.01
C			1	0.75	0.75	1	1	0.1	0	0	0	0.01
D				1	0.1	0.75	0.75	0.1	0	0	0	0.01
E					1	0.75	0.75	0.1	0	0	0	0.01
F						1	1	0.75	0	0	0	0.01
G							1	0.75	0	0	0	0.01
H								1	0	0	0	0.01
I									0	0	0	0
J										0	0	0
K											0	0
L												1

	time slice 2: 25-15 Ma											
	A	B	C	D	E	F	G	H	I	J	K	L
A	1	1	0.75	0.1	0.75	0.75	0.75	0.1	0	0	0.01	0.01

B		1	0.75	0.75	0.75	0.75	0.75	0.1	0	0	0.01	0.01
C			1	0.75	0.75	0.75	0.75	0.1	0	0	0.01	0.01
D				1	0.75	0.75	0.75	0.75	0	0	0.1	0.01
E					1	0.75	0.75	0.1	0	0	0.01	0.01
F						1	0.75	0.75	0	0	0.01	0.01
G							1	0.1	0	0	0.01	0.01
H								1	0	0	0.75	0.01
I									0	0	0	0.01
J										0	0	0.01
K											1	0.1
L												1
time slice 3: 15 Ma to present												
	A	B	C	D	E	F	G	H	I	J	K	L
A	1	1	0.75	0.1	0.75	0.75	0.1	0.1	0.01	0.01	0.01	0.01
B		1	0.75	0.1	0.75	0.75	0.75	0.1	0.1	0.01	0.01	0.01
C			1	0.75	0.75	0.75	0.75	0.1	0.75	0.01	0.01	0.01
D				1	0.75	0.75	0.75	0.75	0.75	0.75	0.75	0.01
E					1	0.75	0.75	0.1	0.75	0.1	0.01	0.01
F						1	0.75	0.75	0.75	0.1	0.01	0.01
G							1	0.1	0.75	0.1	0.01	0.01
H								1	0.75	0.75	0.75	0.01
I									1	0.75	0.75	0.01
J										1	0.75	0.75
K											1	0.75
L												1

1207

1208

1209 **References**

- 1210 Condamine, F.L., Sperling, F.A.H., Kergoat, G.J., 2013. Global biogeographical pattern of swallowtail  
 1211 diversification demonstrates alternative colonization routes in the Northern and Southern  
 1212 hemispheres. *J. Biogeogr.* 40, 9–23.
- 1213 Dong, J., Robillard, T., 2016. The *Cardiodactylus* crickets from Eastern New Guinea, with description  
 1214 of five new species (Orthoptera: Gryllidae: Eneopterinae), in Robillard, T., Legendre, F.,  
 1215 Villemant, C., Leponce, M. (Eds.), *Insects of Mount Wilhelm, Papua New Guinea*. Muséum  
 1216 national d'Histoire naturelle, Paris, pp. 203–258.
- 1217 Grandcolas, P., Murienne, J., Robillard, T., Desutter-Grandcolas, L., Jourdan, H., Guilbert, E.,  
 1218 Deharveng, L., 2008. New Caledonia: a very old Darwinian island? *Phil. Trans. R. Soc. B.* 363,  
 1219 3309–3317.

- 1220 Hall, R., 2002. Cenozoic geological and plate tectonic evolution of SE Asia and the SE Pacific:  
 1221 computer-based reconstructions, model and animations. *J. Asian Earth Sci.* 20, 353–431.
- 1222 Hall, R., 2009. Southeast Asia's changing palaeogeography. *Blumea*. 54, 148–161.
- 1223 Hall, R., 2013. The palaeogeography of Sundaland and Wallacea since the Late Jurassic. *J Limnol* 72,  
 1224 1–17.
- 1225 Neall, V.E., Trewick, S.A., 2008. The age and origin of the Pacific islands: a geological overview. *Phil.  
 1226 Trans. R. Soc. B* 363, 3293–3308.
- 1227 Robillard, T., Gorochov, A.V., Poulain, S., Suhardjono, Y.R., 2014. Revision of the cricket genus  
 1228 *Cardiodactylus* (Orthoptera, Eneopterinae, Lebinthini): the species from both sides of the  
 1229 Wallace line, with description of 25 new species. *Zootaxa*, 3854, 1–104.
- 1230 Spakman, W., Hall, R., 2010. Surface deformation and slab-mantle interaction during Banda arc  
 1231 subduction rollback. *Nat. Geosci.* 3, 562–566.
- 1232 Toussaint, E.F.A., Balke, M., 2016. Historical biogeography of *Polyura* butterflies in the oriental  
 1233 Palaeotropics: trans-archipelagic routes and South Pacific island hopping. *J. Biogeogr.* 43,  
 1234 1560–1572.
- 1235 Walia, M., Knittel, U., Suzuki, S., Chung, S., Pena, R.E., 2012. No Paleozoic metamorphics in Palawan  
 1236 (the Philippines)? Evidence from single grain U-Pb dating of detrital zircons. *J. Asian Earth Sci.*  
 1237 52, 134–145.

1238 **Appendix S3.** Summary of ancestral area estimation with different models and  
 1239 dispersal rate multipliers with time slices (**Table S3a**) and without time slices  
 1240 (**Table S3b**). The gray line highlights the model with the highest statistical  
 1241 support.

1242 **Table S3a.**  
 1243

Multipliers sets	max_range_size	Speciation model	LnL	Parameter estimates	
				d	e
(0, 0.01, 0.1, 0.25, 0.5, 0.75, 1.0)	2	DEC	-128.05	0.024	0.0175
		DIVALIKE	-126.55	0.024	0.0137
		BAYAREALIKE	-140.47	0.036	0.0445
	3	DEC	-131.32	0.016	0.0162
		DIVALIKE	-131.19	0.018	0.0139
		BAYAREALIKE	-143.99	0.019	0.0537
	4	DEC	-131.55	0.015	0.0154
		DIVALIKE	-131.51	0.018	0.0134
		BAYAREALIKE	-145.04	0.016	0.0584
(0, 0.01, 0.1, 0.25, 1.0)	2	DEC	-128.99	0.038	0.0168
		DIVALIKE	-127.65	0.039	0.0133
		BAYAREALIKE	-142.26	0.055	0.0421
	3	DEC	-132.57	0.026	0.0157

		DIVALIKE	-132.70	0.029	0.0135
		BAYAREALIKE	-146.60	0.030	0.0538
(0, 0.01, 0.1, 0.5, 1.0)	4	DEC	-132.86	0.024	0.0150
		DIVALIKE	-132.99	0.028	0.0131
		BAYAREALIKE	-147.61	0.025	0.0594
		DEC	-130.83	0.022	0.0172
(0, 0.01, 0.1, 0.75, 1.0)	2	DIVALIKE	-129.53	0.022	0.0139
		BAYAREALIKE	-143.73	0.032	0.0436
		DEC	-134.27	0.015	0.0160
	3	DIVALIKE	-134.48	0.017	0.0141
		BAYAREALIKE	-147.39	0.017	0.0545
		DEC	-134.42	0.014	0.0153
	4	DIVALIKE	-134.80	0.016	0.0136
		BAYAREALIKE	-148.17	0.014	0.0602
		DEC	-132.14	0.015	0.0175
1244 1245 1246 1247 1248	2	DIVALIKE	-130.88	0.016	0.0143
		BAYAREALIKE	-144.67	0.022	0.0446
		DEC	-133.82	0.010	0.0158
	3	DIVALIKE	-135.75	0.012	0.0144
		BAYAREALIKE	-147.93	0.012	0.0549
		DEC	-135.47	0.009	0.0155
	4	DIVALIKE	-136.10	0.011	0.0140
		BAYAREALIKE	-148.59	0.010	0.0607

**Table S3b (without time slices)**

Multipliers sets	max_range_size	Speciation model	LnL	Parameter estimates	
				d	e
(0, 0.01, 0.1, 0.25, 0.5, 0.75, 1.0)	2	DEC	-111.70	0.016	0.0122
		DIVALIKE	-105.83	0.015	0.0066
		BAYAREALIKE	-131.77	0.005	0.0342
	3	DEC	-113.29	0.012	0.0109
		DIVALIKE	-108.70	0.012	0.0056
		BAYAREALIKE	-138.14	0.002	0.0358
	4	DEC	-113.23	0.011	0.0093
		DIVALIKE	-120.49	0.003	0.0065
		BAYAREALIKE	-138.69	0.002	0.0369

#### Appendix S4. Sampling of species groups for the BAMM analyses.

Because *C. javarere* and *C. kolombangara* show intermediate characters between *Novaeguineae* and *Efordi* species groups (Dong and Robillard, 2016), these two species form a third species group, hereby referred as the *Javarere* species group. Therefore, for the purpose of the BAMM analyses we considered that there are 60 species in *Novaeguineae* species group, 20 in *Efordi* species group and two in *Javarere* species group. In total, there are 35 species of the *Novaeguineae* species

1259 group and one of the *Efordi* species group in SEA. The number of species in each  
1260 species group and the sampling fraction in BAMM analyses were given in TableS4.

1261

1262 **Table S4.** Species sampling fraction in BAMM analyses.

Species group	Total numbers	Numbers in SEA	Sampling fraction
<i>Novaeguineae</i>	60/35	35/28	0.58
<i>Efordi</i>	20/5	1/0	0.25
'Javarere'	2/1	0/0	0.5

1263

1264 Note: Numbers (\*/\*) in the column named “Total numbers” correspond to the total  
1265 numbers in each species group (left of sign /) and the species numbers in this study  
1266 (right of sign /), respectively. Numbers (\*/\*) in the column named “Numbers in SEA”  
1267 correspond the total numbers in each species group distributed in SEA (left of sign /)  
1268 and the species numbers in this study in SEA (right of sign /), respectively. “Sampling  
1269 fraction” corresponds the proportion of the number of species sampled in this study  
1270 vs total numbers of each species group.

1271

1272 **Appendix S5.** Gene trees inferred for each marker: 16S (a), 12S (b), COI (c), COII

1273 (d), Cytb (e), 18S (f), 28S (g), EF1a (h), H3 (i).

1274 **16S (a):**



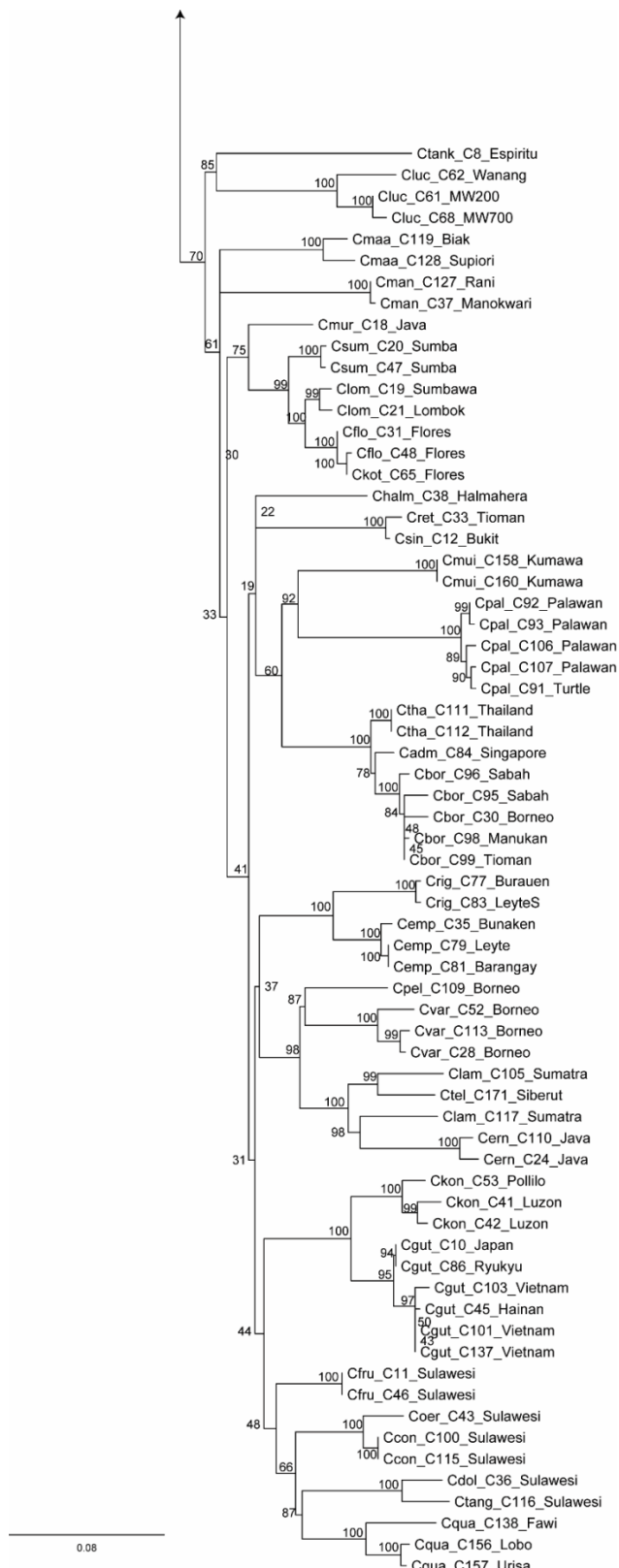
1275

(continued)

1276

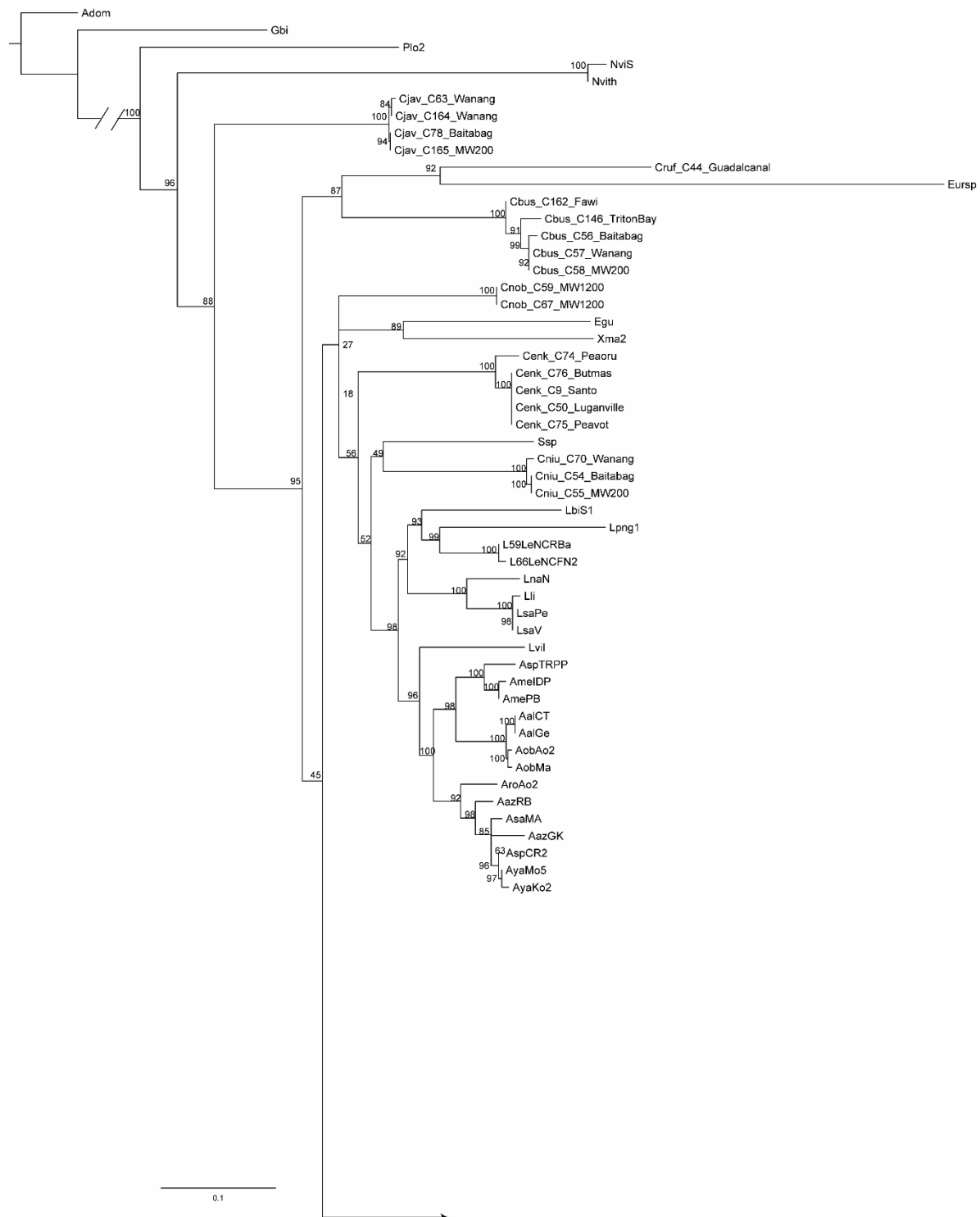
1277

1278

1280 **16S (a): continued**

1283

1284 **12S (b):**



1285

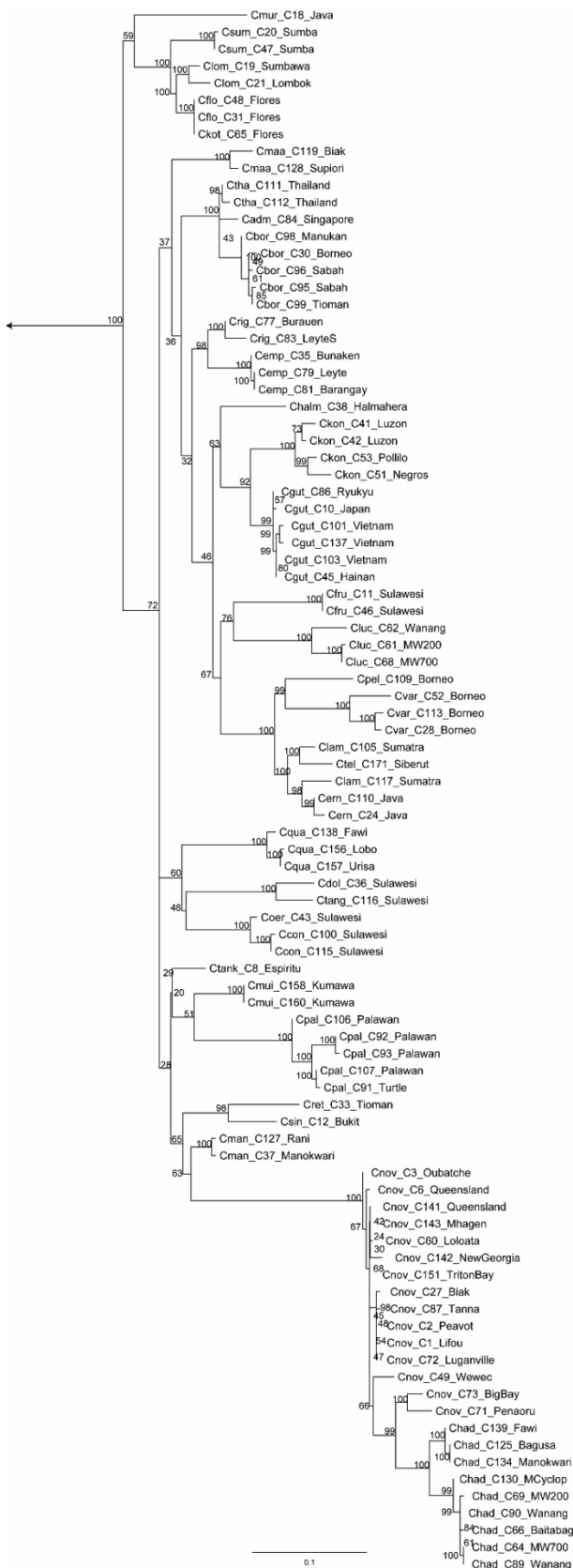
1286

(continued)

1287

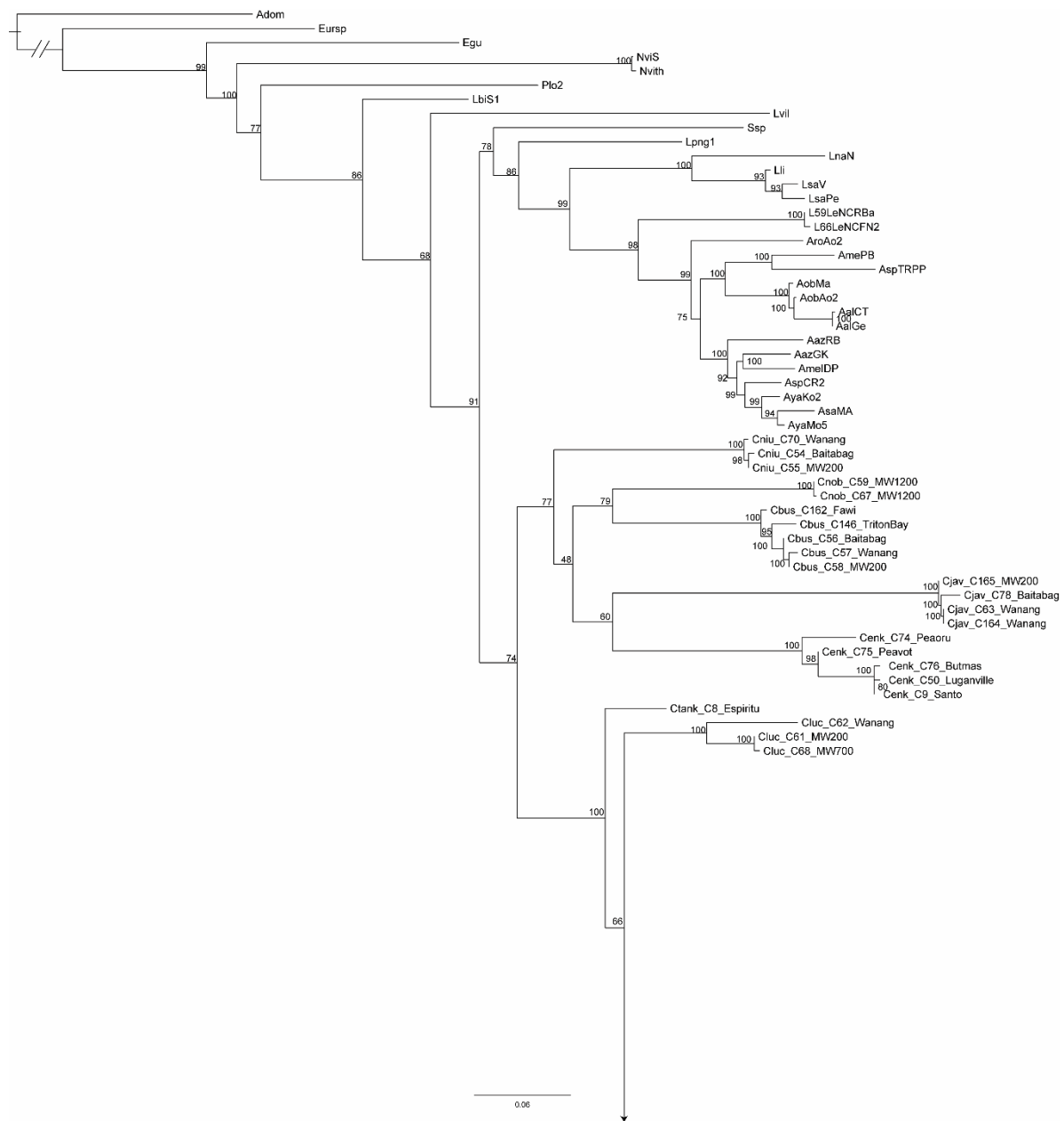
1288

## 1290 12S (b): continued



1293

1294 COI (c):



1295

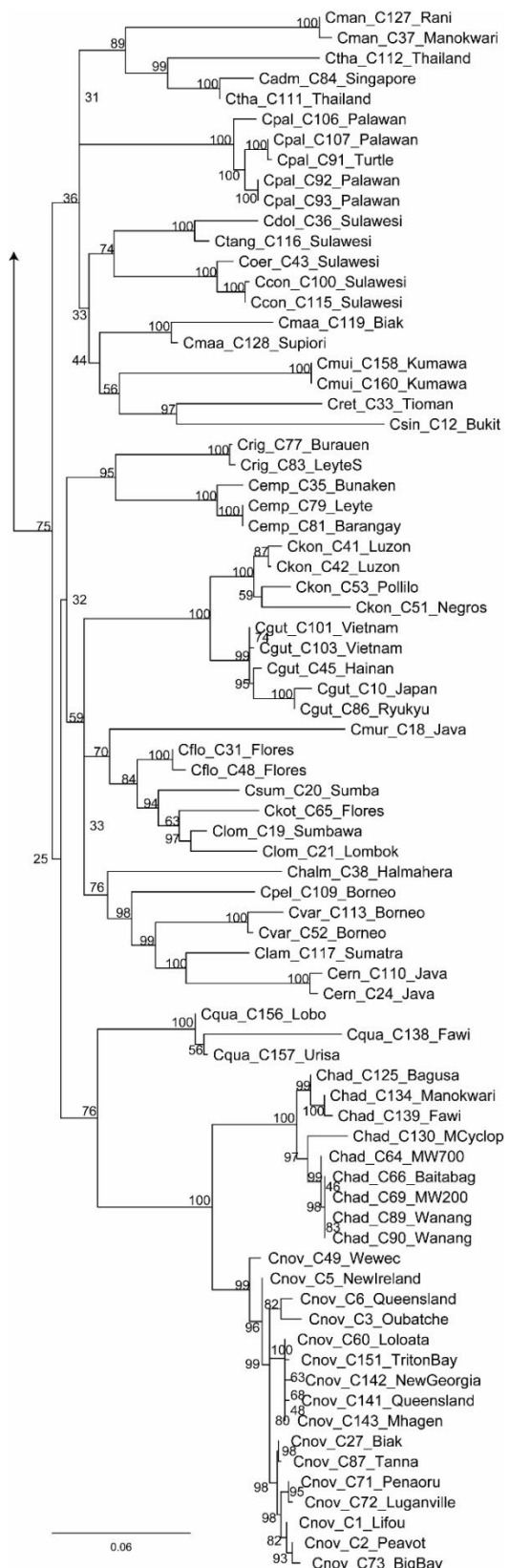
1296

*(continued)*

1297

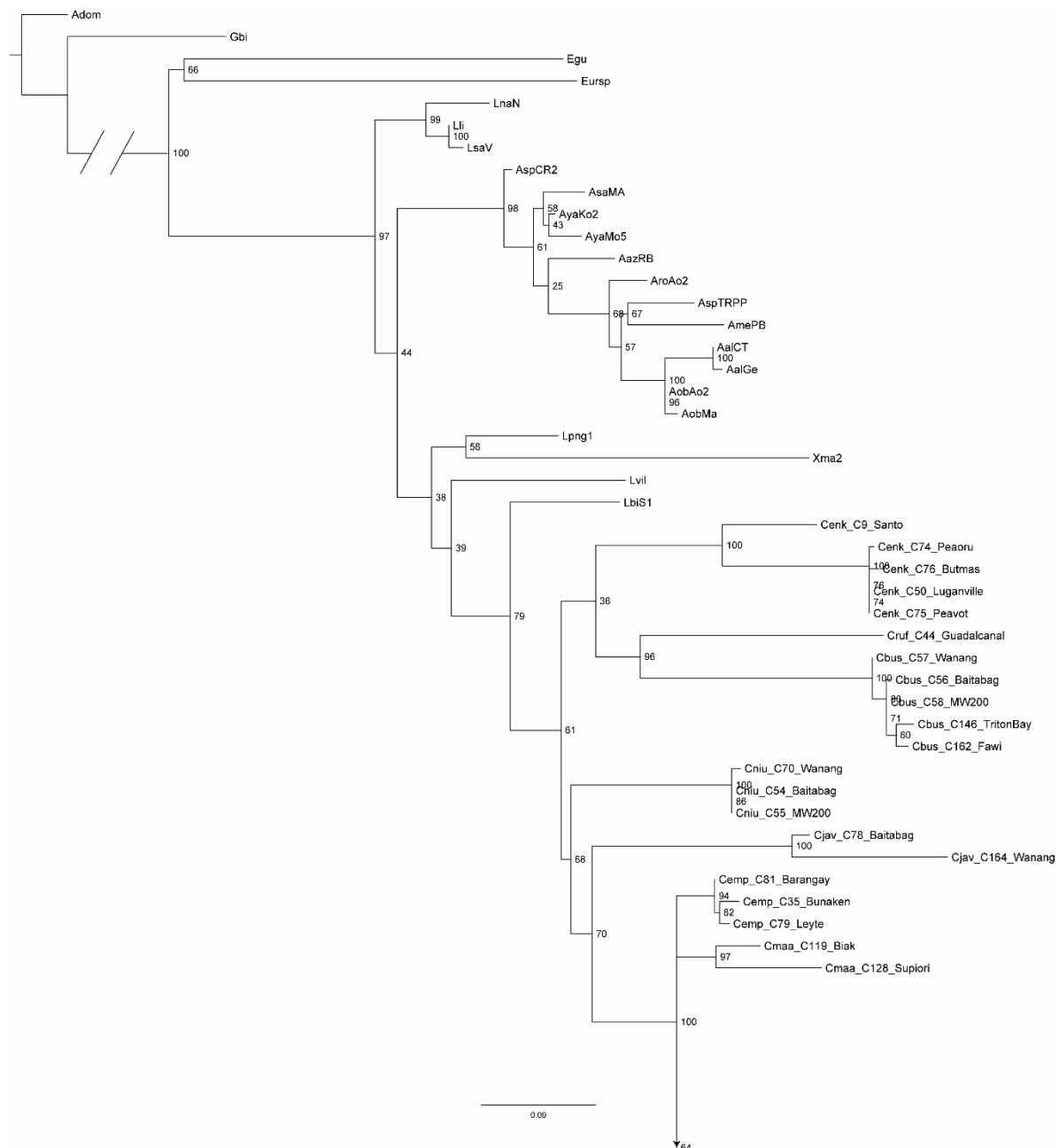
1298

1299



1305

1306 **COII (d):**



1307

1308

(continued)

1309

1310

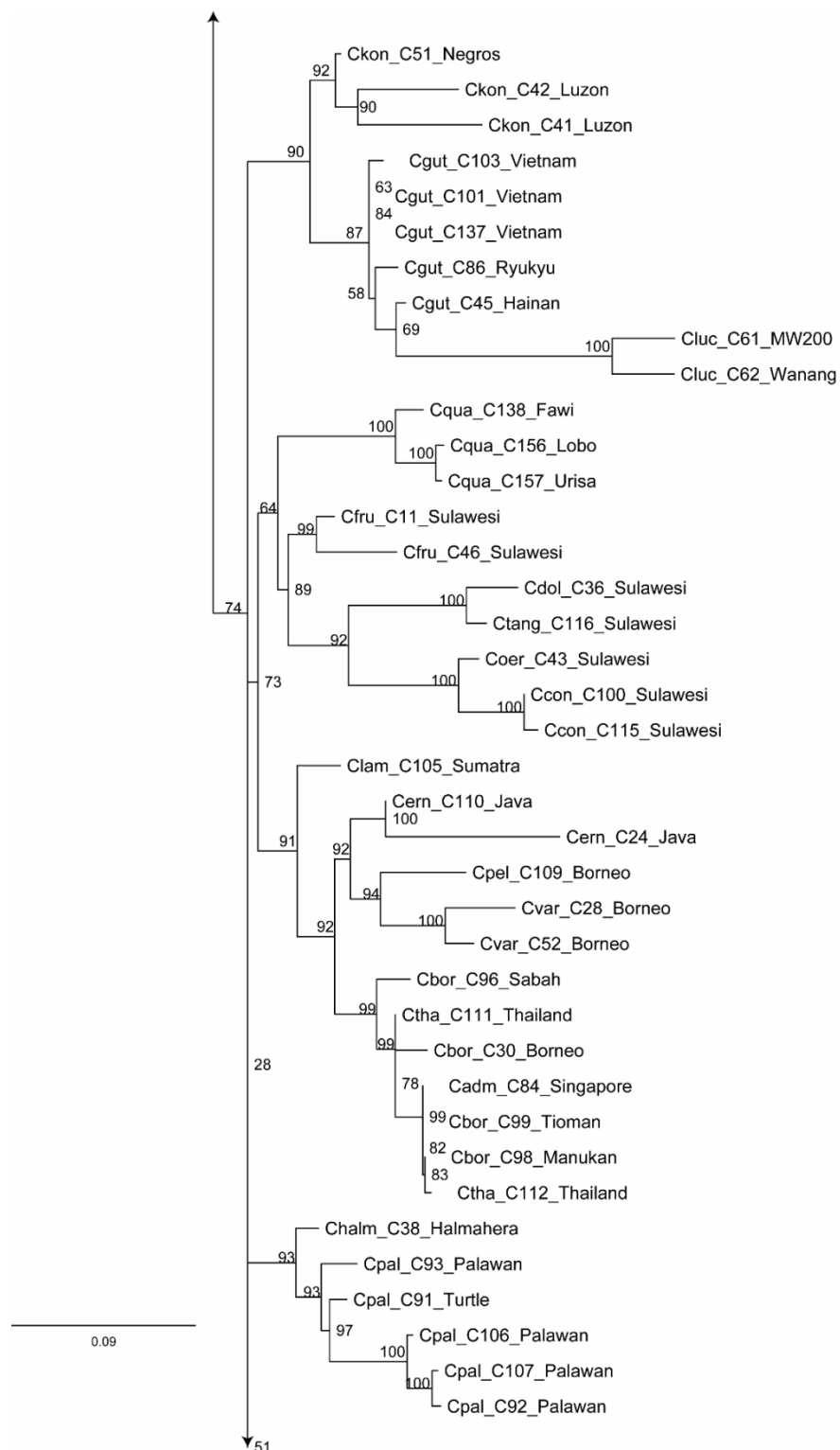
1311

1312

1313

1314

1315 **COII (d): continued**



1316

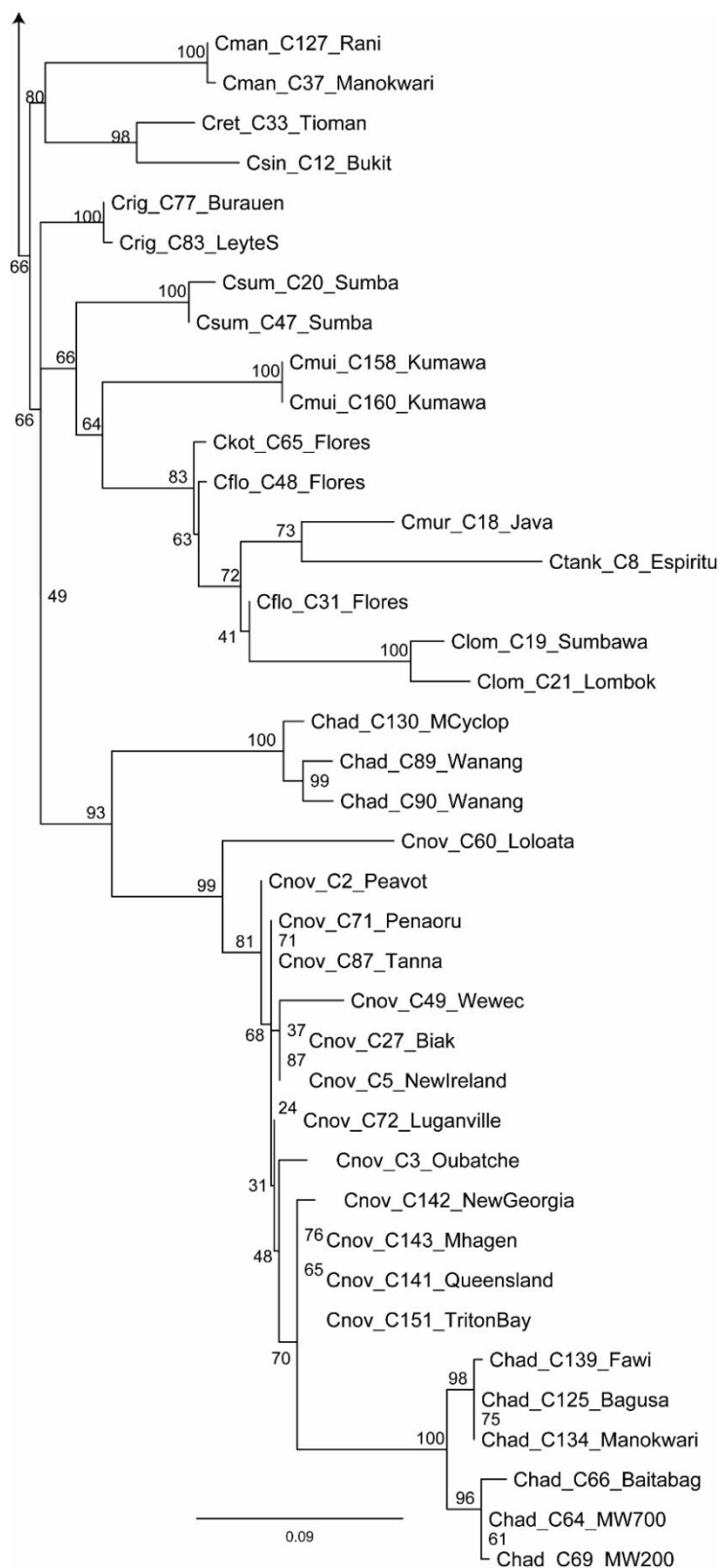
1317

(continued)

1318

1319

1320 **COII (d): continued**

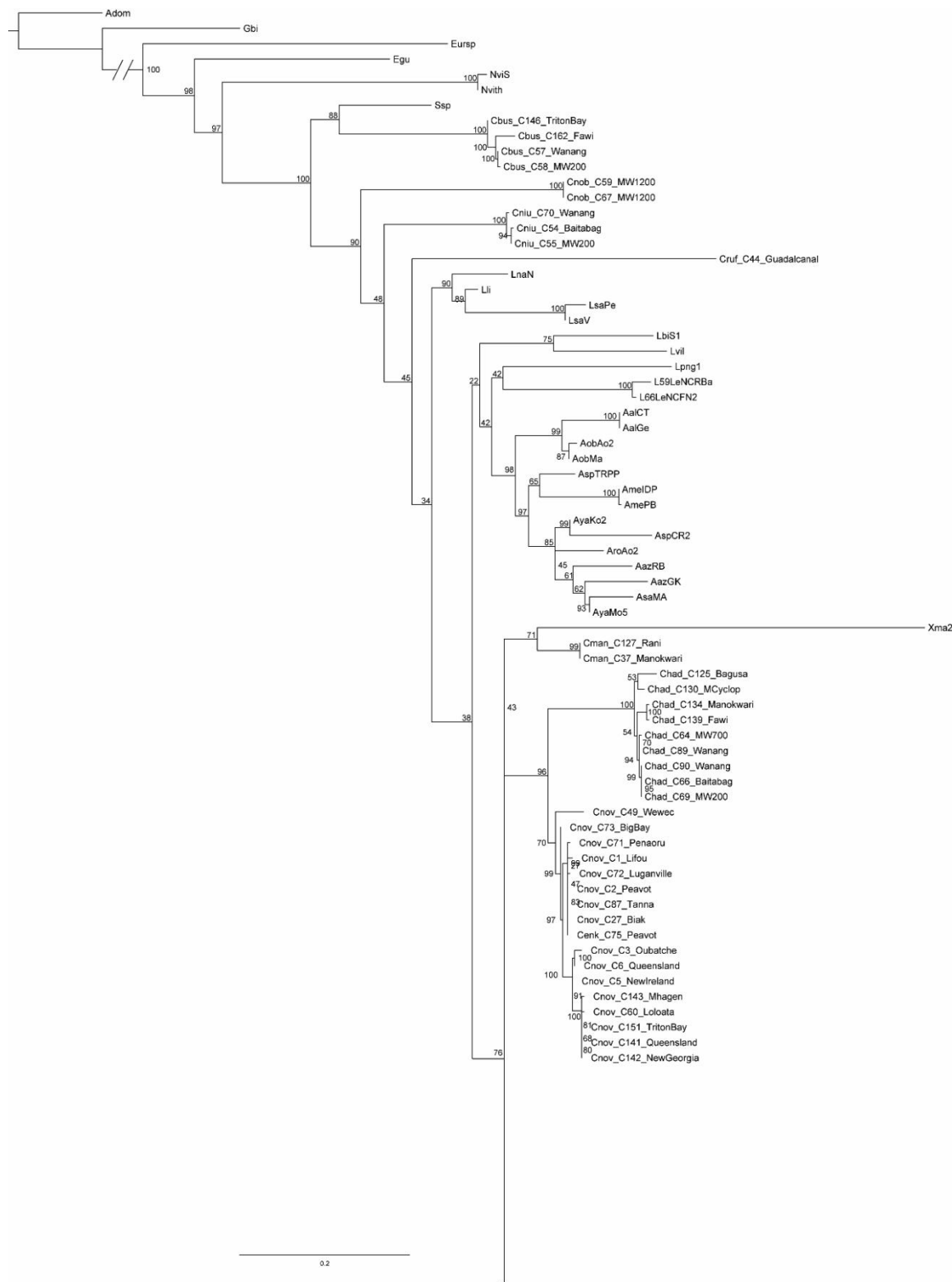


1321

1322

1323

1324 Cytb (e):



1325

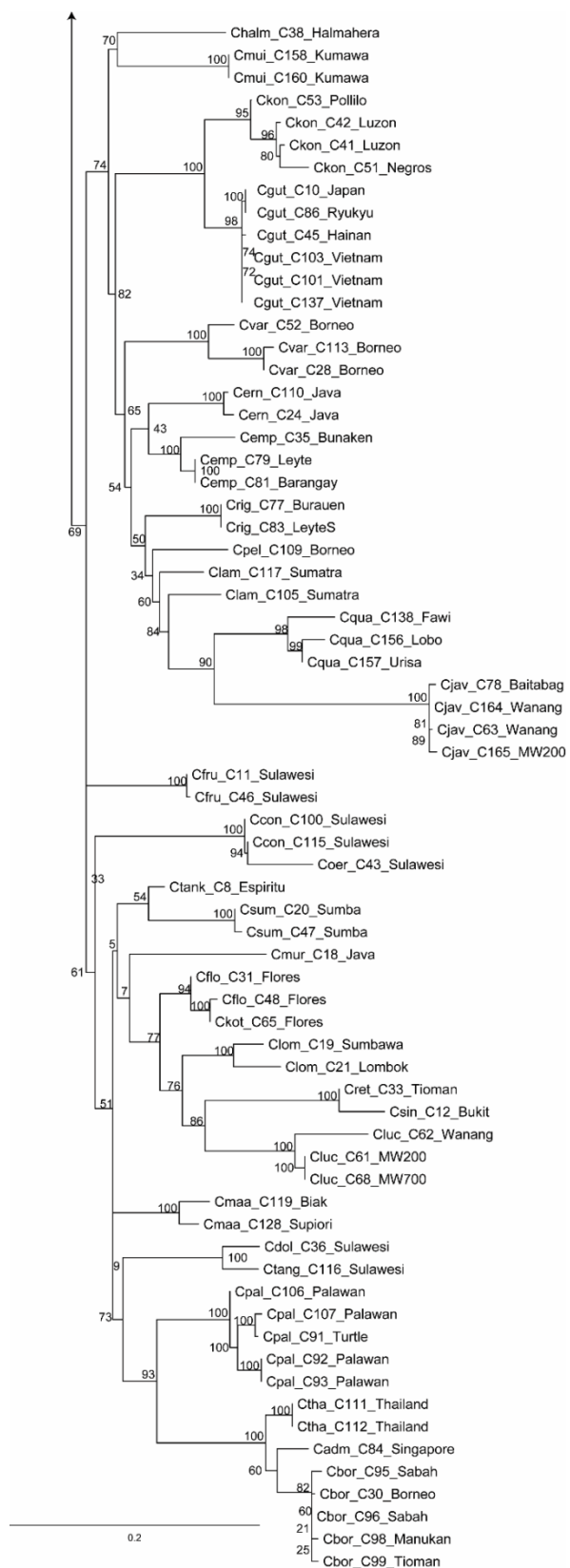
1326

(continued)

1327

1328

1329 **Cytb (e): continued**

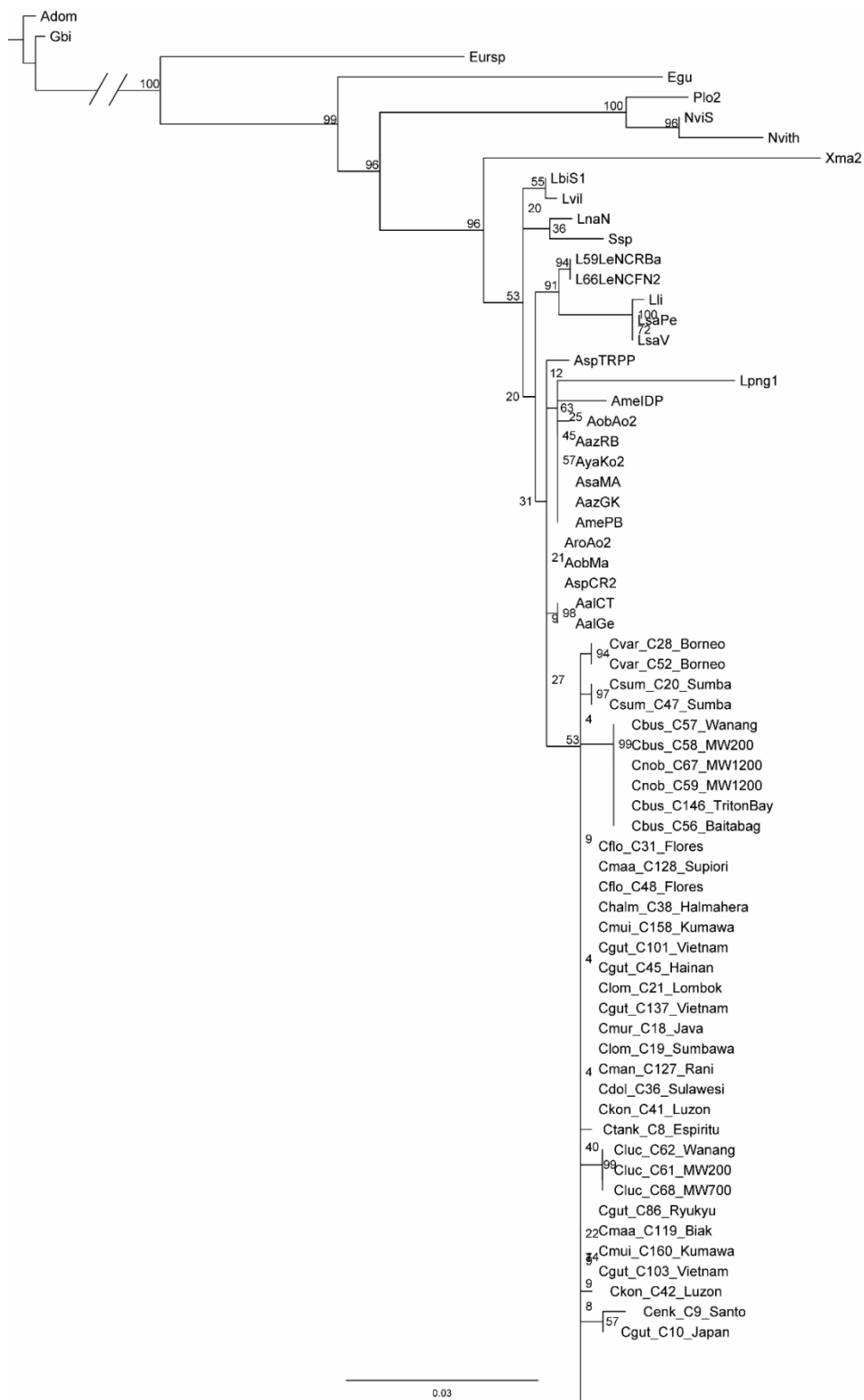


1330

1331

1332

1333 **18S (f):**



1334

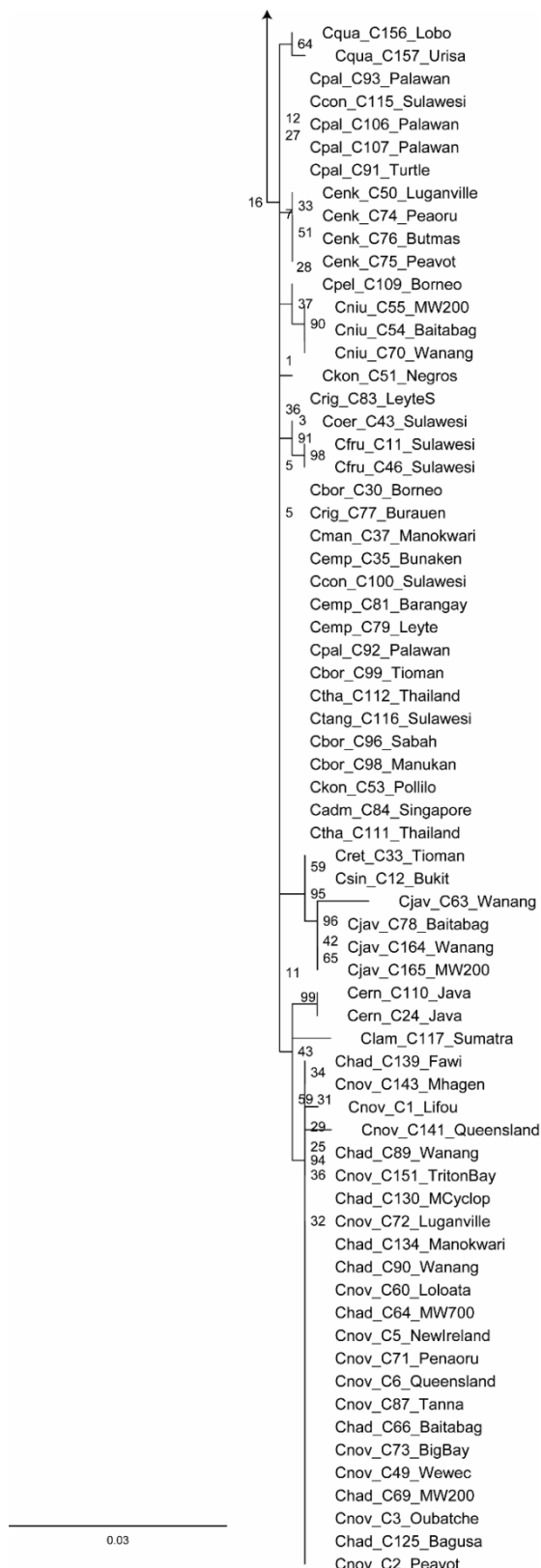
1335

(continued)

1336

1337

1338 **18S (f): continued**

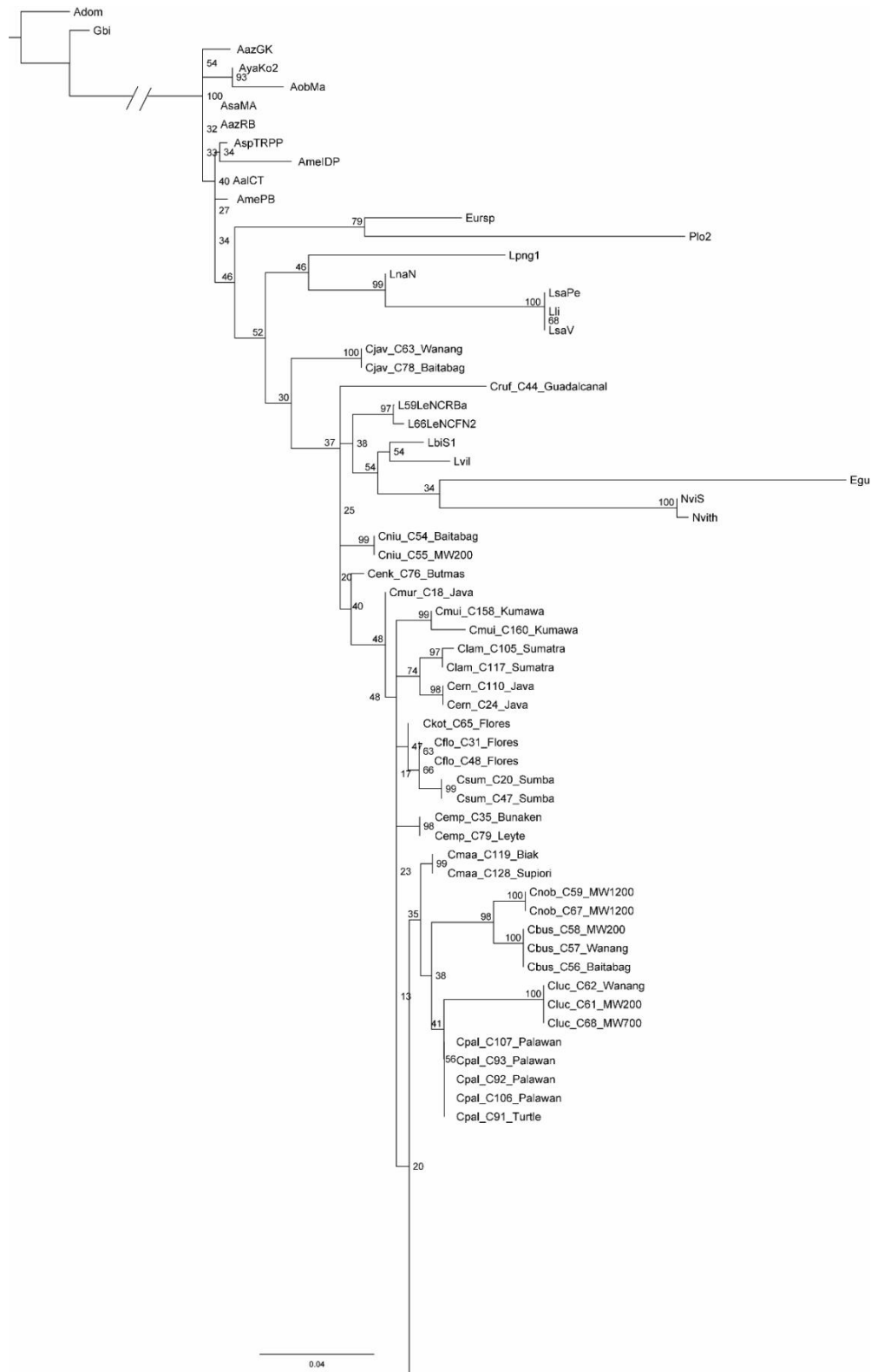


1339

1340

1341

1342 28S (g):



1343

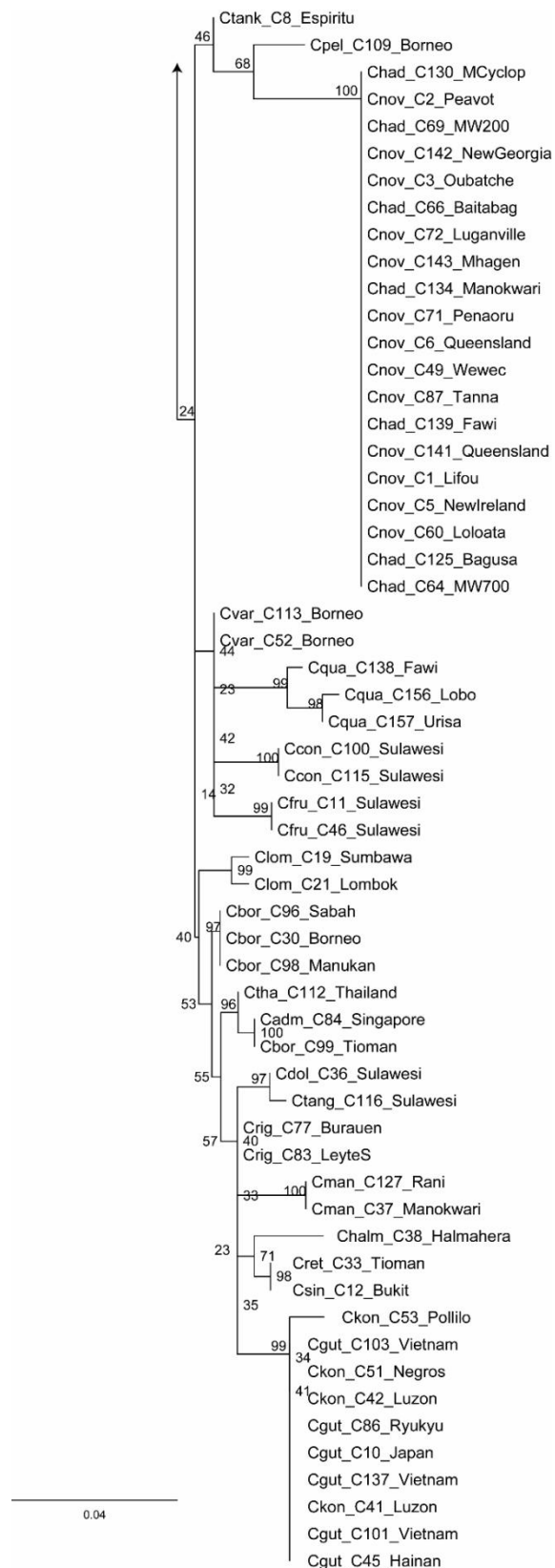
1344

(continued)

1345

1346

1347 **28S (g): continued**



1348

1349

1350

1351 EF1a (h):



1352

1353

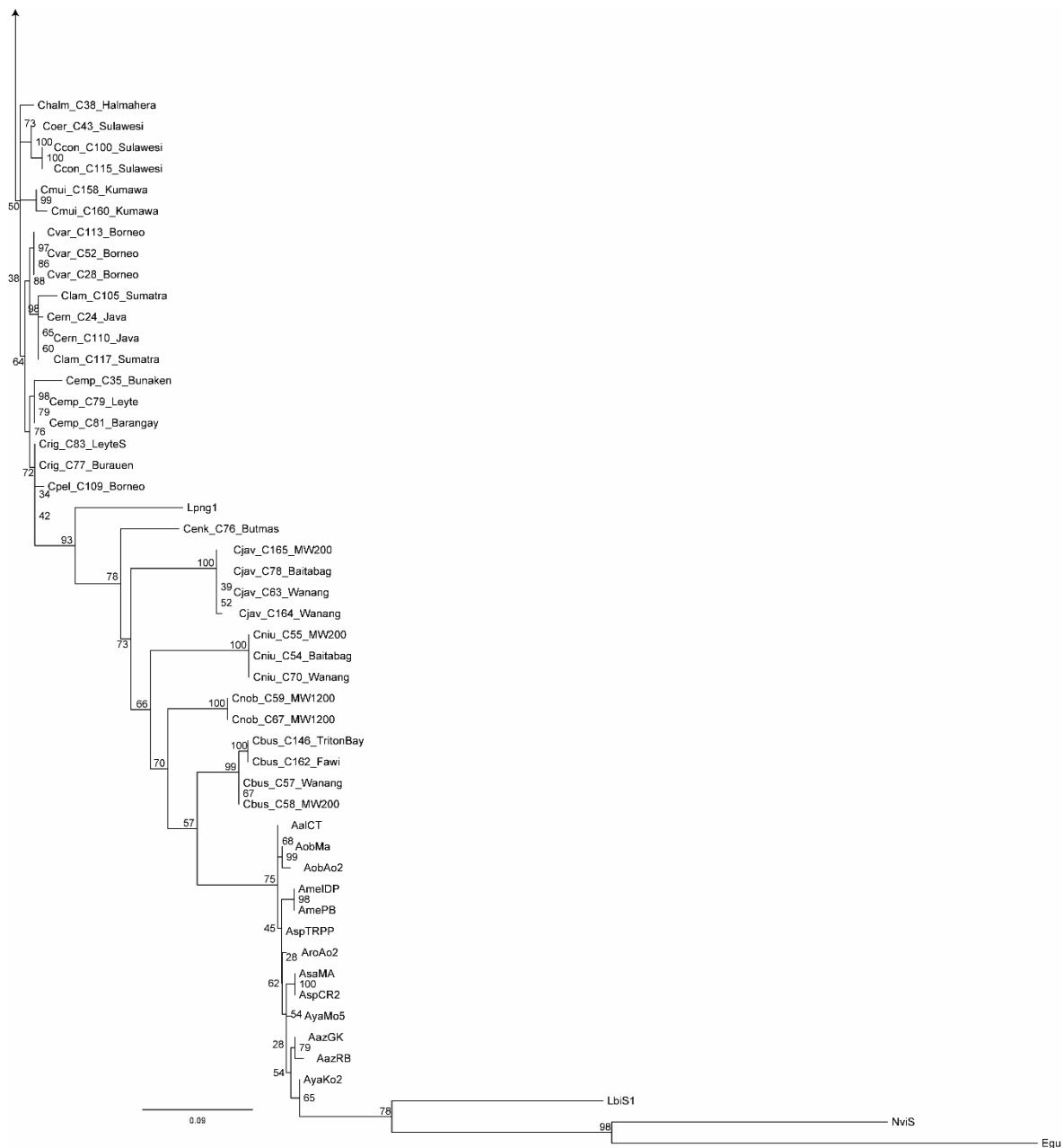
(continued)

1354

1355

1356

## 1357 EF1a (h): continued



1358

1359

1360

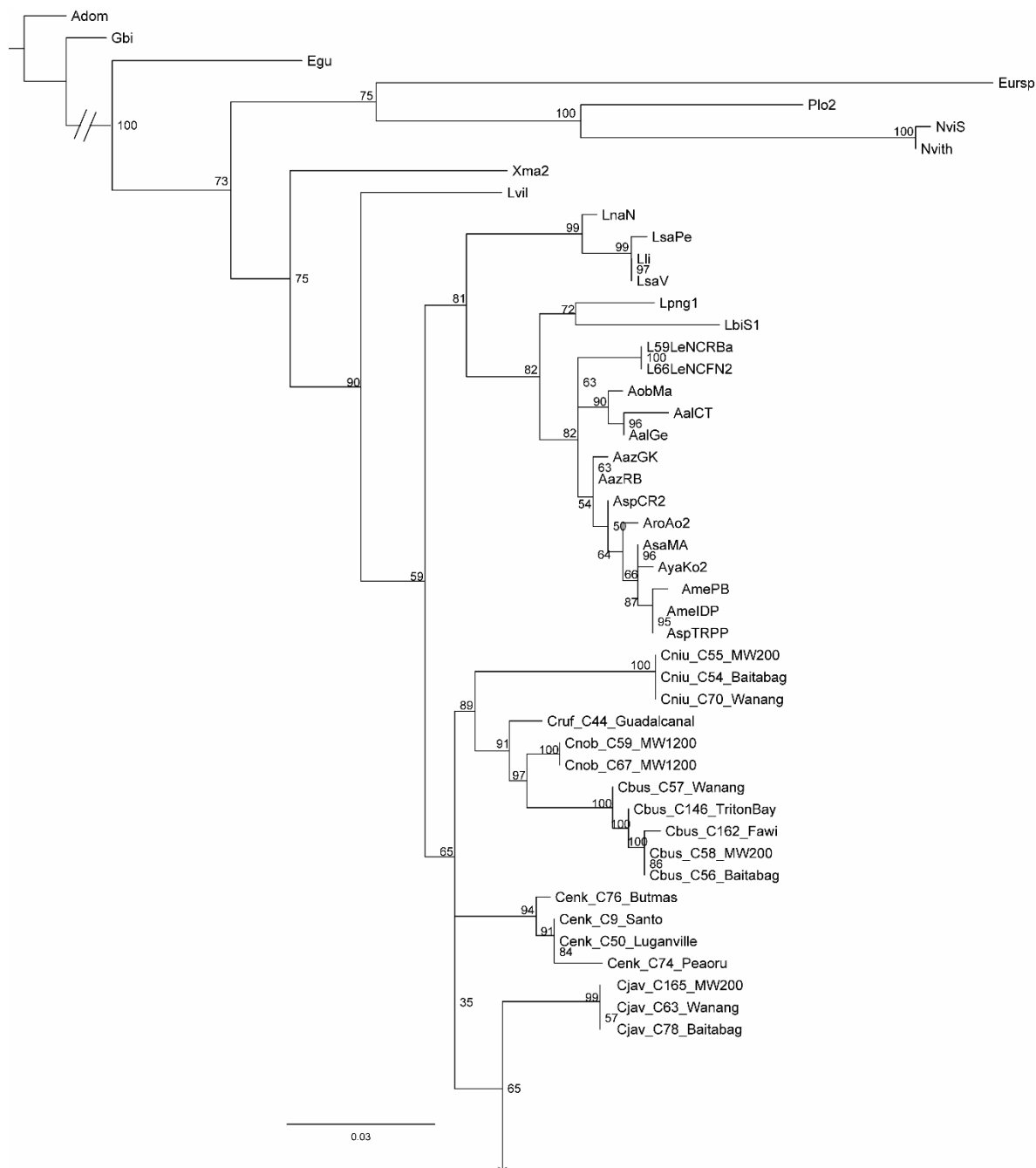
1361

1362

1363

1364

1365

**H3 (i):**

1366

1367

(continued)

1368

1369

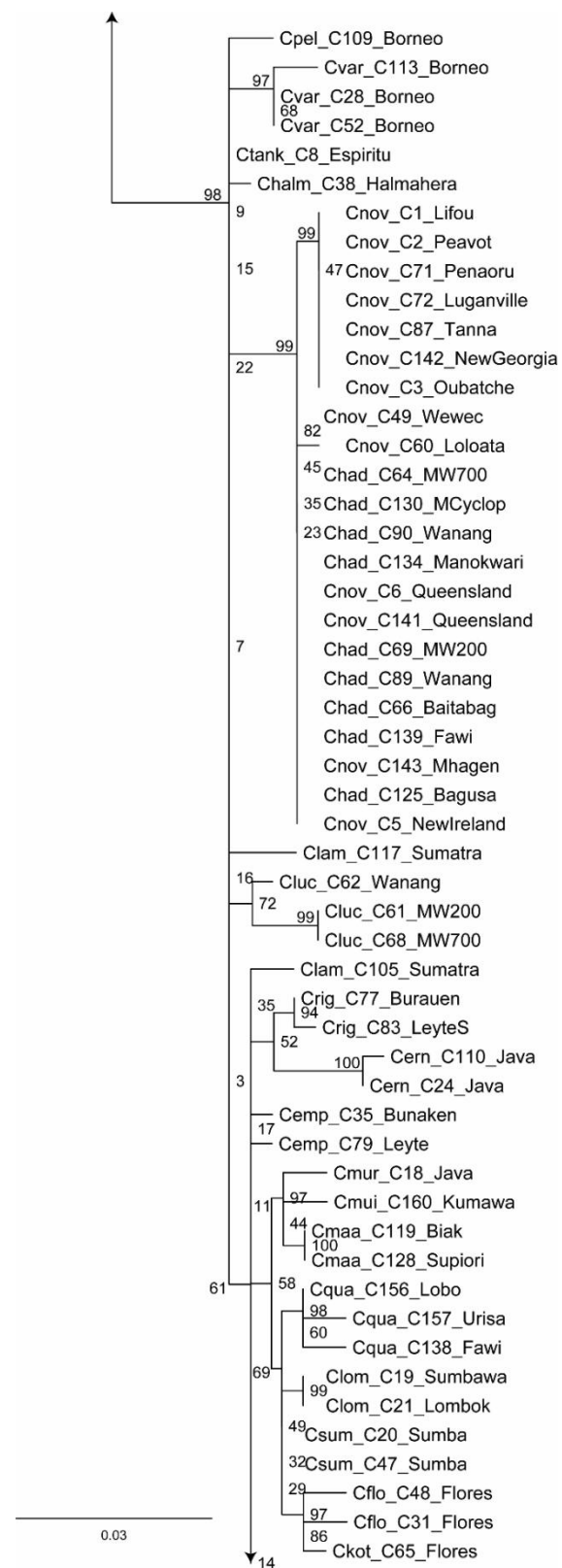
1370

1371

1372

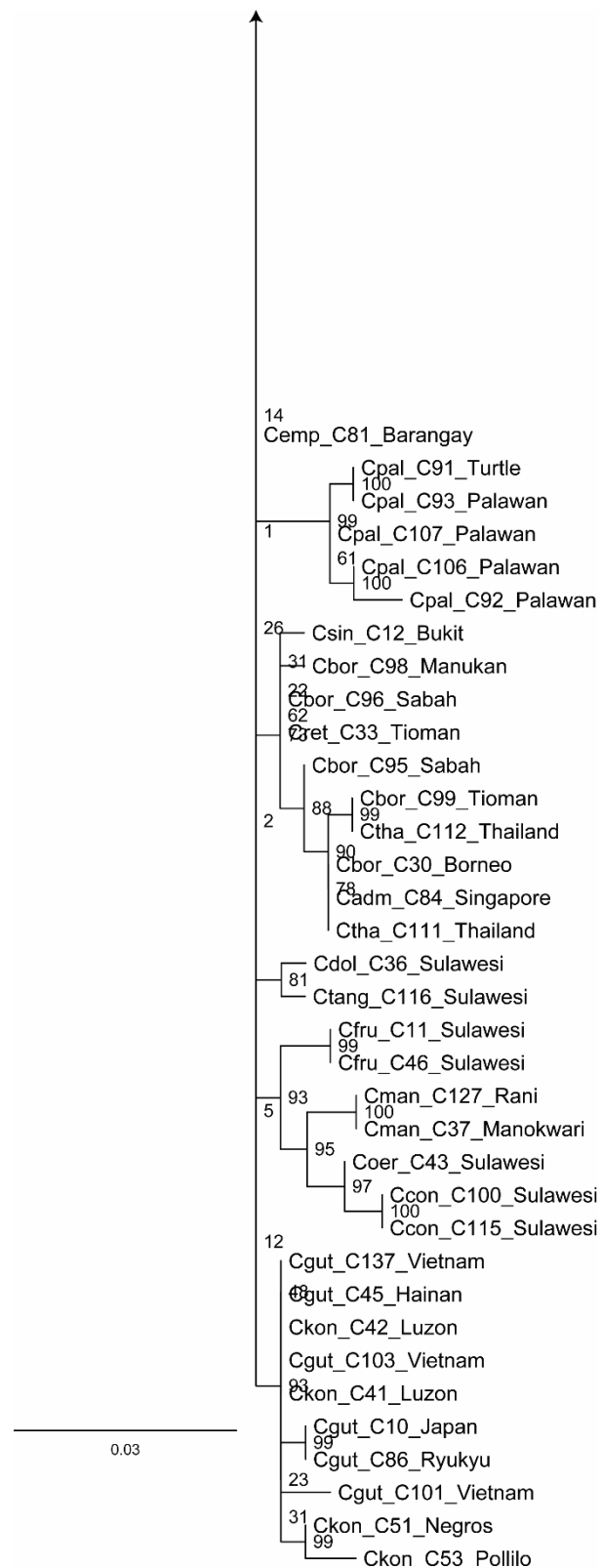
1373

## 1375 H3 (i): continued



1379

1380 H3 (i): continued



1381

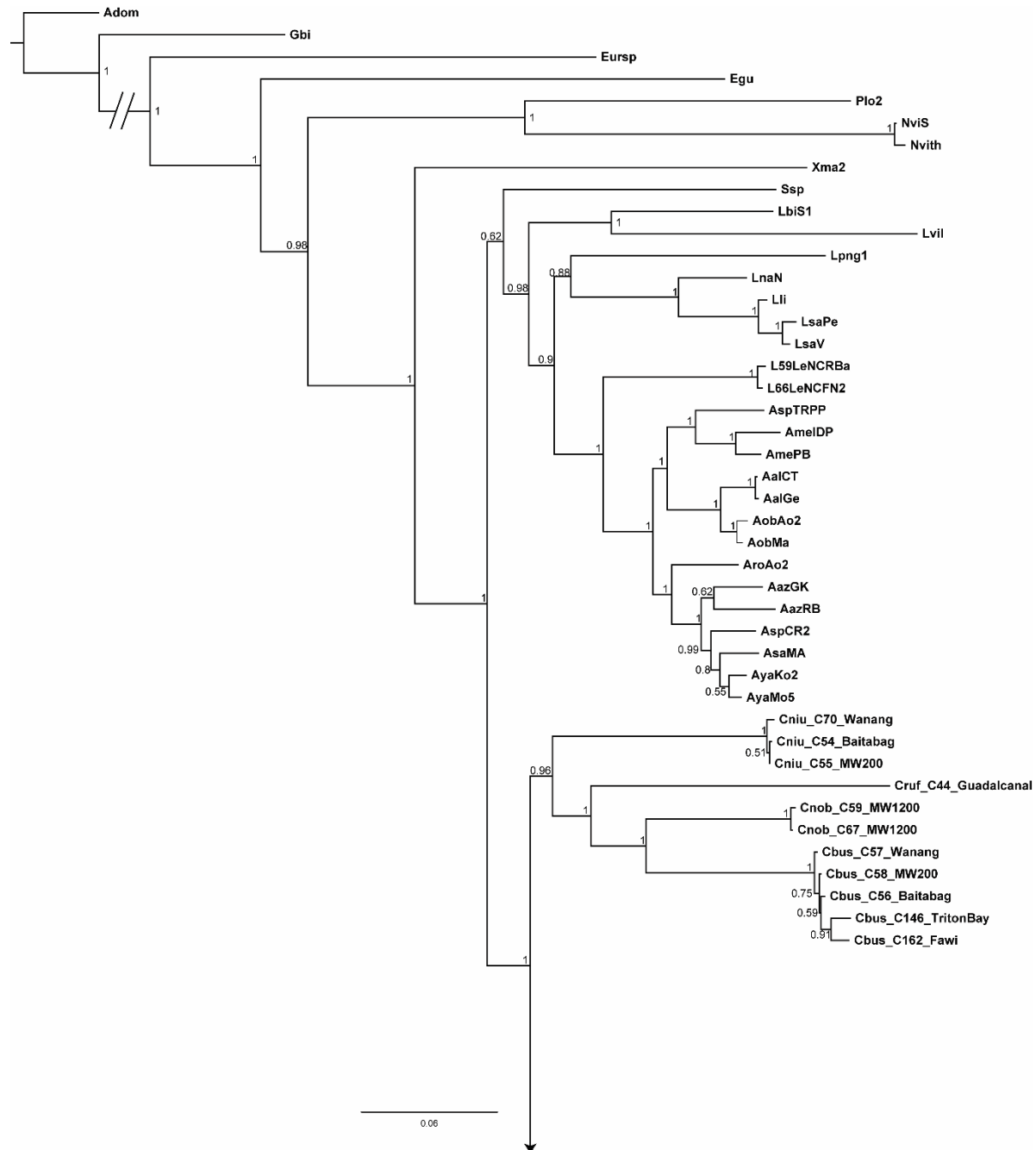
1382

1383

1384

1385 **Appendix S6.** Original output results of Bayesian inference (BI) and maximum  
1386 likelihood (ML) analyses for the concatenated dataset.

1387 **BI maximum consensus tree (concatenated dataset):**



1388

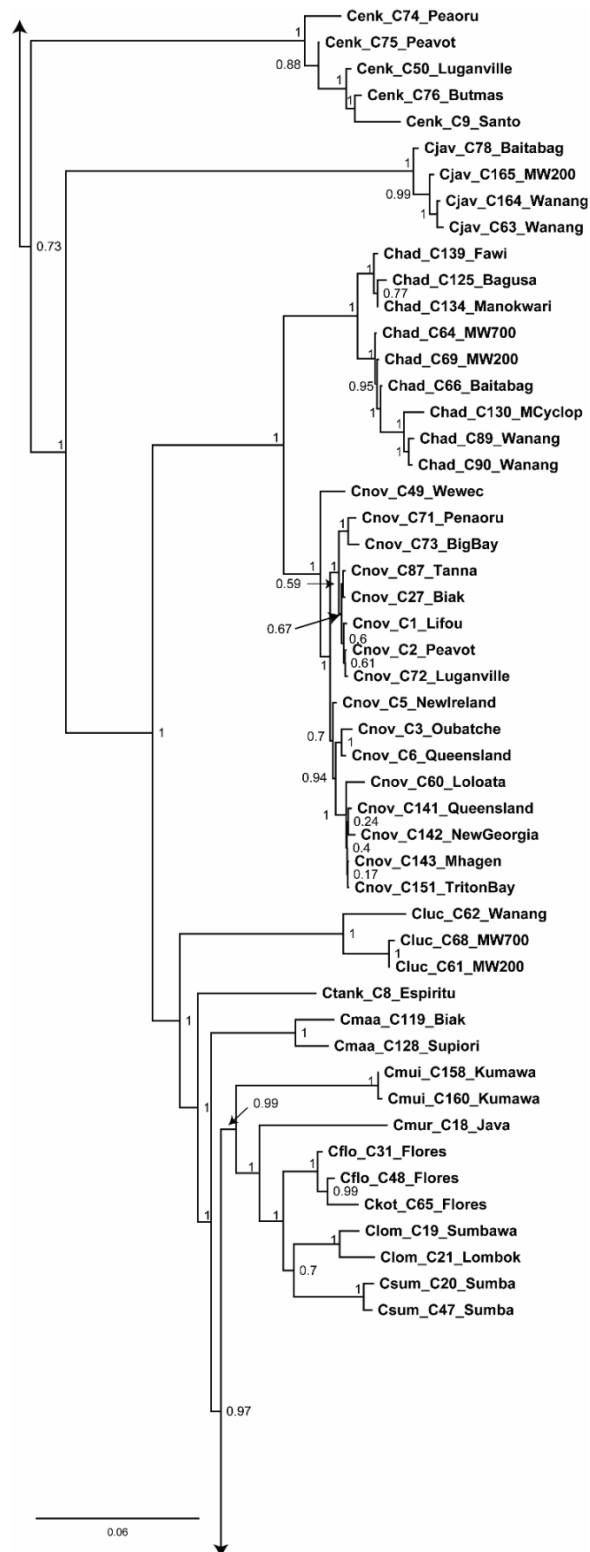
1389 *(continued)*

1390

1391

1392

1393 BI maximum consensus tree (concatenated dataset): continued



1394

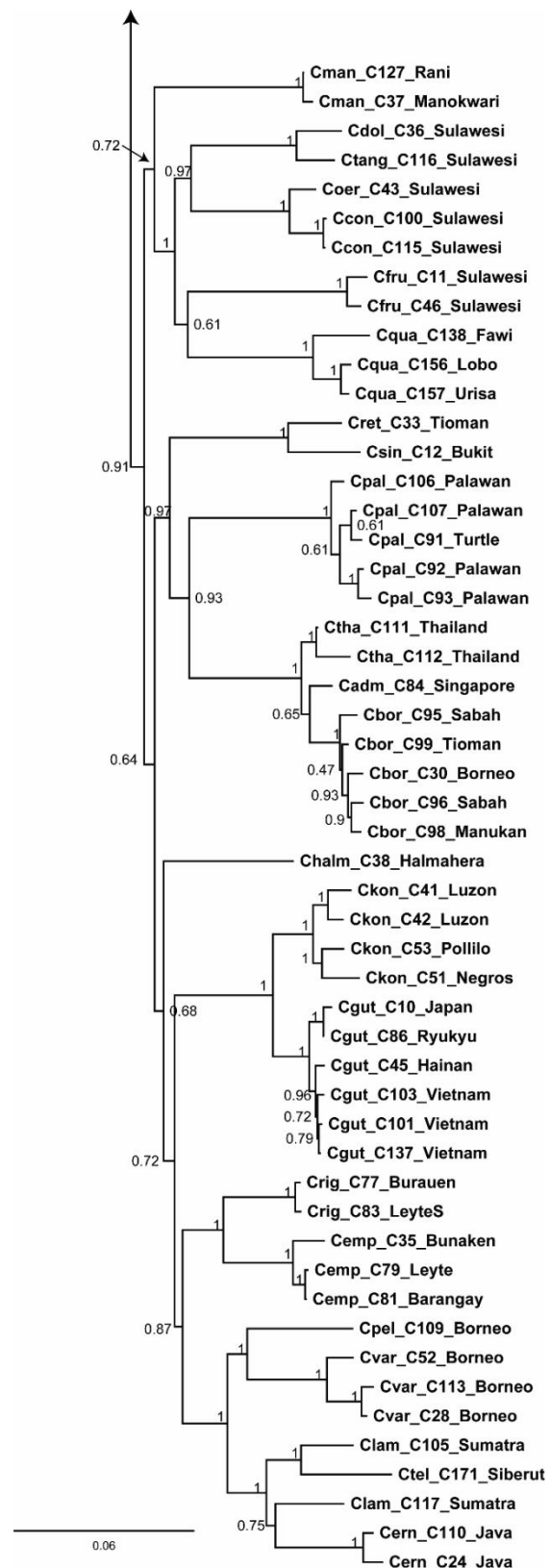
1395

1396

1397

(continued)

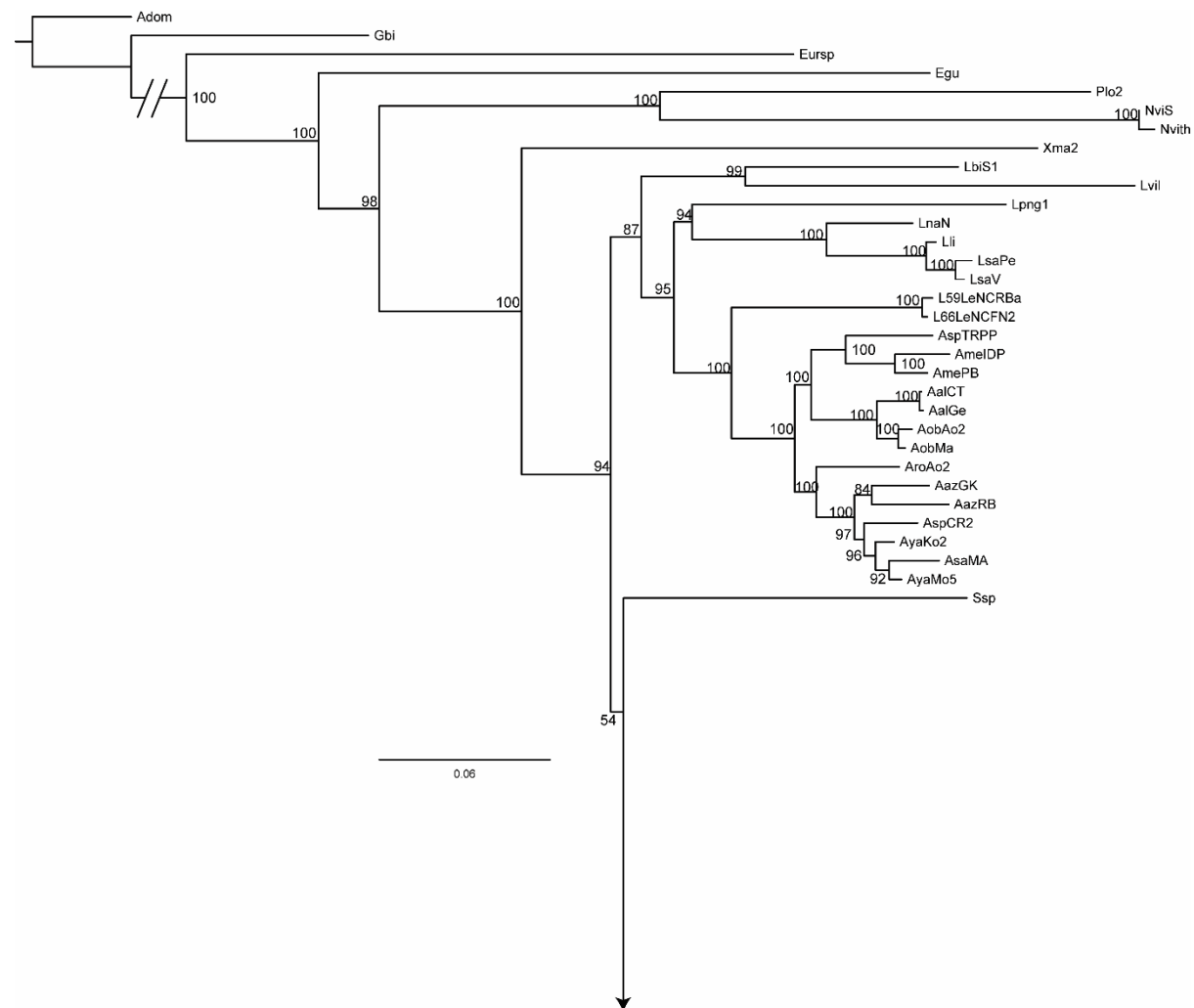
## 1399 BI maximum consensus tree (concatenated dataset): continued



1402

1403

**Best ML tree, RAxML (concatenated dataset):**



1404

1405

(continued)

1406

1407

1408

1409

1410

1411

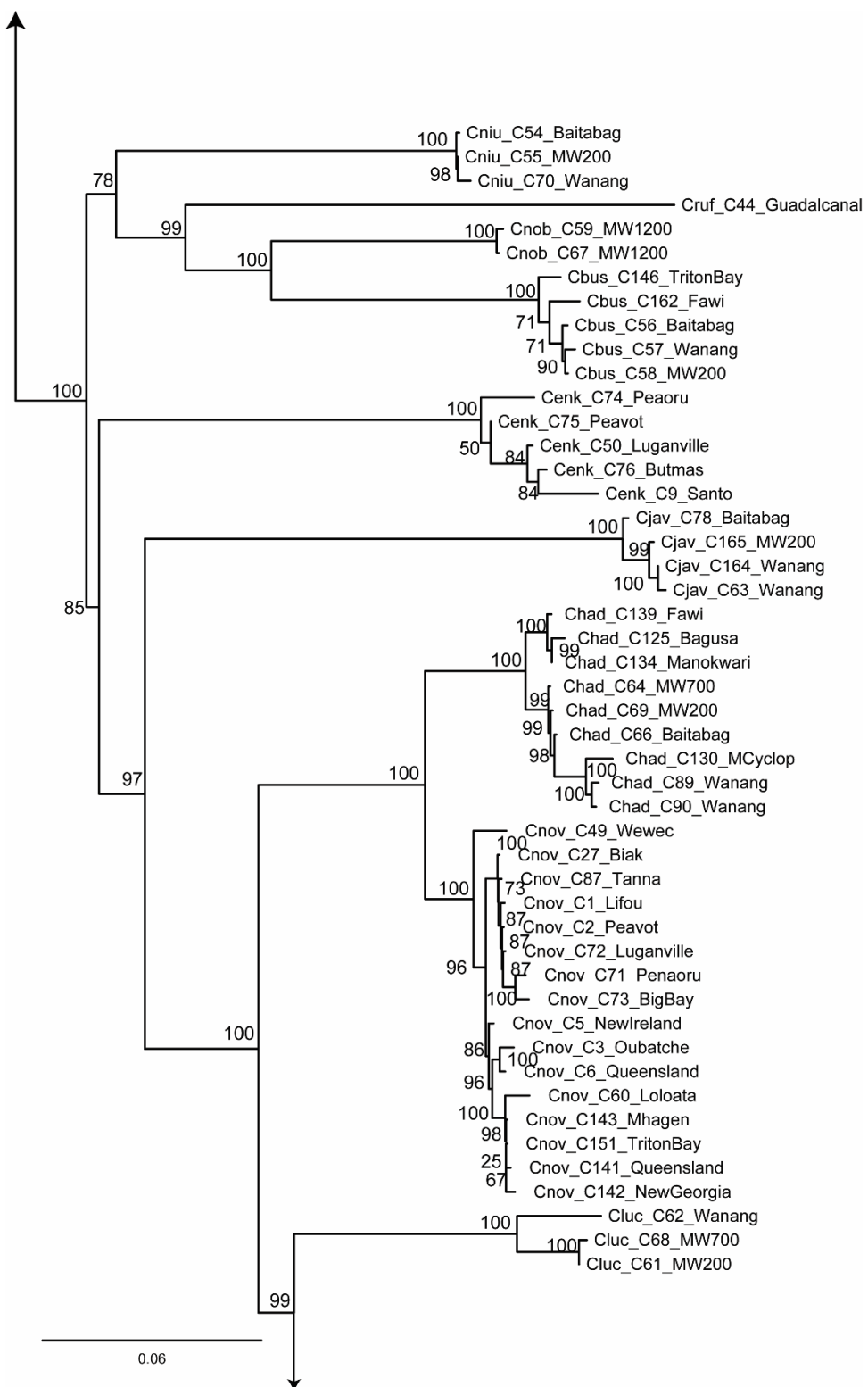
1412

1413

1414

1415

1416 **Best ML tree, RAxML (concatenated dataset): continued**



1417

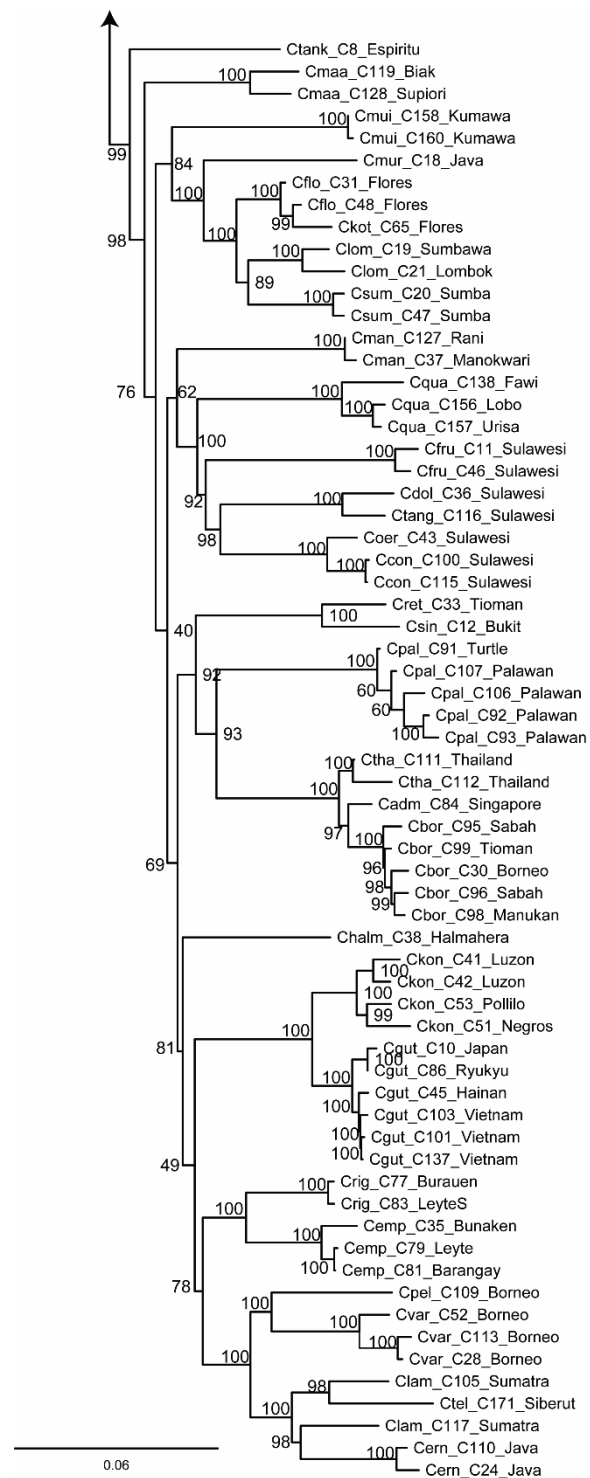
1418

(continued)

1419

1420

1421 **Best ML tree, RAxML (concatenated dataset): continued**



1422

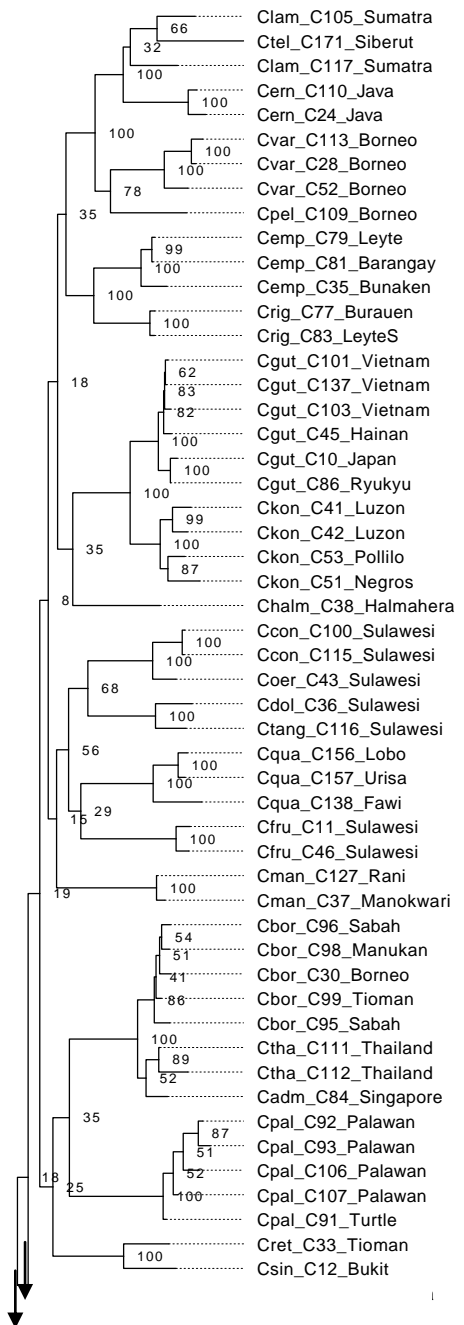
1423

1424

1425

1426

1427 **Best ML tree, IQ-TREE:**



(continued)

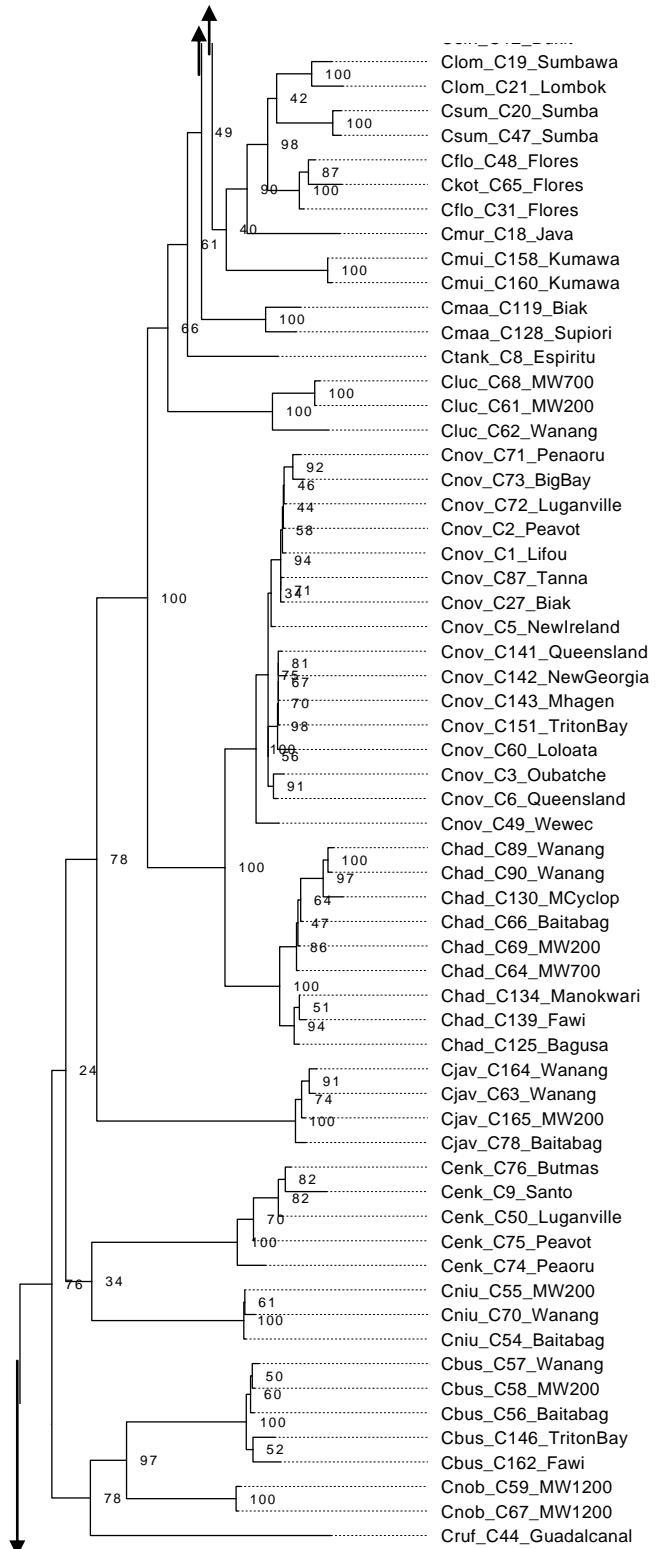
1428

1429

1430

1431 **Best ML tree, IQ-TREE (concatenated dataset): continued**

1432



(continued)

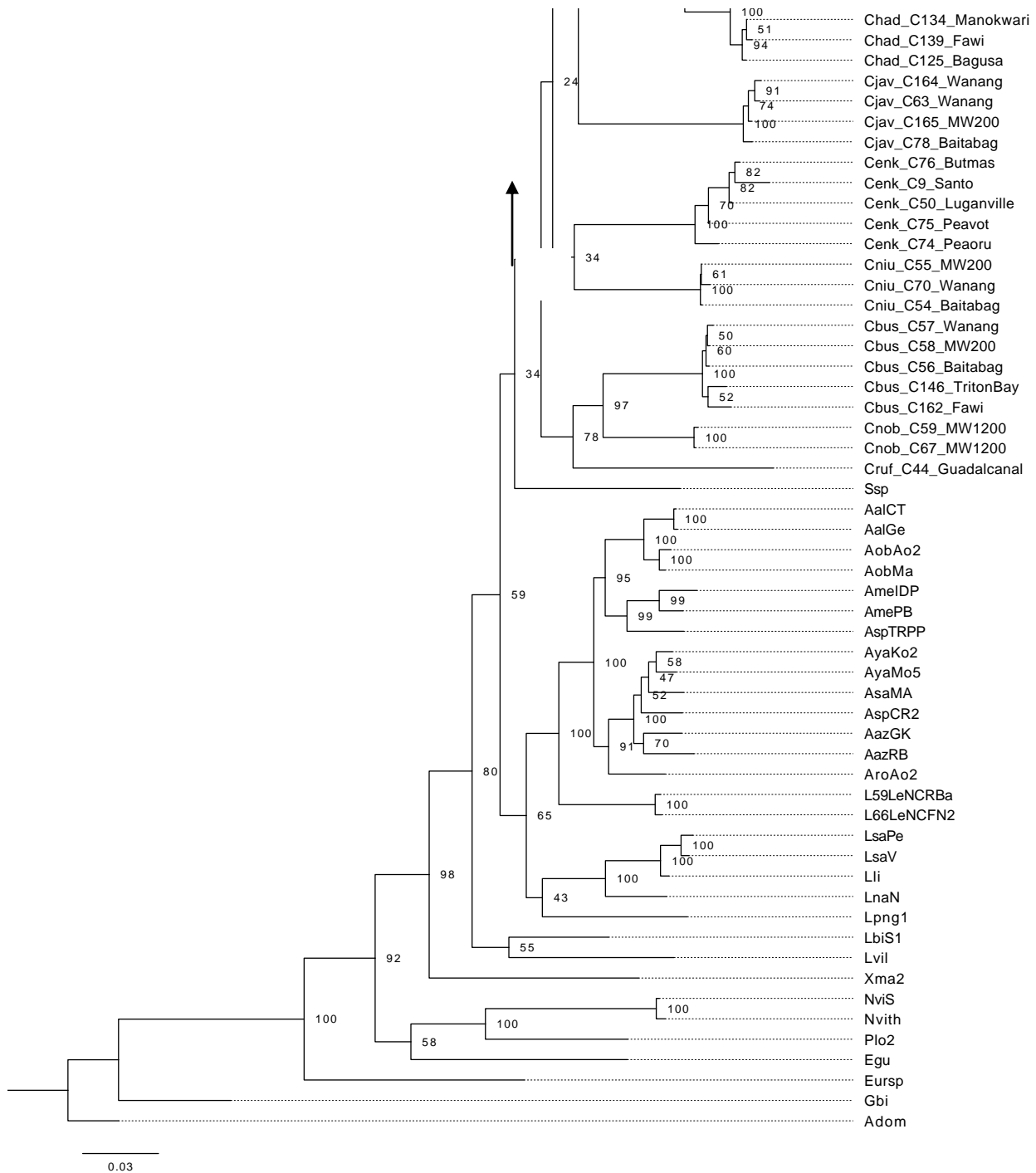
1433

1434

1435

1436

1437 **Best ML tree, IQ-TREE (concatenated dataset): continued**



1438

1439

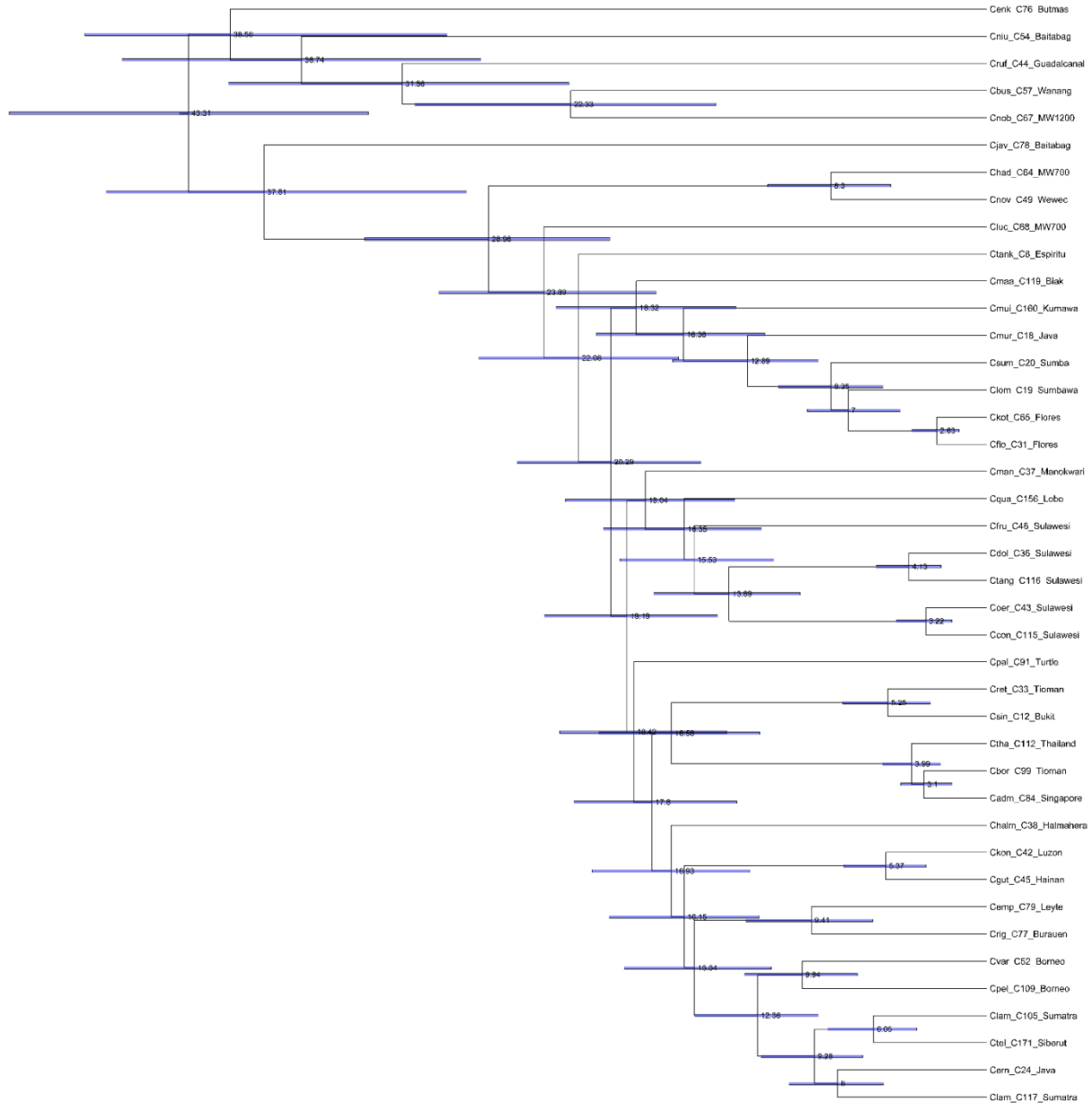
1440

## 1441 Appendix S7. Original outputs for dating analyses.

1442

1443 Dated phylogeny resulting from BEAST analyses relying on the *unlinked*

## 1444 *branch lengths* option of PartitionFinder:



1445

1446

1447

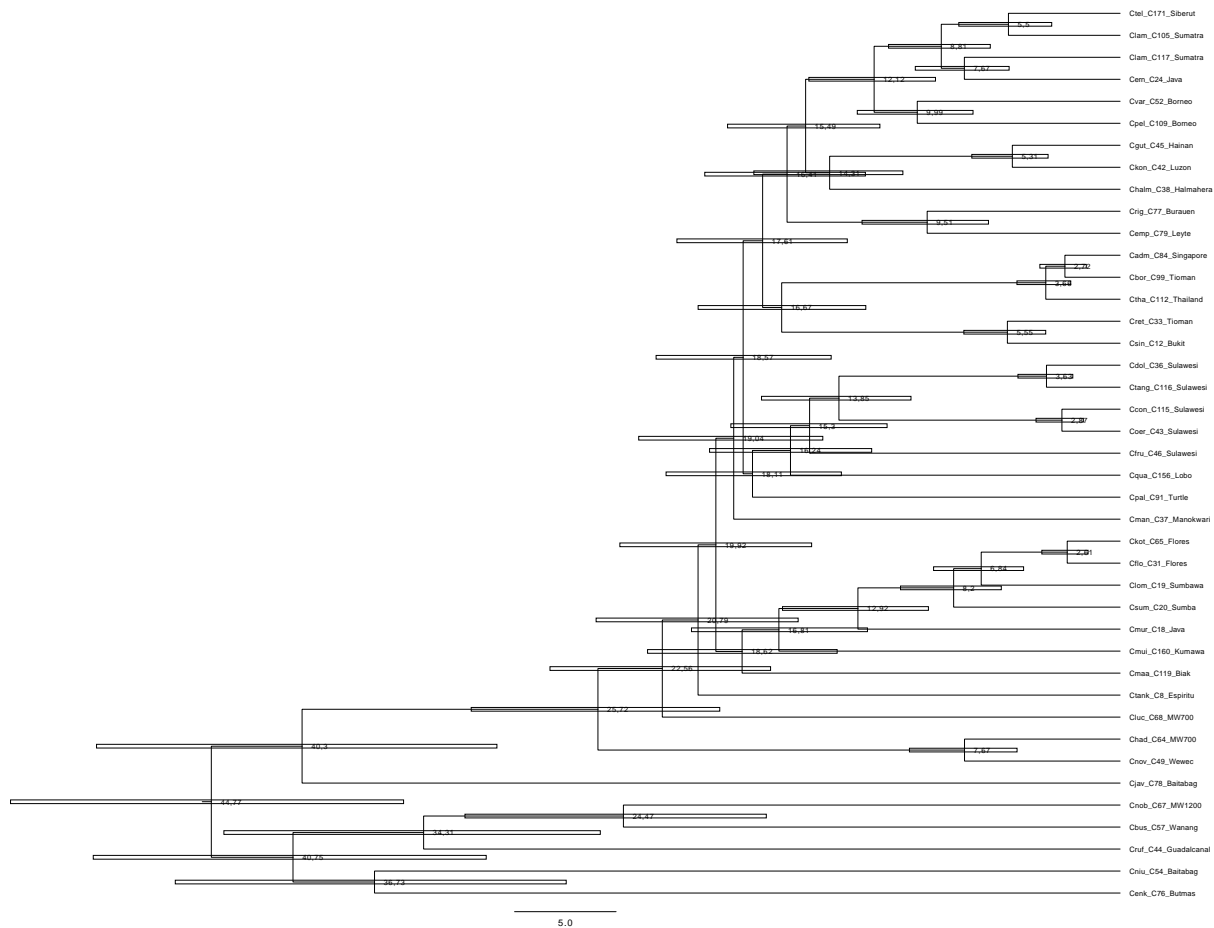
1448

1449 Dated phylogeny resulting from BEAST analyses relying on the *linked branch*

1450 *lengths* option of PartitionFinder:

1451

1452



1453

5.0

1454

1455

1456

1457

1458

1459

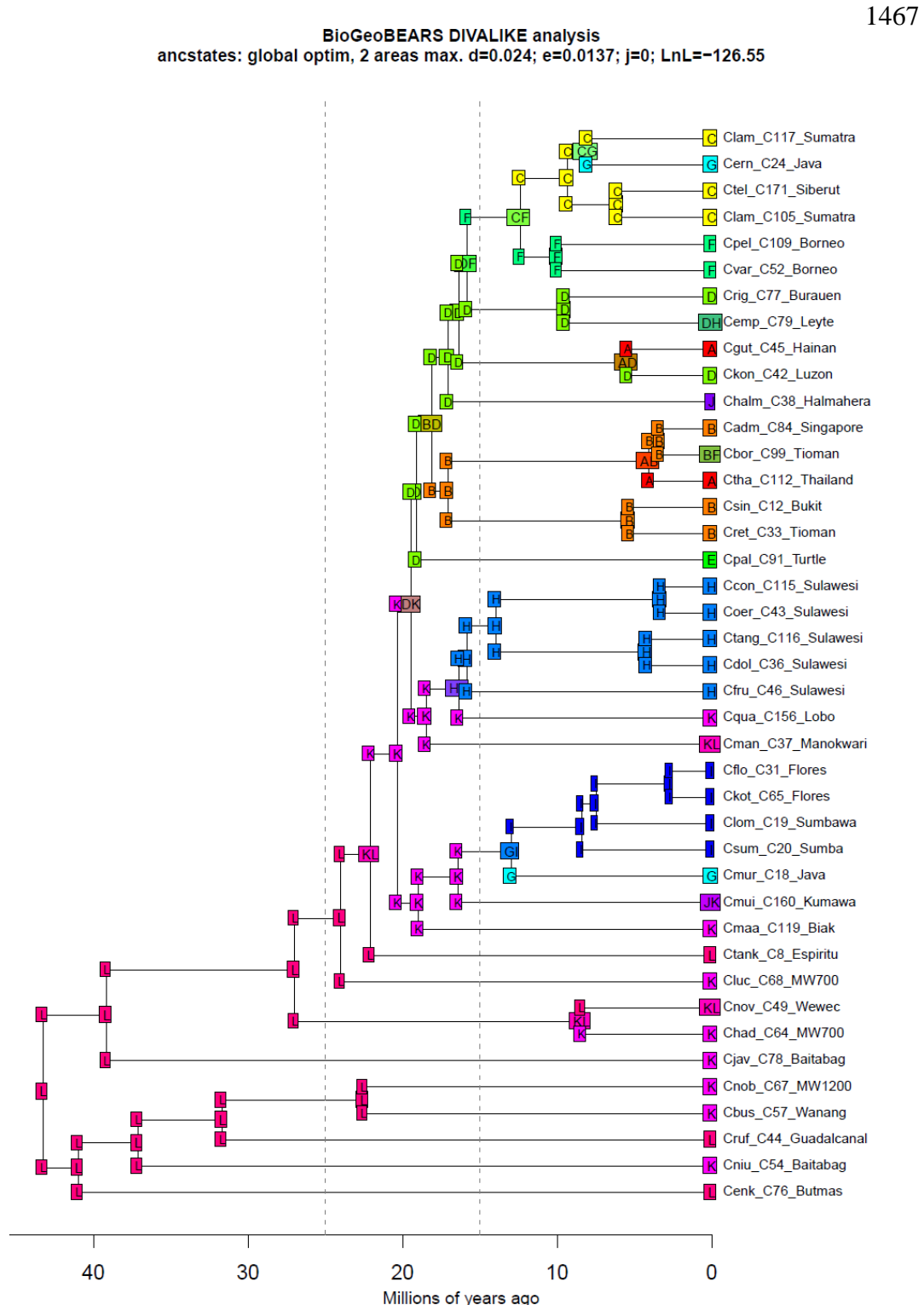
1460

1461

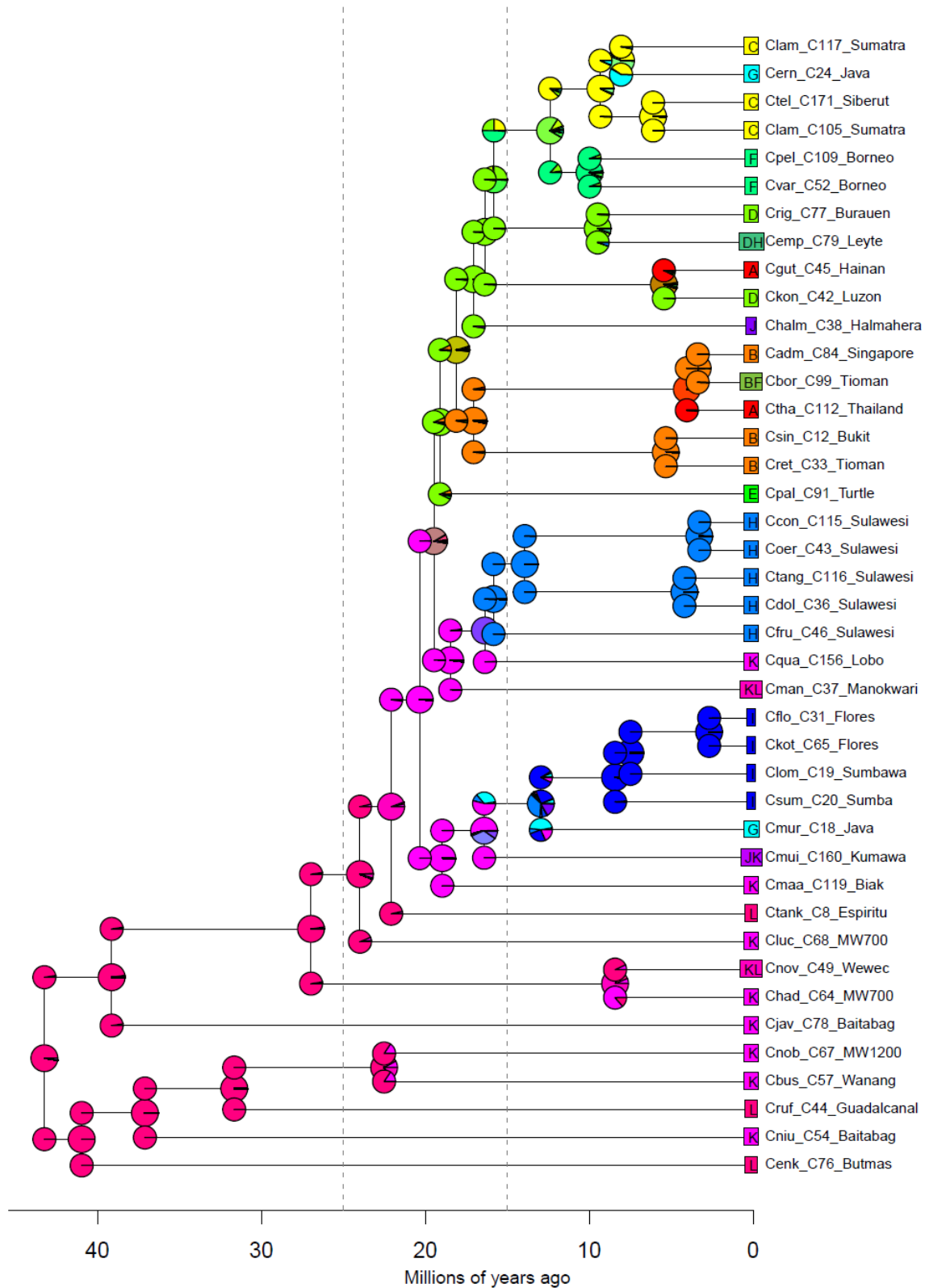
1462

1463

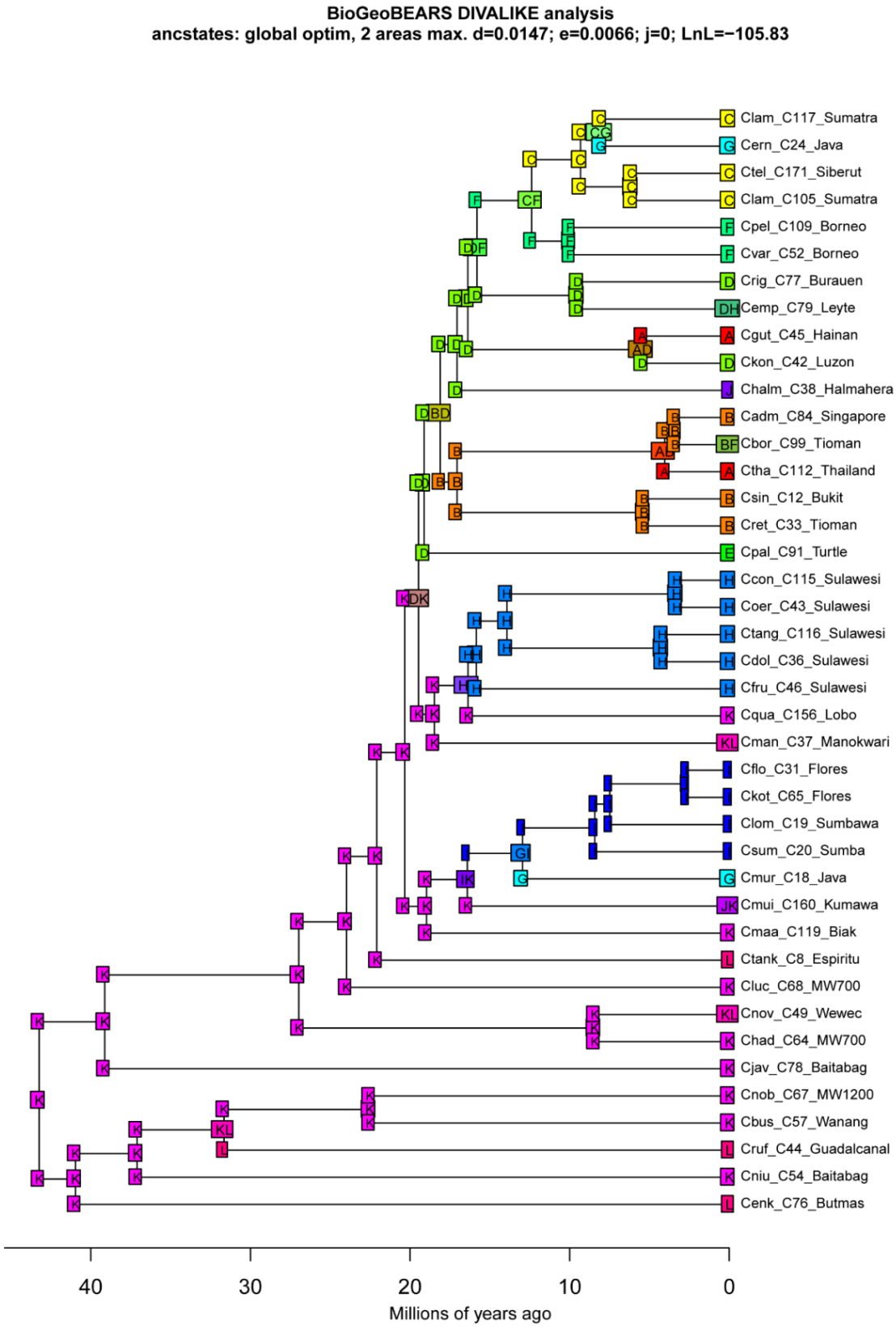
1464 **Appendix S8.** Results of ancestral area estimation in BioGeoBEARS based on the  
 1465 most complex set of dispersal rate multipliers with three time slices, two maximum  
 1466 ancestral areas and DIVALIKE speciation model.



**BioGeoBEARS DIVALIKE analysis**  
 ancstates: global optim, 2 areas max. d=0.024; e=0.0137; j=0; LnL=-126.55

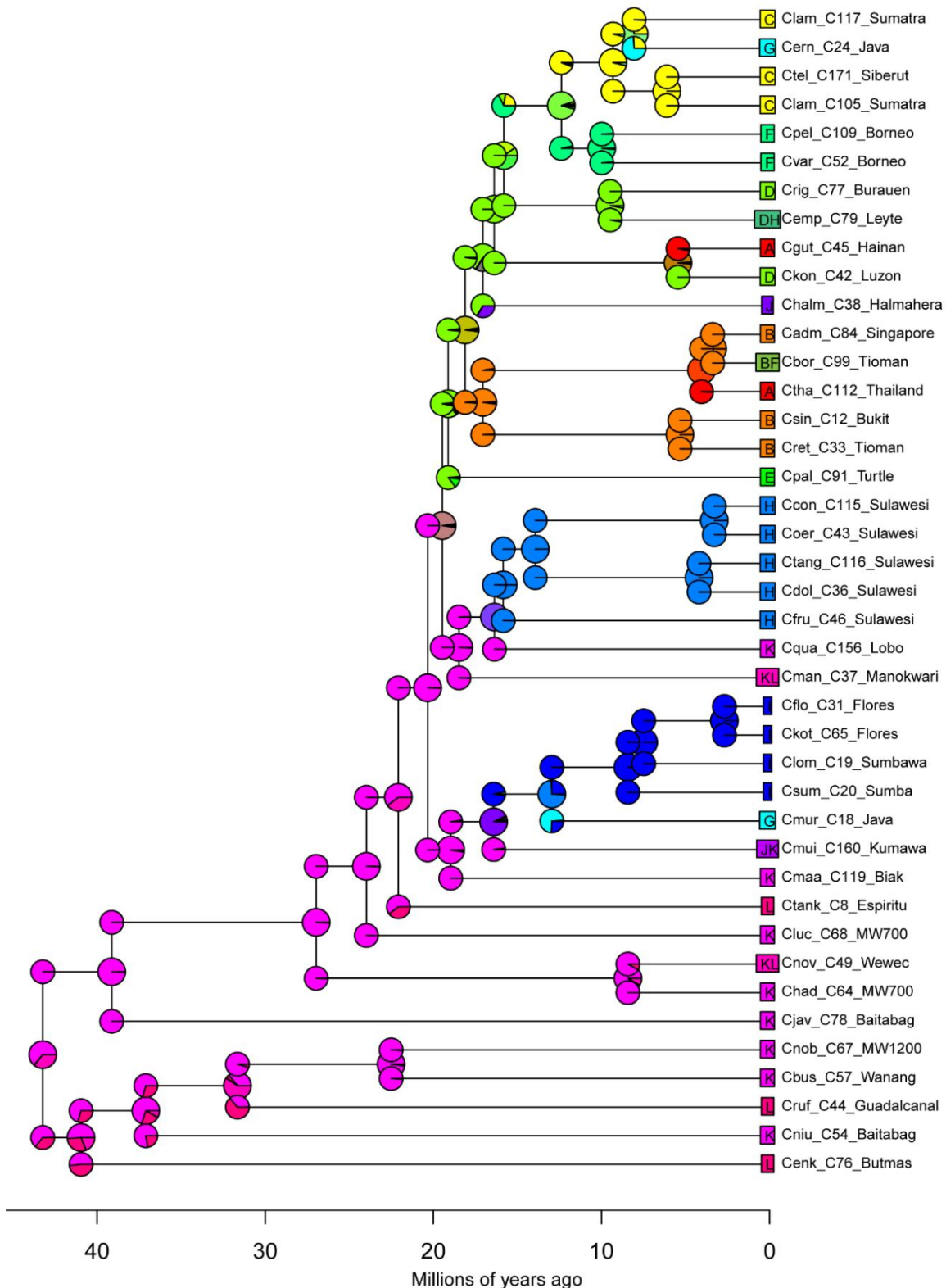


1469 **Appendix S9.** Results of ancestral area estimation in BioGeoBEARS based on the  
 1470 most complex set of dispersal rate multipliers without time slices, two maximum  
 1471 ancestral areas and DIVALIKE speciation model.



1472

**BioGeoBEARS DIVALIKE analysis**  
 ancstates: global optim, 2 areas max. d=0.0147; e=0.0066; j=0; LnL=-105.83



1474  
1475  
1476  
1477

**Appendix S10.** Summary of diversification rate under BAMM analysis with gradient  
of prior values ranging from 0.1 to 1.0. The gray line highlights the model with  
the highest statistical support.

1478  
1479

<i>poissonRatePrior</i>	effectiveSize (postburn\$N_shifts)	effectiveSize (postburn\$logLik)	speciation rate	extinction rate
0.1	751.8863	706.4032	0.1242214	0.06180068
0.2	516.7889	646.3655	0.1201581	0.0575648
0.3	590.2721	404.8521	0.1207902	0.05841862
0.4	737.7893	105.6895	0.1222049	0.05950429
0.5	1088.348	970.286	0.1201945	0.05787543
0.6	612.6263	570.5625	0.1205574	0.05654984
0.7	743.6326	658.2969	0.120278	0.05735786
0.8	569.0992	483.0941	0.118358	0.0551307
0.9	590.9629	510.6484	0.119574	0.05630469
1.0	622.4329	630.815	0.118121	0.05380159

1480  
1481